KASDI MERBAH UNIVERSITY OF OUARGLA

Faculty of New Technologies for Information and Communication
Department of Electronics and Communication

Year :

N° of registration:

/…../…../…../…../

Thesis

In Candidacy of the Degree of "Magister"
In Electronics. Option: Microwaves and Signal Processing

Study and Design of Tunable Filters Based on Planar Technology

Presented and submitted in public
By:

Miss Fentiz Saida

The 8th june 2014

In front of a board of examiners of:

BENATIA Djamel	Professor	University of Batna	Chairman
BOULAKROUNE M'Hamed	Maitre de conference A	University of Ouargla	Supervisor
CHALLAL Mouloud	Maitre de conference B	University of Boumerdes	Supervisor
FORTAKI Tarek	Professor	University of Batna	Member
BOUTTOUT Farid	Professor	University of B. Bouarréridj	Member

2014

Acknowledgements

I want to thank first and foremost, **God Almighty** who gave me during all my years of education health, courage and patience to get to this day.

This thesis would not have been possible without the help, continuous support, patience, motivation and enthusiasm of my principal supervisor, **Dr. Boulakroune M'hamed**, not to mention his advice and immense knowledge. The good advice, support of my second supervisor, **Dr. Challal Mouloud**, has been invaluable for which I am extremely grateful. I could not have imagined having a better supervisor and mentors for my magister study.

I extend my thanks to all the jury members, in particular to **Prof. Benatia Djamel and Prof. Fortaki Tarek** from the University of Batna and **Prof. Bouttout Farid** from the University of B.Bouarréridj who have made me the honor to accept to be part of the jury and review my work.

Last but not least, I would like to thank my parents for their unconditional support, both financially and emotionally throughout my degree. In particular, the patience and understanding shown by my mum, dad and husband during these years are greatly appreciated.

I also thank my family and friends who encouraged me and prayed for me throughout the time of my research. I thank all who in one way or another contributed in the completion of this thesis.

Contribution

The developed work during this thesis generated presentations in international conferences and publication of article in national magazine. The following papers were published and/or under review:

"Synthesis of a Tunable Bandpass Filter," International Congress on Telecommunication and Application'14 University of A.MIRA Bejaia, Algeria, 23-24 April 2014.

"A Novel Tunable Circular Bandpass Patch Filter," Journal AST "Annale des sciences et technologies", Magazine of University Kasdi Merbah Ouargla, Algeria.

This article is under review:
"A Reconfigurable Bandpass Patch Filter with Varactor," - The Second International Conference on Electrical Engineering and Control Applications, *ICEECA 2014* November 18 - 20, 2014, Constantine, Algeria

Abstract

The objective of this thesis is the design and synthesis of tunable bandpass filter at microwave frequencies using planar patch resonators. The characteristics of the designed filter, such as center frequency, bandwidth, and/or selectivity, are electronically adjusted by a DC voltage control.

A design and synthesis of tunable patch filters is developed and applied to circular filter topologies. The complete simulations combine the results of the 3D electromagnetic (EM) simulation of the filter layout with the results of the electrical stimulation of the tuning devices was presented. This allows the correct model of the tuning effect and the definition of the tuning possibilities and limits. The minimum dimensions are greater than 0.5 mm, ensuring a low cost fabrication process. The filter is a tunable triple-mode patch filter using a circular resonator with four slots, across which the varactor diodes are connected.

Résumé

L'objectif de ce mémoire est la synthèse d'un filtre RF passe-bande reconfigurable basé sur des résonateurs de type "Patch". Les caractéristiques du filtre étudié à savoir: sa fréquence de fonctionnement, sa bande passante et sa sélectivité peuvent être ajustées dynamiquement à l'aide d'une tension de commande DC. La technique de synthèse repose sur une analyse électromagnétique des modes propres des résonateurs « Patch ».

Le filtre reconfigurable a été optimisé à l'aide de simulation électromagnétique 3D en incluant le modèle électrique des composants localisés qui sont les diodes varactors et les capacités fixes. Les dimensions minimales du « layout » ont été choisies afin d'être compatibles avec une technologie à bas coût, la dimension la plus faible n'étant pas inférieure à 0,5 mm. Le filtre étudié est un filtre triple mode utilisant un résonateur de type circulaire avec quatre fentes radiales chacune munie d'un varactor.

ملخص

الهدف من هذه المذكرة هو تصميم وتركيب مرشح ممرر الموجة قابل للضبط على ترددات الموجة الصغيرة باستخدام صفيحة معدنية مستوية. خصائص المرشح المصمم، مثل مركز التردد، عرض النطاق الترددي، و / أو الانتقائية، يتم تعديلها الكترونيا عن طريق السيطرة على الجهد DC.

لقد تم تطوير وتصميم مرشحات قابلة للتصحيح الانضباطي وتطبيقها على طبولوجيا مرشح دائري. المحاكاة كاملة تجمع بين نتائج المحاكاة الكهرومغناطيسية 3D (EM) لتخطيط المرشح مع نتائج التحفيز الكهربائي لأجهزة الضبط. هذا ما يسمح للنموذج الصحيح بالتأثر بالضبط وتعريف احتمالات وحدود الضبط. الحد الأدنى لأبعاد هذا المرشح أكبر من 0.5 ملم مع ضمان عملية تصنيع منخفضة التكلفة. المرشح هو عبارة عن فلتر ثلاثي قابل للانضباط باستخدام صفيحة دائرية الشكل مع أربعة فتحات، والتي ترتبط عبرها الصمامات الثنائية القابلة للتعديل.

Table of contents

Chapter III: Results and discussion

Introduction

Filters play important roles in many RF/microwave applications. They are used to separate or combine different frequencies. The electromagnetic spectrum is limited and has to be shared [1][2][3].

Today's modern telecommunication systems become multi-standard, having multiband coverage and multi-functionality. Hence, they require a wide variety of analog circuits containing several amplifiers, filters, oscillators, antennas… etc, for each specific application frequency. This trend demands the development of tunable and reconfigurable filters that constitute a key component in the radio frequency (RF) chain. Electronically tunable and reconfigurable filters have a control circuit to adjust their characteristics such as center frequency, bandwidth, and/or selectivity in a predetermined and controlled manner, replacing the need for multiple channels, improving overall system reliability, reducing size, weight, complexity, and cost [4].

The applications of these filters can be classified according to their behavior. For example, a filter capable of selecting different frequency bands may replace a conventional filter bench, reducing size and cost. Radar systems may employ a tunable bandwidth filter to eliminate out-of-band jamming spectral components. Communication systems with multiband transceivers may also adapt a filter capable of synchronizing different information channels [4][5].

Several types of tunable filters have been presented in the literature using different technologies, topologies, and tuning mechanisms. Despite the great development of planar filters using microstrip resonators tuned by varactor diodes, PIN diodes, or Micro-electromechanical systems (MEMS), planar patch resonators have been rarely investigated [4][5][6][7].

In the meantime, advances in computer-aided design (CAD) tools such as Advanced Design System (EM) simulators have revolutionized filter design [1].

In this work tunable patch filters were to be designed and optimized through complete simulations including 3D electromagnetic (EM) responses of the filters layout and the electrical influence of the discrete components on these responses.

A final analysis was envisaged evaluating the tuning ranges in terms of center frequency, bandwidth, and selectivity. This thesis is organized as follows:

Some terms describing the performance of a tunable filter was introduced in the first chapter with a bibliographical study of tunable filters. It describes the evolution of microwave tunable filters in different technologies and with different tuning mechanisms. This chapter also presents a tuning analysis which consists in determining the tuning element and its equivalent circuit model.

Although the physical realization of filters at RF/microwave frequencies may vary, the circuit network topology is common to all. Therefore, the second chapter begins with section 1, which introduces basic concepts and theories for designing general RF/microwave filters (including microstrip filters). Section 2 describes various network concepts and equations; these are useful for the analysis of filter networks. Then, a third section presents a basic theory of planar filters, classified into the one-dimensional or the two-dimensional (patch) filters, depending on the type of the used resonator, also providing concepts and formulation of a circular patch resonators, the necessary formulation to calculate a coupling matrix relative to the designed patch filter, followed by the basic concepts of coupling matrices are described.

In the last chapter we analyze and design a tunable triple-mode filter using two different circular patch resonators. The filters are designed and characterized and then the simulated frequency responses of the filters are presented. The DC biasing is then discussed. Finally, a discussion of the filter performance is presented indicating the limits of the tuning range, the filter losses, and the calculated unloaded quality factor. The tunable filters with circular patch resonators are compared to the tunable filters presented in the literature in terms of operating frequency, tuning elements, DC bias voltage of the tuning element. Momentum/ADS EM 3D software was used for the analysis, optimization and simulation of the performance of the filters. Finally a conclusion is carried out.

References:

[1] Jia-Sheng Hong & M. J. Lancaster, "Microstrip Filters for RF/Microwave Applications," John Wiley & Sons, Inc., New York, 2001.

[2] I. C. Hunter, L. Billonet, B. Jarry and P. Guillan, "Microwave Filters-Applications and Technology," IEEE Trans. Microwave Theory Tech., vol 50, March 2002, pp. 794-805.

[3] J. Uher, and J. R. Hofer, "Tunable microwave and milimeter-wave bandpass filters," IEEE Trans. Microwave Theory Tech., vol 39, April 1991, pp. 643-653.

[4] M. Makimoto, S. Yamashita, "Microwave resonators and filters for wireless communication: theory, design and application," New York: Springer, 2001.

[5] I. C. Hunter, "Theory and design of microwave filters," New York: Artech House, 2001.

[6] D. M.Pozar, “Microwave Engineering”, John Wiley & Sons, Inc .New York, 1998.

[7] Y.-M. Chen et al., “A reconfigurable bandpass-bandstop filter based on varactor-loaded closed-ring resonators [Technical Committee],” *IEEE Microwave Magazine*, vol. 10, no. 1, pp. 138-140, Feb. 2009.

Chapter I
State of the art

I.1. Introduction

Tunable filter applications in microwave/millimeter-wave systems fall into three major areas: military systems, measurement equipments and communication systems (satellite, cellular radio, etc) [1][2]. Invention of radar systems led to significant development in filters. Basically, one of the critical parts of any military system, such as radars and tracking receivers, is the electronic support measures (ESM) system [3].

The ESM system detects and classifies incoming radar signals by amplitude, frequency, pulse width, etc. The electronic countermeasures (ECM) system which is associated with ESM system, can then take appropriate countermeasures, such as jamming. One method of classifying signals by frequency is to split the complete microwave band of interest into smaller sub-bands. This can be done either by using a contiguous multiplexer, which consists of separate mechanically tunable bandpass filters whose pass-bands cross over at their 3 dB frequencies [4], or an electronically or magnetically tunable filter to scan the whole receive band. Of course, the tuning speed of the filter should be fast enough to keep track of all the signals appear in the whole band of interest.

Since the appearance of the first tunable filters at microwave frequencies during the 1950s, the study of tunable filters has been strongly attached to the fixed filters technology. Most tunable filters described in the literature fall into three basic types: mechanically tunable, magnetically tunable and electronically tunable filters. In this chapter, we cover some of the most important work that has been done in the area of microwave bandpass tunable filters.

I.2. Microwave tunable filters

Before discussing various technologies for frequency agility, some terms describing the performance of a tunable filter are introduced here.

I.2.1 Tunability or relative tunability

The tunability T or relative tunability T_r of a tunable bandpass filter is defined as:

$$T = \frac{f_{max}}{f_{min}} \quad \text{(I. 1)}$$

$$T_r = \frac{f_{max} - f_{min}}{f_{max}} \times 100\% \quad \text{(I. 2)}$$

Where: f_{max}, f_{min} are the maximum and minimum centre frequency of the filter respectively. A large tunability or a wide tuning bandwidth is usually desirable in frequency agile applications.

I.2.2 Loss

Low loss is an essential requirement for such filters to maintain good receiver noise figure and selectivity [5]. The insertion loss (IL) is a measure of the filter loss performance, which is often expressed in dB as [6]:

$$IL = 10logP_{LR} \quad [dB] \quad \text{(I. 3)}$$

Where P_{LR} is the power loss ratio of a network, defined as incident power divided by the actual power delivered to the load. A power loss ratio of 50 % is equivalent to - 3 dB insertion loss. The quality factor Q of a resonator circuit is defined as [7]:

$$Q = w\frac{average\ energy\ stored}{average\ energy\ dissipated} \quad \text{(I. 4)}$$

Resonator Q is a measure of the frequency selectivity and loss performance. For a filter consisting of resonators, a higher resonator Q implies a lower loss and better frequency selectivity of the filter. The resonator quality factor Q can be evaluated as [7]:

$$Q = \frac{w_0 L}{R} = \frac{1}{w_0 LC} \quad \text{(I. 5)}$$

For a series RLC resonant circuit, and:

$$Q = \frac{R}{w_0 L} = w_0 LC \quad \text{(I. 6)}$$

For a parallel RLC resonant circuit, where $w_0 = 1/\sqrt{LC}$ is the resonant frequency.

I.2.3 Tuning speed

The tuning speed of a tunable filter refers to the delay time required by the filter to change between two frequencies or two states. A tuning speed over 1 GHz/µs is required in modern communication systems [8].

I.2.4 Linearity

In a linear system, the output signal has the same frequency as the input signal, it only differs in the amplitude and phase. However, practical microwave devices are generally nonlinear and exhibit intermodulation distortion (IMD).

I.2.5 RF power handling capability

Power handling capability of a RF/microwave device is the ability to transmit high microwave power level without breakdown or unacceptable intermodulation distortion of the in-band signals. A large power handling capability is required for filters in applications such as wireless or radio base station transmitters and diplexers, satellite output filters and multiplexers, and transmitters in radar systems [9].

I.2.6 Fractional bandwidth (FBW_{3dB})

In view of the many different applications existing nowadays, a narrower or wider bandwidth does not necessarily means a best characteristic. The bandwidth is discussed along this work and is defined as the absolute 3-dB (FBW_{3dB}) defined in eq. (4), where (f_{3dB} *up* - f_{3dB} *low*) is the difference between the upper and lower frequencies at the passband when the insertion loss drops 3 dB relative to the center frequency f_c.

$$FBW_{3dB} = \frac{ABW_{3dB}}{f_c} = \frac{f_{3dBup} - f_{3dBlow}}{f_c} \quad \text{(I. 7)}$$

In addition to the above, other performance parameters such as operating frequency, power consumption, and tuning voltage as well as many others specify the tuning technology requirements.

I.3. Different Techniques for Filter Tuning

Throughout the next two decades, a fast spread of the tuning concept was experienced and several designs were developed with either mechanical tuning by using movable metallic or dielectric walls[10], or tuning screws[11], or magnetic

tuning, using pieces of ferrites inside the cavities [12][13]. Most tunable filters described in the literature fall into three basic types: mechanically tunable, magnetically tunable and electronically tunable filters [14].

I.3.1 Mechanical tuning

Mechanically tunable bandpass filter's large power handling capability and low insertion loss are often important factors if a tunable filter is required for long-distance communication (satellite or transponder) or radar systems. They are usually realized using either coaxial or waveguide resonators [15]. The main disadvantages of these filters are their tuning speed and size. Their tuning speed is very low. They can be tuned manually or electrically if the filter is combined with a remotely controlled motor. Their size is large and they are bulky.

I.3.2 Magnetical tuning

Magnetically tunable filters have been used in microwave systems for a long time. The most popular type uses ferromagnetic resonators and gyromagnetic coupling. The first filter of this kind was reported in 1958 [16]. Since they usually contain single-crystal Yttrium-Iron-Garnet (YIG) spheres in their resonators, they are commonly termed YIG filters. They have multioctave tuning range, spurious-free response, low insertion loss and high quality factor resonators [15][17]. They are often used between 0.5-18 GHz for military and commercial purposes, such as tracking receivers, radars, etc. The design principles for multi-stage YIG filters from 0.5 to 40 GHz are described in [15][18][19].

Magnetic resonator filters have also been developed for millimeter-wave applications. Instead of using YIG spheres, they employ highly anisotropic hexagonal ferrites. The 4-pole filter reported in [20] has been tuned from 50 to 75 GHz with an insertion loss of about 6 dB and a relative bandwidth of 1%. As mentioned above, the important problems associated with YIG filters are size, tuning speed and power consumption. Compare to mechanically tunable filters they have smaller size, but because they are not planar structures, they cannot be used in integrated systems. The YIG filter is tuned by changing the biasing current of the ferromagnetic resonator.
This current is in the order of hundreds of mill-amperes, which is not acceptable in most modern low power RF transceivers. YIG filters have moderate tuning speed,

which is not usually less than 1-2 GHz/ms which is not enough for applications which require very fast tuning (electronic warfare, signal intelligence, etc).

I.3.3 Electrical tuning

Electrically tunable filters can be tuned very fast over a wide (an octave) tuning range, and they offer compact size and are good candidates for highly integrated RF front ends. The best way of tuning an RF filter electronically is using tunable capacitors as part of the resonator. The capacitor value and the resonator frequency are changed by adjusting the biasing voltage across the tunable capacitor. There are three major technologies applied for this type of RF filter tuning:

- Semiconductor Gallium-Arsenide (GaAs), Silicon (Si) or Silicon-Germanium (SiGe) varactors;
- Ferroelectric thin film tunable capacitors;
- Radio frequency micro-electromechanical systems (RF MEMS) switches and varactors.

I.4. Tuning analysis

The tuning analysis consists in determining the tuning element, which can be varactor diodes, MEMS switches or capacitances, PIN diodes, or any type of commercial or custom device that changes the filter response as the desired tuning behavior.

Microwave tunable filters can be divided in two groups, filters with discrete tuning, and filters with continuous tuning. Filter topologies presenting a discrete tuning generally use PIN diodes or MEMS switches. On the other hand, filter topologies using varactor diodes, MEMS capacitors, ferroelectric materials or ferromagnetic materials are frequently used to obtain a continuous tuning device.

I.4.1 MEMS-based Tunable Filters

RF MEMS reconfigurable devices have good compatibility with technologies used in semiconductor industries. They offer small size and good integration capabilities with microwave electronics. RF MEMS in general require low currents to be operated, thus they consume low power compared to solid state devices, and they also can exhibit linear transmission with low signal distortion.

a. Tunable filters using MEMS switches

The MEMS switches can be either a cantilever or a bridge type, and can be capacitive type switches or direct contact switches. Switches can have two states: on or off. Direct contact switches will generally make a metal to metal contact in the on state, direct contact switches are commonly used for low frequency applications as can be seen in figureI.1.

Capacitive switches will present two capacitances, one in the on state and another one in the off state, these switches can be used for high frequency operation.

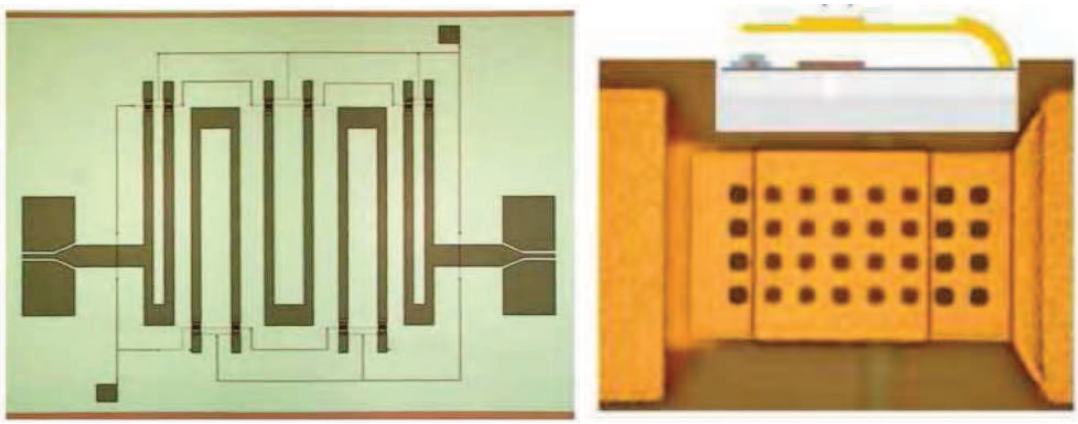

Figure I.1: Tunable bandpass filter using direct contact MEMS cantilever switches [10].

b. Tunable filters using MEMS varactors

The use of MEMS varactors can result in low filter insertion losses, and are used to provide a continuous filter parameter reconfiguration. MEMS varactors are suitable for miniature lumped element filters due to the high quality factor presented by the MEMS varactors, compared with conventional components like the metal insulator metal capacitor. MEMS varactors can also be used to load distributed resonators to achieve tunable filters.

I.4.2 Ferroelectric materials-based tunable filters

Ferroelectric materials can change permittivity values proportionally to an applied DC electric field where some ferroelectrics are suitable for thin film deposition. This section focuses on tunable microwave filters using three of the most common ferroelectrics used to date, the Barium-Strontium-Titanate oxide (BST), the Strontium-Titanate Oxide (STO), and the lead Strontium-Titanate oxide (PST).

Other ferroelectric materials considered for microwave tunable devices are the sodium potassium niobium oxide or the bismuth zincniobate oxide ferroelectric which are not covered in this section. Ferroelectrics have been very attractive due to their compatibility with planar microwave electronics and technologies to produce high speed reconfigurable devices.

a. Tunable filters using ferromagnetic materials

Tunable filters using ferromagnetic materials like Yttrium-Iron-Garnet (YIG), results in high unloaded quality factor resonators with high power handling capabilities and high power consumption. Resonators using YIG spheres have been traditionally used (Carter, 1961), despite the high unloaded quality factors obtained, the filters require very precise fabrication involving high costs, and also other drawbacks are a low tuning speed and a complex tuning mechanism involving coils near the spheres.

I.4.3 Mechanically tuned filters

Mechanically adjustable dielectric or metallic tuning screws are commonly used to tune microwave filters. These techniques are frequently used to compensate fabrication tolerances, where the screws can be moved manually while monitoring the measured response. Automated tuning programs can automatically find an optimum filter response by iterating tuning screw positions until a user defined response is found.

The tuning screws can be placed strategically on top or near microwave resonators to tune the resonant frequency of individual resonators. The screws can be placed between resonators to modify inter-resonator coupling coefficients, or screws can be placed between the input/output coupling structure to the filter and the first/last resonator to adjust the input and output coupling to the filter.

Also the type of screw is important depending on the electric and magnetic field distribution near the resonator to be tuned; in general, dielectric tuning screws are mostly used where the electric field maximums around the resonator can be found. Similarly metallic tuning screws are mostly used where magnetic field maximums around the resonator are found.

I.4.4 MMIC Tunable filters

The silicon integrated reconfigurable filter can tune center frequency, bandwidth and transmission gain, photography of the chip is shown in figure I.2.

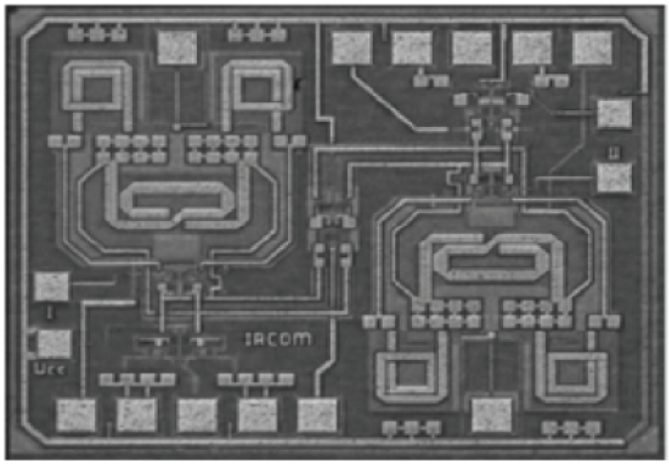

Figure I.2: MMIC tunable bandpass filter [10].

I.4.5 Tunable filters using active devices

This covers tunable filters that use semiconductor based tuning elements. Devices using diodes are attractive below 10 GHz where diodes can still show quality factors above 50 with low bias voltages. Diodes usually involve simple packages and can be mounted on microwave boards.

a. Tunable filters using transistors

A gallium arsenide field effect transistor is based on a combline topology and can tune its center frequency as can be seen in figure I.3.

Center frequency tuning has been achieved on a two pole filter configuration using two metal semiconductor field effect transistors; one transistor is used for center frequency tuning and the other to provide a negative resistance to the circuit. The negative resistance technique can raise the resonator unloaded quality factor resulting in an improved filter response.

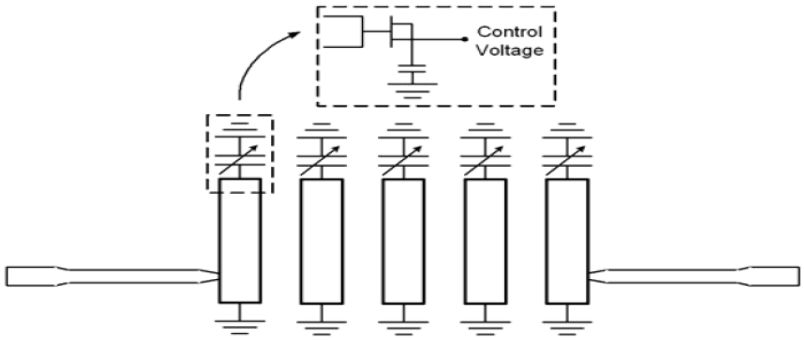

Figure I.3: Tunable bandpass filter using transistors [10].

b. Tunable filters using PIN diodes

PIN diodes are frequently used to produce reconfigurable discrete states on a filter response, and are very attractive for low cost implementations. An example of a switchable bandstop filter using PIN diode is shown in the following figure:

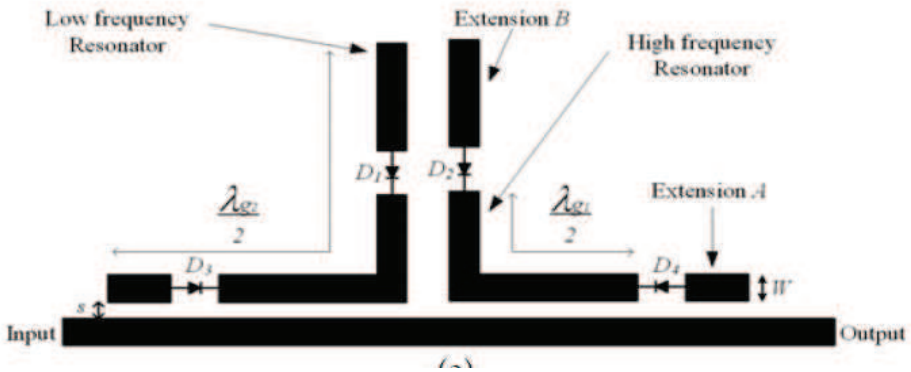

Figure I.4: switchable bandstop filter using PIN diodes [10].

c. Tunable filters using varactor diodes

Varactors are typically used for continuous tuned filters. Varactor diodes use the change in the depletion layer capacitance of a p-n junction as a function of applied bias voltage. Varactor tuned devices have been used for high tuning speeds; these devices do not exhibit hysteresis. Tuning speeds of varactor tuned filters are limited only by the time constant of the bias circuit. Varactor based tunable filters are mainly distributed.

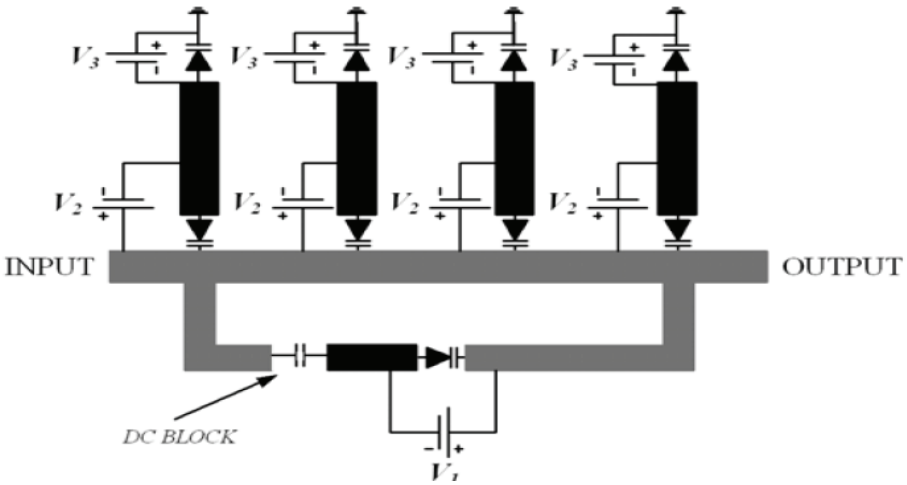

Figure I.5: Tunable bandstop filter using varactor diodes [10].

The tuning element used in these filters is a varactor diode. Varactor diode is a semiconductor diode that, when reversed biased below its breakdown voltage, acts as a voltage-controlled variable capacitance. The reverse voltage changes the width of its depletion layer, changing the diode junction capacitance.

When modeling an encapsulated varactor diode, one should take into account the parasitic elements that are mostly due to the package, in order to obtain an accurate equivalent electrical circuit model at the frequency band at which the diode will operate. For the filters developed in this work, the classical model used is shown in Figure I.6, where *Rs* represents the parasitic series resistance of the diode die, *Ls* and *Cp* are the parasitic inductance and capacitance due to the package.

In this model, *Rs* and *Ls* vary with the applied voltage. In general, the capacitance *Cp* is absorbed by *Cj* due to its very low value, and the model becomes a simple series *RLC*. At higher microwave frequencies, say above 10 GHz, a more complete model should be extracted, taking into account *Cp*, the package material, the wires bonding, etc.

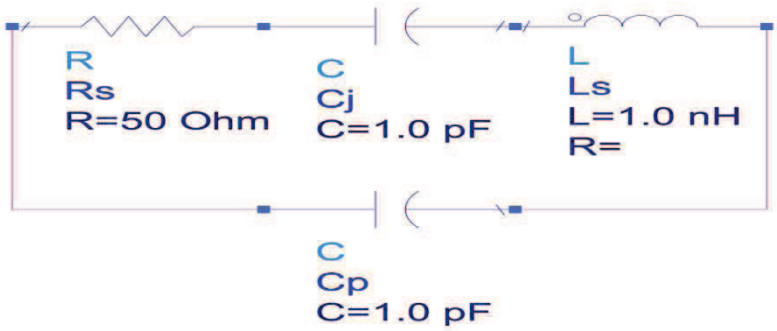

Figure I.6: Equivalent electrical model of a reversed biased varactor diode.

Normally, a typical curve Cj (V) is given by the manufacturer for each varactor diode, as shown in Figure I.7. With these curves, the more suitable diode capacitance values can be chosen for the design of the reconfigurable filters.

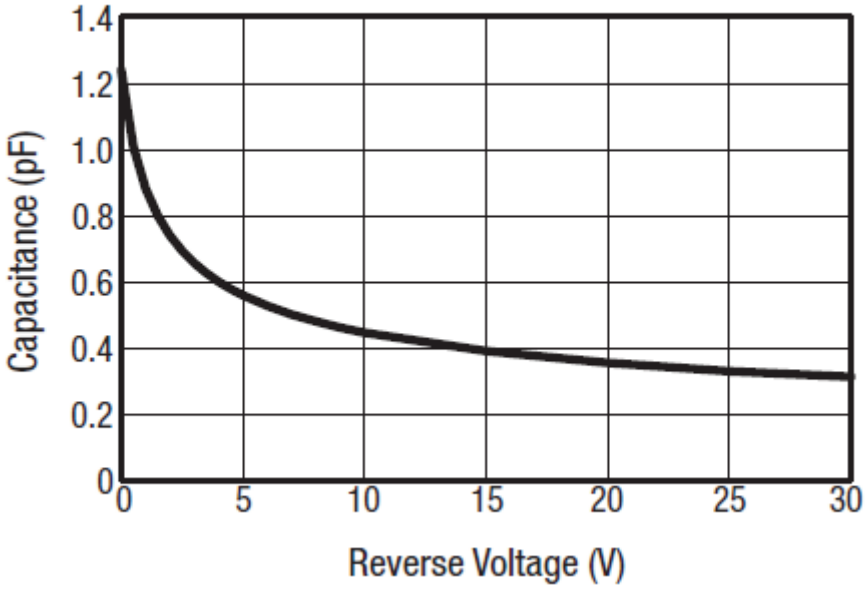

Figure I.7: Capacitance vs Reverse Voltage (SMV1430, used in this work).

Figure I.7 shows the curve of the SMV1430 GaAs diode, from SKYWORKS, which was available to be used in this work. The available data given by the manufacturer is the capacitance range vs. the reverse voltage from 0.45 pF (20 V) to 2.3 pF (0.1 V) at 1 MHz, $\gamma = 0.75$, $Ls = 0.45$ nH, and $Q = 4500$ (at 50 MHz). The Q-factor is defined in eq. (I.8).

$$Q_{u\,varactor} = \frac{1}{2\pi f R_s C} \qquad (\text{I}.8)$$

I.5. Conclusion

In order to reduce the area of a single-mode patch filter, a useful technique is to insert a perturbation in the resonator geometry. The perturbation is inserted into the resonator to increase the electrical current path of a resonant mode and thus, the corresponding modal frequency decreases. If the dominant frequency of a patch resonator is reduced without changing its dimensions, one can consider the filter miniaturized, because in order to reduce the frequency, the filter dimensions should increase.

The dual-mode concept increases the order of the filter without increasing the number of resonators. A dual-mode patch resonator is a single-mode resonator with perturbations in its geometry, which bring the frequency of a particular mode closer to the frequency of another mode, forming the filter passband. Each of these modes works as a resonant circuit, determining a pole in the passband. From an electrical point of view, a dual-mode patch resonator is equivalent to a doubly-tuned resonant circuit and thus, a second order filter is constructed with a single resonator. Hence, the number of resonators needed to build a filter with a given order is halved thus decreasing the filter size.

Therefore, it is possible to design patch filters with two important characteristics: miniaturization and selectivity. Miniaturization occurs at two levels: by increasing the electrical current path, which reduces the modal frequency without changing the patch resonator area, and by increasing the order of the filter without increasing the number of resonators. Selectivity is also improved when changing specific resonant frequencies or when increasing the order of the filter.

References:

[1] I. C. Hunter, L. Billonet, B. Jarry and P. Guillan, "Microwave Filters-Applications and Technology," IEEE Trans. Microwave Theory Tech., vol 50, March 2002, pp. 794-805.

[2] J. Uher, and J. R. Hofer, "Tunable microwave and milimeter-wave bandpass filters," IEEE Trans. Microwave Theory Tech., vol 39, April 1991, pp. 643-653.

[3] R. M. Fano andW. Lawson, "Micorwave Transmission Circuits," ser. M.I.T. Rad. Lab. New York: McGraw-Hill, 1948, vol. 9, ch. 9, 10.

[4] J. B. Tsui, "Microwave Receivers with Electronic Warfare Applications," New York: Wiley, 1992.

[5] J. Nath, D. Ghosh, J. P. Maria, A. I. Kingon, W. Fathelbab, P. D. Franzon, and M. B. Steer, "An electronically tunable microstrip bandpass filter using thin-film Barium-Strontium-Titanate (BST) varactors", IEEE Transactions on Microwave Theory and Techniques, vol. 53, no. 9, pp. 2707-2712, 2005.

[6] N. K. Pervez, P. J. Hansen, and R. A. York, "High tunability barium strontium titanate thin films for RF circuit applications", Applied Physics Letters, vol. 85, no. 19, pp. 4451-4453, 2004.

[7] V. Pleskachev and I. Vendik, "Tunable microwave filters based on ferroelectric capacitors", in 15th International Conference on Microwaves, Radar and Wireless Communications2004, pp. 1039-1043.

[8] E. Marsan, J. Gauthier, M. Chaker, and K. Wu, "Tunable microwave device: status and perspective", in IEEE-NEWCAS Conference2005, pp. 279-282.

[9] A. Tombak, J. P. Maria, F. Ayguavives, Zhang Jin, G. T. Stauf, A. I. Kingon, and A. Mortazawi, "Tunable barium strontium titanate thin film capacitors for RF and microwave applications", Microwave and Wireless Components Letters, vol. 12, no. 1, pp. 3-5, 2002.

[10] W. Sichak and H. Augenblick, "Tunable Waveguide Filters", Proceedings of the IRE, vol. 39, no. 9, pp. 1055-1059, Sep. 1951.

[11] M.H.N. Potok, "Capacitive-iris-type mechanically tunable waveguide filters for the Xband", Proceedings of the IEE Part B: Electronic and Communication Engineering, vol. 109, no. 48, p. 505, Nov. 1962.

[12] C. Nelson, "Ferrite-Tunable Microwave Cavities and the Introduction of a New Reflectionless, Tunable Microwave Filter", Proceedings of the IRE, vol. 44, no. 10, pp. 1449-1455, Oct. 1956.

[13] P.S. Carter, "Magnetically-Tunable Microwave Filters Using Single-Crystal Yttrium-Iron-Garnet Resonators", IEEE Transactions on Microwave Theory and Techniques, vol. 9, no. 3, pp. 252-260, May. 1961.

[14] J. Uher, and J. R. Hofer, "Tunable microwave and milimeter-wave bandpass filters", IEEE Trans. Microwave Theory Tech., vol 39, April 1991, pp. 643-653.

[15] G. L. Matthaei, E. Young, and E. M. T. Jones, "Microwave Filters, Impedance-Matching Networks, and Coupling Structures", Norwood, MA: Artech House, 1980

[16] R. W. deGreese, "Low-loss gyromagnetic coupling through single crystal garnets", J. Appl. Physics, vol. 30, pp. 1555-1559, 1958.

[17] W. J. Keane, "YIG filters aid wide open receivers", Microwave J., vol. 17, no. 8, Sept. 1980.

[18] P. S. Carter, "Equivalent circuit of orthogonal-loop-coupled magnetic resonance filters and bandwidth narrowing due to coupling resonance", IEEE Trans. Microwave Theory Tech., vol 18, Feb. 1970, pp. 100-105.

[19] R. F. Fjerstad, "Some design considerations and realizations of iris-coupled YIG-tuned filters in the 12-40 GHz region", IEEE Trans. Microwave Theory Tech.,vol 18, Apr. 1970, pp. 205-212.

[20] H. Tanbakuchi et al, "Magnetically tunable osillators and filters", IEEE Trans. Magn., vol 25, Sept. 1989, pp. 3248-3253.

[21] Advanced Design System (ADS). Agilent Technologies web site: http://www.home.agilent.com/agilent/product.jspx?cc=SG&lc=eng&ckey=1297113&nid=-34346.0.00&id=1297113.

Chapter II

Basic concepts and Theories of filters

II.1. Introduction

An electric filter is a network that transforms an input signal in some specific ways to yield a desirable output signal. Considered in frequency domains, a filter is a frequency-selective circuit which passes signals of desirable frequencies and blocks unwanted signals of other frequencies.

Filters are indispensable components in a huge variety of electric systems that explore the usage of frequency spectrum, including mobile communications, satellite communications, radar, navigation, sensing and other systems [1][2]. With the advancement of these systems, the finite electromagnetic spectrum must accommodate more and more systems. Thus, the limited frequency resources have to be divided, cared for, and treated with respect. RF signals of each system should be confined within the assigned spectral range. Filters are widely employed to select or confine RF signals within the spectral limits.

This section describes basic concepts and theories that form the foundation for design of general RF/microwave filters.

II.2. Fundamentals

II.2.1 Electromagnetic spectrum

The electromagnetic spectrum is represented by the range of all frequencies of electromagnetic radiation (EMR). The electromagnetic radiation is a form of energy that travels and spread out as it goes; it is sometimes referred to as wave-like behavior.

Microwave frequencies are wavelengths located between 300 MHz and 300 GHz of the electromagnetic spectrum, they range from one millimeter to one meter and it also falls under ultra high frequency (UHF) to super high frequency (SHF) of the radio-wave spectrum.

II.2.2 Basic filters

Radio frequency (RF) and microwave filters are designed to operate on frequencies ranging from megahertz to gigahertz. Basic functionalities includes allowing signal to pass through within passband frequency and attenuates signal in the stopband frequency. The four general filters are lowpass, highpass, bandpass and bandstop responses [3].

II.2.2.1 Low-Pass Filter (LPF)

A low-pass filter passes low frequency signals, and rejects signals at frequencies above the filter's cutoff frequency(f_C).

II.2.2.2 High-Pass Filter (HPF)

The opposite of the low-pass is the high-pass filter, which rejects signals below its cutoff frequency(f_C).

II.2.2.3 Band-Pass Filter (BPF)

A band pass filter allows signals with a range of frequencies($f_{Clow,}f_{Cup}$). (passband) to pass through and attenuates signals with frequencies outside this range.

II.2.2.4 Band-Stop Filter (BSF)

A filter with effectively the opposite function of the band-pass is the band-reject or notch filter.

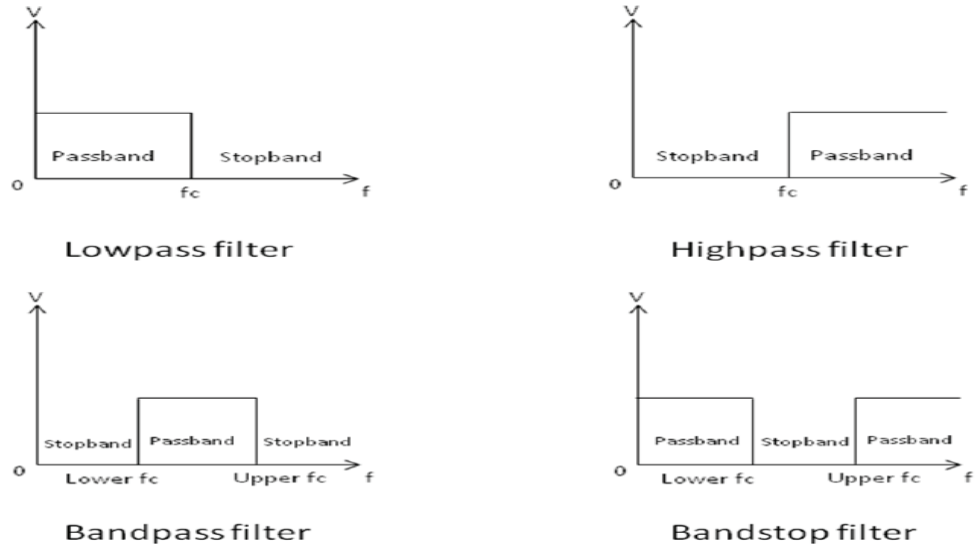

Figure II.1: Basic filters topologies.

II.2.3 Filter Characteristics

Filter characteristics are comprises of butterworth, elliptic and chebyshev. Butterworth filter have maximum flat magnitude response in the passband with no ripple, but exhibits a low rate of attenuation. Elliptic have sharp cut-off frequency with ripples in passband and stopband, however its designs are complicated. Chebyshev have a better rate of attenuation as compared to butterworth, and a sharp transition between passband and stopband produces small absolute errors and faster execution speed. Chebyshev type 1 filter allows ripple in the passband and Chebyshev type 2 filters allows ripple in the stopband [4].

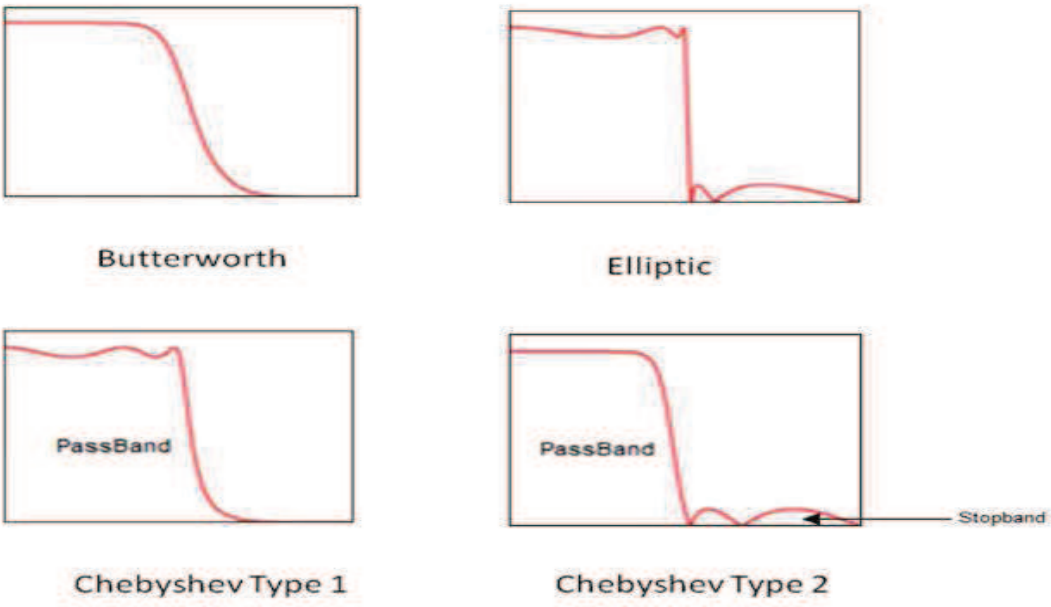

Figure II.2: Filter characteristics.

II.2.4 Terms used in filters

II.2.4.1 Transfer functions

The transfer function of a two-port filter network is a mathematical description of network response characteristics, namely, a mathematical expression of S_{21}. On many occasions, an amplitude-squared transfer function for a lossless passive filter network is defined as:

$$|S_{21}(j\Omega)|^2 = \frac{1}{1 + \varepsilon^2 F_n^2(\Omega)} \quad \text{(II. 1)}$$

Where ε is a ripple constant, $F_n(\Omega)$ represents a filtering or characteristic function, and Ω is a frequency variable.

II.2.4.2 Insertion loss

For a given transfer function the insertion loss response of the filter, following the conventional definition in Eq. (II.1), can be computed by:

$$L_A(\Omega) = 10log\frac{1}{|S_{21}(j\Omega)|^2}dB \quad \text{(II. 2)}$$

II.2.4.3 Return loss

Since $|S11|^2 + |S21|^2 = 1$ for a lossless passive two-port network, the return loss response of the filter can be found using Eq. (II.3):

$$L_R(\Omega) = 10log\lfloor 1 - |S_{21}(j\Omega)|^2 \rfloor dB \quad \text{(II. 3)}$$

II.2.4.4 Phase

If a rational transfer function is available, the phase response of the filter can be found as:

$$\emptyset_{21}(\Omega) = ArgS_{21}(j\Omega) \quad \text{(II. 4)}$$

II.2.4.5 Group-delay

The group-delay response of this network can then be calculated by:

$$\tau_d(\Omega) = -\frac{d\emptyset_{21}(\Omega)}{d\Omega} \quad \text{(II. 5)}$$

Where $\emptyset_{21}(\Omega)$ is in radians and Ω is in rad/s.

II.3. Network analysis

Filter networks are essential building elements in many areas of RF/microwave engineering. Such networks are used to select/reject or separate/combine signals at different frequencies in a host of RF/microwave systems and equipments. Although the physical realization of filters at RF/microwave frequencies may vary, the circuit network topology is common to all.

At microwave frequencies, the use of voltmeters and ammeters for the direct measurement of voltages and currents do not exist. For this reason, voltage and current, as a measure of the level of electrical excitation of a network, do not play a primary role at microwave frequencies. On the other hand, it is useful to be able to describe the operation of a microwave network, such as a filter, in terms of voltages, currents, and impedances in order to make optimum use of low-frequency network concepts [5].

It is important to describe various network concepts and provide equations that are useful for the analysis of filter networks.

II.3.1 Network variables

Most RF/microwave filters and filter components can be represented by a two-port network, as shown in Figure (II.3), where V_1, V_2 and I_1, I_2 are the voltage and current variables at ports 1 and 2, respectively, Z_{01} and Z_{02} are the terminal impedances, and E_s is the source or generator voltage.

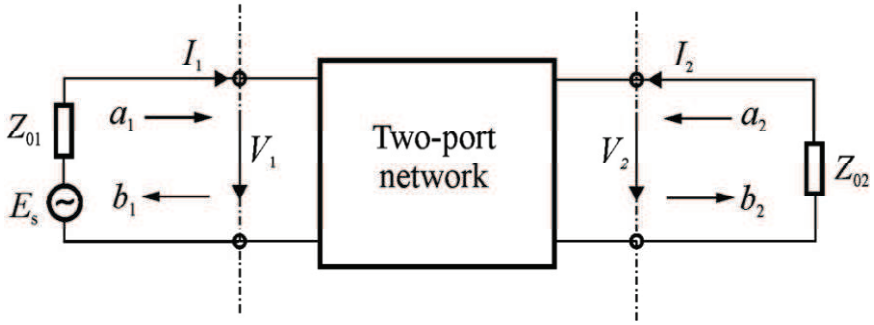

Figure II.3: Two-port network.

We can then make the following transformations:

$$v_1(t) = |V_1|\cos(wt + \emptyset) = Re\left(|V_1|e^{j(wt+\emptyset)}\right) = Re\left(V_1 e^{jwt}\right) \qquad \text{(II. 6)}$$

We can identify the complex amplitude V_1 defined by:

$$V_1 = |V_1|e^{j\emptyset} \qquad \text{(II. 7)}$$

Because it is difficult to measure the voltage and the current at microwave frequencies, the wave variables a_1, b_1 and a_2, b_2 are introduced, with *a* indicating the incident waves and *b* the reflected waves. The relationships between the wave variables and the voltage and current variables are defined as:

$$\begin{aligned} V_n &= \sqrt{Z_{on}}(a_n + b_n) \\ I_n &= \frac{1}{\sqrt{Z_{on}}}(a_n - b_n) \end{aligned} \quad for\ n = 1\ and\ 2 \qquad (II.8)$$

Or

$$\begin{aligned} a_n &= \frac{1}{2}\left(\frac{V_n}{\sqrt{Z_{on}}} + \sqrt{Z_{on}} I_n\right) \\ b_n &= \frac{1}{2}\left(\frac{V_n}{\sqrt{Z_{on}}} - \sqrt{Z_{on}} I_n\right) \end{aligned} \quad for\ n = 1\ and\ 2 \qquad (II.9)$$

The above definitions guarantee that the power at port *n* is:

$$P_n = \frac{1}{2} Re(V_n \cdot I_n^*) = \frac{1}{2}(a_n a_n^* - b_n b_n^*) \qquad (II.10)$$

It can be recognized that $a_n a_n^*/2$ is the incident wave power and $b_n b_n^*/2$ is the reflected wave power at port *n*.

II.3.2 Scattering parameters

The scattering or *S* parameters of a two-port network are defined in terms of the wave variables as [6]:

$$\begin{aligned} S_{11} &= \frac{b_1}{a_1}\Big|_{a_2=0} \quad S_{12} = \frac{b_1}{a_2}\Big|_{a_1=0} \\ S_{21} &= \frac{b_2}{a_1}\Big|_{a_2=0} \quad S_{22} = \frac{b_2}{a_2}\Big|_{a_1=0} \end{aligned} \qquad (II.11)$$

Where a_n = 0 implies a perfect impedance match (no reflection from terminal impedance) at port *n*. These definitions may be written as:

$$\begin{bmatrix} b_1 \\ b_2 \end{bmatrix} = \begin{bmatrix} S_{11} & S_{12} \\ S_{21} & S_{22} \end{bmatrix} \cdot \begin{bmatrix} a_1 \\ a_2 \end{bmatrix} \qquad (II.12)$$

The parameters S_{11} and S_{22} are also called the reflection coefficients, whereas S_{12} and S_{21} are the transmission coefficients. These are the parameters directly measurable at microwave frequencies. The *S* parameters are, in general, complex, and it is convenient to express them in terms of amplitudes and phases, that is, $S_{mn} = |S_{mn}| e^{j\varphi mn}$ for m, n = 1, 2. Often their amplitudes are given in decibels (dB), which are defined as:

$$20log\ |S_{mn}|\ dB \quad m,n\ =\ 1,2 \tag{II. 13}$$

For filter characterization, we may define two parameters:

$$L_A = -20log|S_{mn}|\ dB\ m,n = 1{,}2\ (m \neq n) \tag{II. 14}$$

$$L_R = 20log|S_{nn}|\ dB\ n = 1{,}2 \tag{II. 15}$$

Where L_A denotes the insertion loss between ports *n* and *m* and L_R represents the return loss at port *n.* Instead of using the return loss, the voltage-standing wave ratio *VSWR* may be used. The definition of *VSWR* is:

$$VSWR = \frac{1 + |S_{nn}|}{1 - |S_{nn}|} \tag{II. 16}$$

Whenever a signal is transmitted through a frequency-selective network, such as a filter, some delay is introduced into the output signal in relation to the input signal. There are two other parameters that play a role in characterizing filter performance related to this delay. The first one is the phase delay, defined by:

$$\tau_p = \frac{\emptyset_{21}}{w} s \tag{II. 17}$$

Where $\emptyset_{21}$ is in radians and ω is in rad/s. Port 1 is the input port and port 2 is the output port.

The phase delay is actually the time delay for a steady sinusoidal signal and is not necessarily the true signal delay, because a steady sinusoidal signal does not carry information; sometimes, it is also referred to as the carrier delay. The more important parameter is the group delay, defined by:

$$\tau_d = \frac{d\emptyset_{21}}{dw} s \tag{II. 18}$$

This represents the true signal (baseband signal) delay and is also referred to as the envelope delay. In network analysis or synthesis, it may be desirable to express the reflection parameter S_{11} in terms of the terminal impedance Z_{01} and the so-called input impedance $Z_{in1} = V_1/I_1$, which is the impedance looking into port 1 of the network. Such an expression can be deduced by evaluating S_{11} in Eq. (II.11) in terms of the voltage and current variables using the relationships defined in Eq. (II.9). This gives:

$$S_{11} = \left.\frac{b_1}{a_1}\right|_{a_2=0} = \frac{V_1/\sqrt{Z_{01}} - \sqrt{Z_{01}}I_1}{V_1/\sqrt{Z_{01}} + \sqrt{Z_{01}}I_1} \tag{II. 19}$$

Replacing V_1 by $Z_{in1}I_1$ results in the desired expression:

$$S_{11} = \frac{Z_{in1} - Z_{01}}{Z_{in1} + Z_{01}} \tag{II. 20}$$

Similarly, we can have:

$$S_{22} = \frac{Z_{in2} - Z_{02}}{Z_{in2} + Z_{02}} \tag{II. 21}$$

Where $Z_{in2} = V_2/I_2$ is the input impedance looking into port 2 of the network. Equations (II.20) and (II.21) indicate the impedance matching of the network with respect to its terminal impedances.

The *S* parameters have several properties that are useful for network analysis. For a reciprocal network we have $S_{12} = S_{21}$. If the network is symmetrical, an addition property, $S_{11} = S_{22}$, holds. Hence, the symmetrical network is also reciprocal. For a lossless passive network, the transmitting power and the reflected power must equal to the total incident power. The mathematical statements of this power conservation condition are:

$$\begin{matrix} S_{21}S_{21}^* + S_{11}S_{11}^* = 1 \\ S_{12}S_{12}^* + S_{22}S_{22}^* = 1 \end{matrix} \quad or \quad \begin{matrix} |S_{21}|^2 + |S_{11}|^2 = 1 \\ |S_{12}|^2 + |S_{22}|^2 = 1 \end{matrix} \tag{II. 22}$$

II.3.3 *ABCD* parameters

The *ABCD* parameters of a two-port network are given by:

$$A = \left.\frac{V_1}{V_2}\right|_{I_{2=0}} \quad B = \left.\frac{V_1}{-I_2}\right|_{V_{2=0}}$$

$$C = \left.\frac{I_1}{V_2}\right|_{I_{2=0}} \quad D = \left.\frac{I_1}{-I_2}\right|_{V_{2=0}} \tag{II. 23}$$

These parameters are actually defined in a set of linear equations in matrix notation. Where the matrix comprised of the *ABCD* parameters is called the *ABCD* matrix. Sometimes, it may also be referred to as the transfer or chain matrix.

$$\begin{bmatrix} V_1 \\ I_1 \end{bmatrix} = \begin{bmatrix} A & B \\ C & D \end{bmatrix} \cdot \begin{bmatrix} V_2 \\ I_2 \end{bmatrix} \tag{II. 24}$$

	ABCD	Y	Z
S_{11}	$\frac{A+B/Z_0-CZ_0-D}{A+B/Z_0+CZ_0+D}$	$\frac{(Y_0-Y_{11})(Y_0+Y_{22})+Y_{12}Y_{21}}{(Y_0+Y_{11})(Y_0+Y_{22})-Y_{12}Y_{21}}$	$\frac{(Z_{11}-Z_0)(Z_{22}+Z_0)-Z_{12}Z_{21}}{(Z_{11}+Z_0)(Z_{22}+Z_0)-Z_{12}Z_{21}}$
S_{12}	$\frac{2(AD-BC)}{A+B/Z_0+CZ_0+D}$	$\frac{-2Y_{12}Y_0}{(Y_0+Y_{11})(Y_0+Y_{22})-Y_{12}Y_{21}}$	$\frac{2Z_{12}Z_0}{(Z_{11}+Z_0)(Z_{22}+Z_0)-Z_{12}Z_{21}}$
S_{21}	$\frac{2}{A+B/Z_0+CZ_0+D}$	$\frac{-2Y_{12}Y_0}{(Y_0+Y_{11})(Y_0+Y_{22})-Y_{12}Y_{21}}$	$\frac{2Z_{12}Z_0}{(Z_{11}+Z_0)(Z_{22}+Z_0)-Z_{12}Z_{21}}$
S_{22}	$\frac{-A+B/Z_0-CZ_0+D}{A+B/Z_0+CZ_0+D}$	$\frac{(Y_0+Y_{11})(Y_0-Y_{22})+Y_{12}Y_{21}}{(Y_0+Y_{11})(Y_0+Y_{22})-Y_{12}Y_{21}}$	$\frac{(Z_{11}+Z_0)(Z_{22}-Z_0)-Z_{12}Z_{21}}{(Z_{11}+Z_0)(Z_{22}+Z_0)-Z_{12}Z_{21}}$

Table II.1: *S* Parameters in Terms of *ABCD*, *Y*, and *Z* Parameters.

II.4. Microstrip filters

The general structure of a microstrip is illustrated in Figure II.4. A conducting strip (microstrip line) with a width *W* and a thickness *t* is on the top of a dielectric substrate that has a relative dielectric constant ε_r and a thickness *h*, and the bottom of the substrate is a ground (conducting) plane.

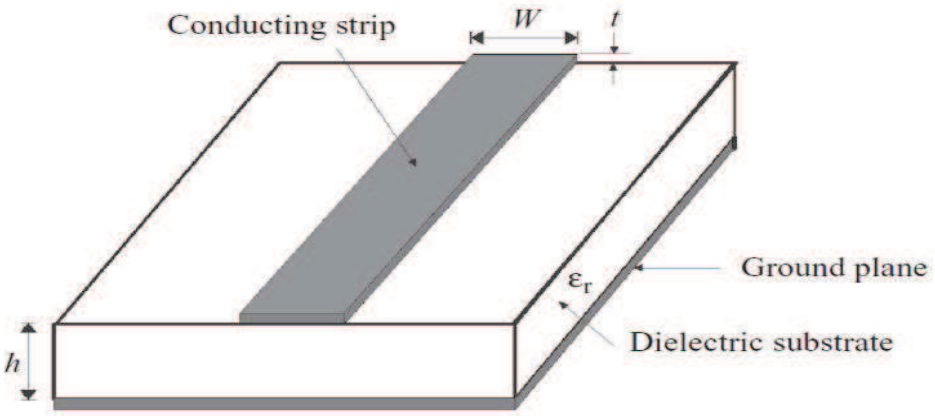

Figure II.4: General microstrip structure.

II.4.1 Microstrip Components

Microstrip components, which are often encountered in microstrip filter designs, may include lumped inductors and capacitors, quasi-lumped elements (namely, short-line sections and stubs), and resonators. In most cases, the resonators are the distributed elements, such as quarter-wavelength and half-wavelength line resonators. The choice of individual components may mainly depend on the types of filters, the fabrication techniques, the acceptable losses or *Q* factors, the power handling, and the operating frequency.

II.4.1.1 Resonators

A microstrip resonator is any structure that is able to contain at least one oscillating electromagnetic field. There are numerous forms of microstrip resonator. In general, microstrip resonators for filter designs may be classified as lumped-element or quasi-lumped element resonators and distributed-line resonators or patch resonators. Some typical configurations of these resonators are illustrated in figure II.5.

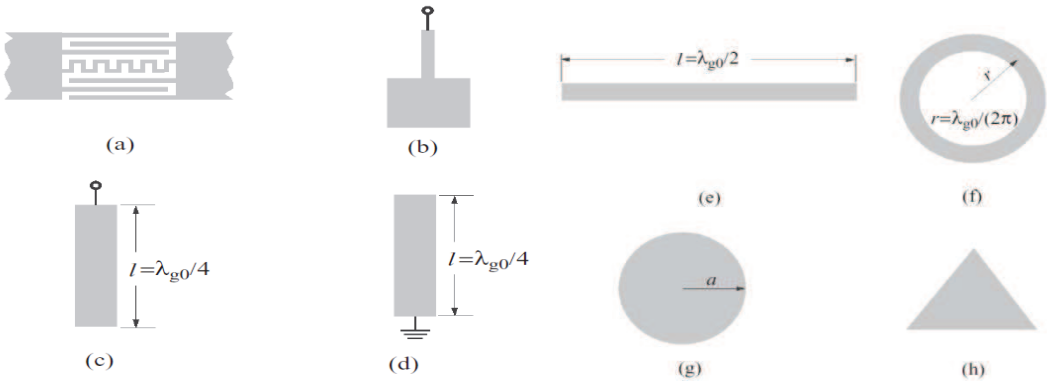

Figure II.5: Some typical microstrip resonators: (**a**) lumped-element resonator; (**b**) quasi-lumped element resonator; (**c**) $\lambda g_0/4$ line resonator (shunt-series -resonance); (**d**) $\lambda g0/4$ line resonator (shunt-parallel resonance); (**e**) $\lambda g_0/2$ line resonator; (**f**) ring resonator; (**g**) circular patch resonator; (**h**) triangular patch resonator.

In the past, much research was conducted and plenty of resonators were proposed. Among the proposed resonators, some were introduced originally for single passband filter applications. Hairpin and open loop resonators are typical examples with the length of half wavelength. These resonators are modified by using stub at the line center to improve the selectivity [6][7].

To reduce circuit size, a compact microstrip resonant cell was proposed and utilized in both lowpass and bandpass filters [8][9]. Besides these single mode resonators, some research focused on dual mode resonators were also introduced for designing wideband filters [10][11]. Moreover, multiple mode resonators were also introduced for designing wideband filters [12][13].

Each of the above resonators primaly operates at one frequency and is only suitable for single passband filters applications. As for dual band filter designs using above resonators, two sets of resonators with different resonant frequencies are required, leading to complicated filter configurations [14][15].

To solve this problem patch resonators was presented, they support different resonant modes, in which the applied energy is split. Each mode resonates at a particular frequency, where the lowest frequency is from the first mode, named fundamental or dominant, and is defined by the characteristics of the resonator. For frequencies higher than the fundamental mode one, there are other resonant modes, which generate spurious bands in the filter response.

When the resonator has a regular geometry, two modes may have the same resonance frequency, despite their different EM field patterns. These modes are called degenerate modes and can occur at several frequencies in the same resonator. In patch resonators, the fundamental modes are degenerate, one presenting an even and the other an odd EM field pattern.

II.4.1.2 Patch resonators

Patch resonators are of interest for the design of microstrip filters, in order to increase the power-handling capability [16][17]. An associated advantage of microstrip patch resonators is their lower conductor losses as compared with narrow microstrip line resonators. Although patch resonators tend to have a stronger radiation, they are normally enclosed in a metal housing for filter applications so that the radiation loss can be minimized. Patch resonators usually are a larger size; however, this would not be a problem for the application in which the power handling or low loss has a higher priority. The size may not be an issue at all for the filters operating at very high frequencies. Depending on the applications, patches may take different shapes, such as circular in Figure II.5g and triangular in Figure II.5h.

These microstrip patch resonators can be analyzed as waveguide cavities with magnetic walls on the sides. The fields within the cavities can be expanded by the TM^{z}_{nm0} modes, where z is perpendicular to the ground plane. For instance, the fields for each of the cavity modes in a circular microstrip patch (disk) resonator may be expressed in a cylindrical coordinate system (φ, r, z) [18] as:

$$E_z = A_{nm} J_n(K_{nm} r/a) \cos(n\emptyset) \quad \text{(II. 25)}$$

$$H_r = \frac{j}{w\mu}\left(\frac{1}{r}\frac{\partial E_z}{\partial \emptyset}\right) = -\frac{j}{w\mu}\frac{n}{r} A_{nm} J_n(K_{nm} r/a) \sin(n\emptyset) \quad \text{(II. 26)}$$

$$H_\emptyset = \frac{-j}{w\mu}\left(\frac{\partial E_z}{\partial r}\right) = \frac{-j}{w\mu}\frac{K_{nm}}{a} A_{nm} J'_n(K_{nm} r/a) \cos(n\emptyset) \quad \text{(II. 27)}$$

$$E_\emptyset = E_r = E_z = 0 \quad \text{(II. 28)}$$

Where A_{nm} is a reference amplitude, J_n is the Bessel function of the first kind of order n, J'_n is the derivative of J_n, and K_{nm} is the mth zero of J'_n. for m=1 the zeros are:

$$K_{n1} = \begin{cases} 3.83171 & n = 0 \\ 1.84118 & n = 1 \\ 3.05424 & n = 2 \\ 4.20119 & n = 3 \end{cases}$$

The resonant frequency of these modes are given by:

$$f_{nm0} = \frac{K_{nm}c}{2\pi a_e\sqrt{\varepsilon_r}} \quad for \quad a_e = a\sqrt{1 + \frac{2h}{\pi a}\left[ln\left(\frac{\pi a}{2h}\right) + 1.7726\right]} \qquad \text{(II. 29)}$$

Where a_e is an effective radius that takes into account the fringing fields ($a_e \approx a$ for $h \ll a$) [19]. Thus, the lowest order or fundamental mode is the TM^z_{110} mode.

A circular patch operating at this mode is a dual-mode resonator as well. Another interesting mode is the TM^z_{010} mode, which does not have current along the edge. This mode has been used to design superconducting filters having higher power-handling capability [20].

II.4.2 Planar filters

Planar filters are basically realized on two metal layers with a dielectric substrate in between, as shown in Figure II.6a. The main substrate characteristics that determine the dimensions of the filter are the thickness *h* of the dielectric layer, its dielectric constant or relative permittivity *εr*, and the thickness *t* of the metal layers. Other parameters such as the dielectric loss tangent tan (*δ*) and the metal conductivity *ζ* affect the filter performance, in terms of insertion loss.

Planar filters are typically fabricated on the top metal layer, as illustrated in Figure II.6b, and sometimes, metal vias are used to make a connection to the ground plane. Some topologies have also electromagnetic band-gap structures (EBG) etched in the ground plane to add a rejection characteristic to the filter response.

Note: Patch filters are fabricated in the same planar technology as the microstrip filters, but employ, instead of strips, resonators.

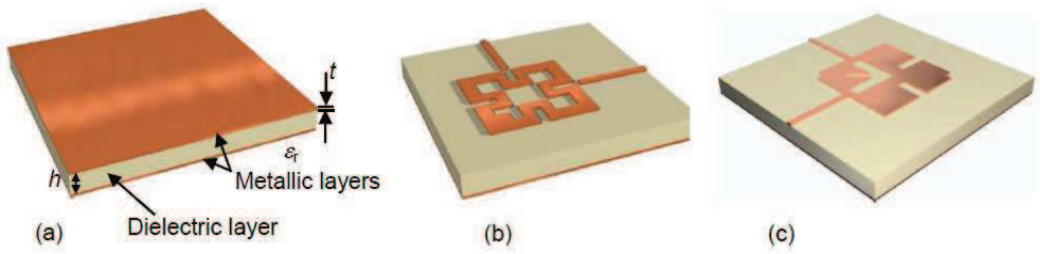

Figure II.6: (a) Planar filters substrate; (b) Example of a fabricated microstrip filter; (c) Example of a fabricated patch filter.

Planar filters can be classified into the one-dimensional or the two-dimensional filters, depending on the type of resonator used, as explained in the following.

II.4.3 The one-dimensional planar bandpass filters

The one-dimensional planar filters are those with resonators based on microstrip transmission line. The more conventional ones are the stepped impedance, coupled lines by the edge or in parallel, hairpin, interdigital and combline. The stepped impedance filters are mostly used in low-pass filters while the others are used in the bandpass filters which will be briefly presented in the following sections.

II.4.3.1 End-Coupled Half-Wavelength Resonator Filters

The general configuration of an end-coupled microstrip bandpass filter is illustrated in Figure II.7, where each open-end microstrip resonator is approximately a half guided wavelength long at the midband frequency f_0 of the bandpass filter. The coupling from one resonator to the other is through the gap between the two adjacent open ends and, hence, is capacitive [21].

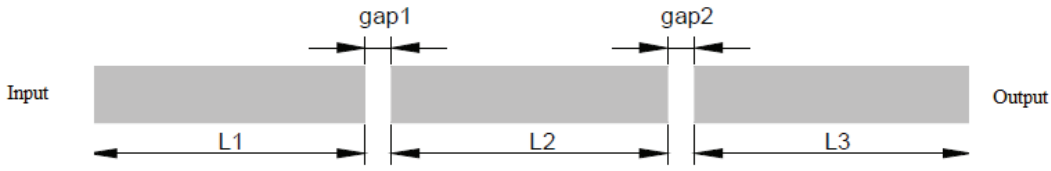

Figure II.7: Layout of a three-pole end-coupled microstrip bandpass filter.

II.4.3.2 Parallel-Coupled Half-Wavelength Resonator Filters

Figure II.8 illustrates a general structure of parallel-coupled (or edge-coupled) microstrip bandpass filters, which use half-wavelength line resonators. They are positioned so that adjacent resonators are parallel to each other along one-half of their length. This parallel arrangement gives relatively large coupling for a given spacing

between resonators and, thus, this filter structure is particularly convenient for constructing filters having a wider bandwidth as compared to the structure for the end-coupled microstrip filters described in the last section.

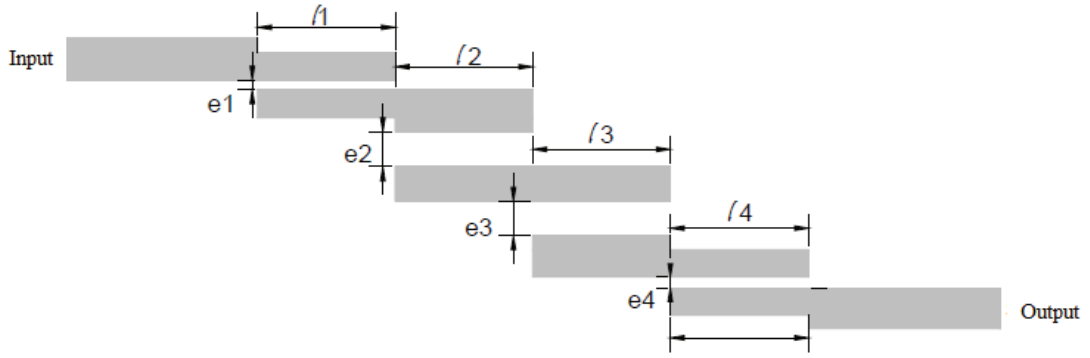

Figure II.8: Layout of four-pole parallel (edge)-coupled microstrip bandpass filter.

II.4.3.3 Hairpin-Line Bandpass Filters

Hairpin-line bandpass filters are compact structures. They may conceptually be obtained by folding the resonators of parallel-coupled, half-wavelength resonator filters, which are discussed in the previous section, into a "U" shape. This type of "U-shape" resonator is the so-called hairpin resonator. Consequently, the same design equations for the parallel-coupled, half-wavelength resonator filters may be used [22].

However, to fold the resonators, it is necessary to take into account the reduction of the coupled-line lengths, which reduces the coupling between resonators. If the two arms of each hairpin resonator are also closely spaced, they function as a pair of coupled lines, which can also have an effect on the coupling.

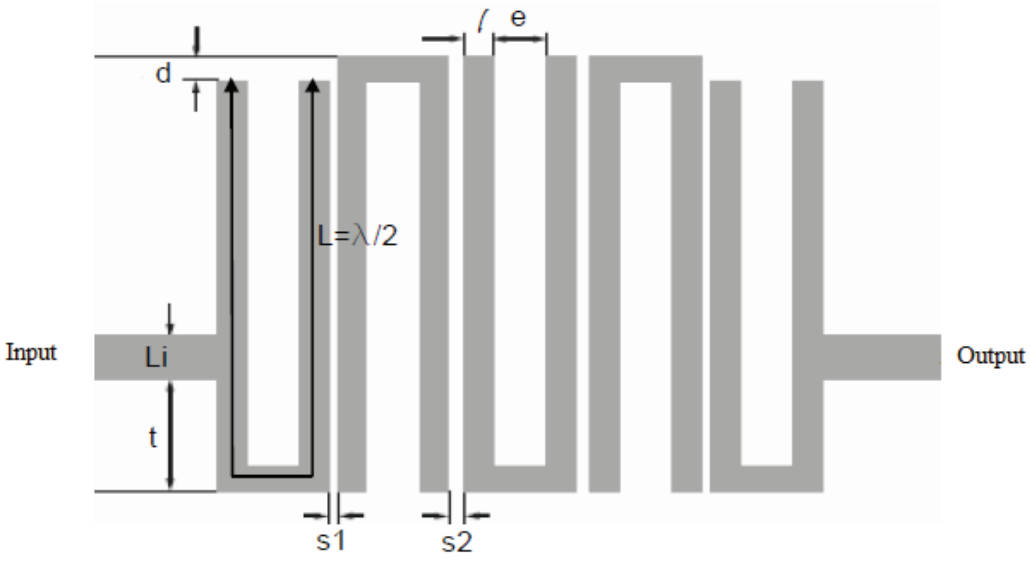

Figure II.9: Layout of a five-pole hairpin filter.

II.4.3.4 Interdigital Bandpass Filters

Figure II.10 shows a type of interdigital bandpass filter commonly used for microstrip implementation. The filter configuration, as shown, consists of an array of n TEM-mode or quasi-TEM-mode transmission-line resonators, each of which has an electrical length of 90◦ at the midband frequency and is short-circuited at one end and open-circuited at the other end with alternative orientation. In general, the physical dimensions of the line elements or the resonators can be different, as indicated by the lengths $l1, l2 \ldots ln$ and the widths $W1, W2 \ldots Wn$. Coupling is achieved by the fields fringing between adjacent resonators separated by spacing $si,i+1$ for $i = 1 \ldots n - 1$.

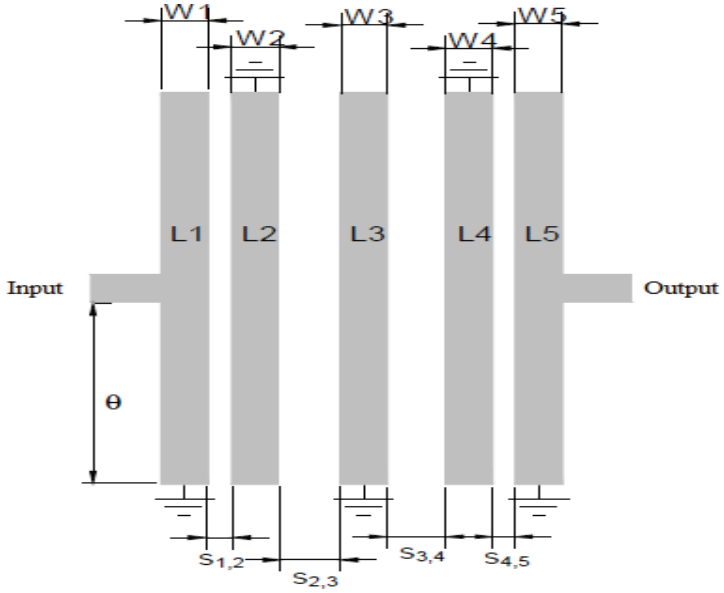

Figure II.10: Configuration of a five pole interdigital bandpass filter.

II.4.3.5 Combline Filters

As shown in Figure II.11, the combline bandpass filter is comprised of an array of coupled resonators. The resonators consist of line elements 1 to n, which are short-circuited at one end, with a lumped capacitance CLi loaded between the other end of each resonator line element and ground. The input and output of filter are through coupled-line elements 0 and $n + 1$, which are not resonators.

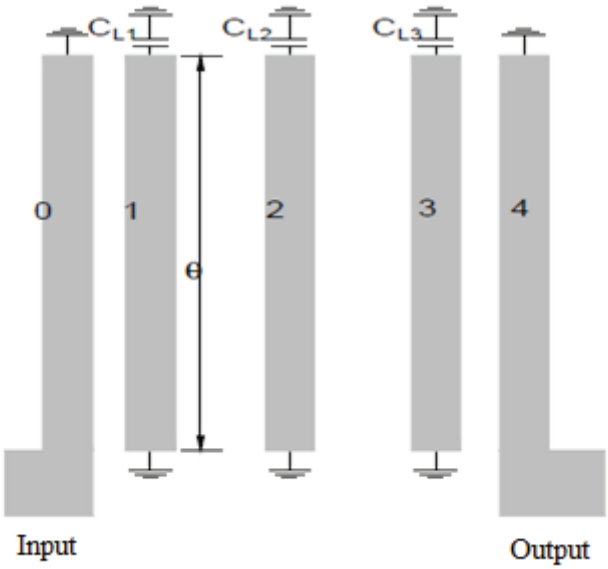

Figure II.11: Layout of a five-pole microstrip interdigital bandpass filter.

II.4.3.6 Meander loop filters

Meander loop filters [22] are composed of ring resonators, whose perimeter is increased by the inclusion of recesses in microstrip used, as shown in Figure 8.

This type of filter works as a resonator in a rectangular or circular ring with elliptic response and is characterized by its small size. Because the current along the resonator go a longer way than a ring would travel common, the frequency of the resonator undergoes reduction and, consequently, the filter built occupies less area than a ring resonator built with the same frequency filter resonance .

The concept of increasing the path through which current flows in a given frequency is of particular importance and will be largely used for the development of design methodology presented in this paper patch filters.

II.4.4 Two dimensional planar bandpass filters

II.4.4.1 Patch filters

The approach to the study of patch filters differs from the filters presented in the previous sections. In the one dimensional planar filters, the study was based on the characteristics of the transmission lines used as resonators and the coupling between them.

The filter uses the conventional microstrip filter as part of the patch resonator leaving only microstrip interfaces for the input and the output.

The analysis of fields in these resonators in the form of geometries is essential for understanding the functionality of patch filters.

The planar resonators can be treated as a cavity waveguide which upper and lower layers are perfect electric walls, surrounded laterally by perfect magnetic walls [23], [24], [25], as illustrated in Figure II.4a. Thus, it is considered that the EM fields in the resonator are Transverse Magnetic perpendicular to the ground plane (TMZ) whose z-axis formulation is well known and has been used for the analysis of the fields.

Every so resonates at a particular frequency, in which there is minimal attenuation. The first mode, called essential or dominant, resonates at a lower frequency permitted by the characteristics of the resonator. Above this, there are other resonant modes that generate spurious bands crossing the frequency response of the filter.

There are cases where two modes have the same resonant frequency, although their EM fields have different distributions. These modes are called degenerate and are a major focus of this work, being widely used for determining characteristics of dual-mode filters [26].

Particularly in TMZ mode, the entire magnetic field in the transverse plane is not having magnetic component in the direction of propagation, only electrical component. Thus, any analysis will be based on the distribution of the electric field on the axis of propagation z (Ez).

As the resonator can support multiple resonant modes, the indices 'm', 'n' and 'p' are used to complete the description of the field distribution in each mode ($TM^{z}_{m,n,p}$) .

This work was developed based on patch resonators a circular geometry. This resonator, besides the regular geometry, have well-defined symmetry axis and therefore support degenerate resonant modes that are of interest to design dual-mode filter.

The 3D planar EM simulator Momentum / Advanced Design System (ADS) [27], the Agilent Technologies, was used to generate the frequency response curves of this resonator.

II.4.4.2 Circular patch resonator

A circular patch resonator is illustrated in Figure II.12, in polar coordinates.

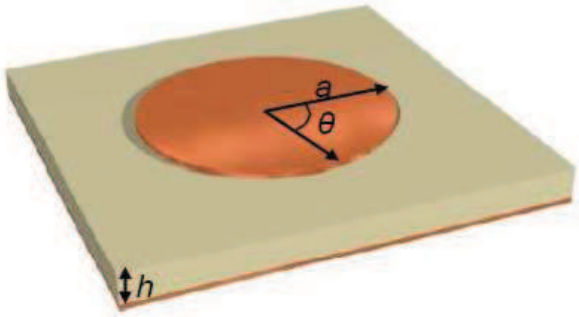

Figure II.12: Circular patch resonator with radius *a*.

The electric field distribution along this type of resonator is given by eq. (II.30) [28]. The field distribution is only related to the resonator physical dimensions and the resonant mode indices *p* and *q*. The modal frequencies depend on those indices and also on the substrate characteristics, calculated from eq. (II.31) [29].

$$E_{z\,circle}(a,\theta) = AJ\left(P,\frac{\alpha_{p,q}r}{a}\right)\cos(p\theta) \qquad \text{(II. 30)}$$

$$freq\ circle(p,q) = \frac{\alpha_{p,q}c}{2\pi r_{ef}\sqrt{\varepsilon_r\mu_r}} \qquad \text{(II. 31)}$$

Where:

J (*p*, *r*) is the Bessel function of first kind and order *p*;

r is the radial variation of the radius from 0 to *a*;

a is the radius of the circular resonator*;*

θ is the angular variation of the radius from 0 to 2π.

p and *q* are the non-negative integer $TMz_{p,q,0}$ mode indices in θ and *r* directions, respectively, with $q \neq 0$;

$\alpha_{p,q}$ is the q^{th} zero of the derivative of the Bessel function of first kind and order *p*;

r_{ef} is the effective radius of the resonator:

For $p = 0$[30]:

$$r_{ef} = a\sqrt{1 + (2h/\pi a\varepsilon_r)\left[ln(a/2h) + \varepsilon_r\sqrt{2} + 1.7726 + (h/a)(0.268\varepsilon_r + 1.65)\right]} \qquad \text{(II. 32)}$$

For $p \neq 0$[31]:

$$r_{ef} = a\sqrt{1 + (2h/\pi a\varepsilon_r)[ln(\pi\, a/2h) + 1.7726]} \qquad \text{(II. 33)}$$

The frequency equation shows that the modal frequencies are directly related to the values of $\alpha_{p,q}$. The lowest values are $\alpha_{0,1} = 3.832$, $\alpha_{1,1} = 1.841$, and $\alpha_{2,1} = 3.054$,

therefore the fundamental mode is $TMz_{1,1,0}$, given by the lowest value $\alpha_{1,1}$. The degenerate modes are orthogonal to each other and can be calculated from (II.30) by simply rotating θ by 90^{o}.

II.5. Coupling matrix

To design microwave filters a basic understanding of coupling and coupling mechanisms is necessary. In this section, the coupling mechanisms in bandpass filters are investigated.

Modeling the circuit in matrix form is particularly useful because matrix operations can then be applied, such as inversion, similarity transformation, and partitioning. Such operations simplify the synthesis, reconfiguration of the topology, and performance simulation of complex circuits. Moreover the coupling matrix is able to include some of the real-world properties of the elements of the filter [32].

Each element in the matrix can be identified uniquely with an element in the finished microwave device. This enables us to account for the attributions of electrical characteristics of each element, such as the Q, values for each resonator, different dispersion characteristics for the various types of mainline coupling and cross-coupling within the filter. This is difficult or impossible to achieve with a polynomial representation of the filter's characteristics.

The synthesis optimization that considers the source/load-multimode couplings results in a coupling matrix with N+2 rows and N+2 columns, where N is the order of the filter. The first row denotes the source, the second row denotes the first resonant mode, the third row denotes the second resonant mode…, up to the penultimate row (N+1), which denotes the last resonant mode, and the last row (N+2), which denotes the load. The columns are related to each filter part: source, resonant modes, and load in an analogous manner [33]. For a third order filter (N=3), its general coupling matrix M is shown in eq. (II.34):

$$M_{3^{rd}order} = \begin{bmatrix} M_{SS} & M_{S1} & M_{S2} & M_{S3} & M_{SL} \\ M_{1S} & M_{11} & M_{12} & M_{13} & M_{1L} \\ M_{2S} & M_{21} & M_{22} & M_{23} & M_{2L} \\ M_{3S} & M_{31} & M_{32} & M_{33} & M_{3L} \\ M_{LS} & M_{L1} & M_{L2} & M_{L3} & M_{LL} \end{bmatrix} \quad \text{(II. 34)}$$

The matrix element placed across a row and a column represents the coupling between the filter parts corresponding to the row and column. All the coupling coefficients of the matrix are normalized, and thus, frequency-independent.

From the coupling matrix, one can obtain the theoretical curves of the reflection coefficient S_{11}, known as return loss (RL) and the transmission coefficient S_{21}, known as insertion loss (IL) as a function of the frequency. For that, the filter network is considered to be excited by a voltage source with internal impedance R_i and magnitude equal to unity, whereas the load terminal impedance is R_0. Using the kirchoff's voltage law, which states that the algebraic sum of the voltage drops around any closed path in a network is zero, one can obtain the loop current equations expressed in a matrix form and grouped in a vector [I] in eq. (II.35) [34].

$$[-jR + w'W + M][I] = [A][I] = -j[e] \quad \text{(II. 35)}$$

Where:

$j^2 = -1$;

[R] is a (N+2) × (N+2) matrix, in which only nonzero entries are $R_{11} = R_i$ and $R_{N+2,N+2} = R_0$, both normalized to 1 (the reference is 50 Ω);

[W] is a (N+2) × (N+2) identify matrix, with $W_{11} = W_{N+2,N+2} = 0$;

w' is the lowpass prototype normalized angular frequency given by eq. (II.36):

$$w' = \frac{w_c}{\Delta w}\left(\frac{w}{w_c} - \frac{w_c}{w}\right) \quad \text{(II. 36)}$$

Where:

w_c is the center angular frequency of the filter;

Δw is the bandwidth of the filter;

[M] is the coupling matrix;

[e] is a (1 × N) vector that represents the filter stimulus, in which only nonzero entry is $e_{11}=1$.

Finally, the scattering parameters curves are given by eq. (II.37) and (II.38) [33].

$$S_{21} = -2j[A^{-1}]_{N+2,1} \quad \text{(II. 37)}$$

$$S_{11} = 1 + 2j[A^{-1}]_{11} \quad \text{(II. 38)}$$

II.6. Coupling scheme

The couplings in a filter can also be expressed in a diagram form, called coupling scheme. The coupling scheme is a diagram where all the filter parts are represented as black nodes (resonant modes) and white nodes (source/load), and the coupling between them, as full- or dotted-lines symbolizing a direct coupling or an admittance inverter. One possible coupling scheme considering all couplings for the example of a 3rd-order filter is shown in Figure (II.13).

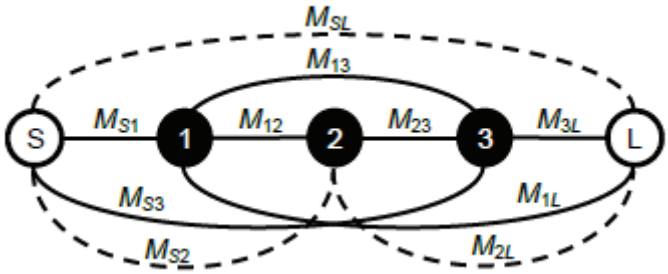

Figure II.13: coupling scheme of a 3rd order filter considering all possible couplings. Source and load are represented by white circles and resonators represented by black circles.

The maximum number of possible transmission zeroes (TZ) of a filter with source/load-multimode couplings is given by the existent path from the source to load. It can be determined by the order of the filter (N) minus the number of resonant modes of the shortest path between source and load. TZ = N means that there is a coupling between source and load and thus, $M_{SL} \neq 0$.

In multimode patch filters, an interpretation of the coupling scheme is necessary as the resonant modes are distributed along the same patch resonator and their equivalent electrical circuits are not obvious. Then, it is important to use powerful tools, such as 3D EM simulators in order to identify the field patterns of interest and better understand their couplings. Concerning configurable filters, a specific synthesis technique has not been carried out yet.

II.7. Conclusion

There is a very extensive literature on the microwave network theory addressing both the theoretical as well as practical aspects. It explains fundamental concepts of microwave circuits such as waveguides, impedance matching, *S*-parameters, filters and the design of microwave filters.

In this chapter, we gave an introduction to microwave network theory that forms the foundation for design of general RF/microwave filters.

An introduction to the planar technology used to design the proposed patch filter was explained, it consists of the one dimensional planar filters and the two dimensional planar filters with some examples.

We finished with some necessary equations for calculating the coupling matrix and provide the coupling scheme that models the filter behavior.

References

[1] G. L. Matthaei, L. Young and E. M. T. Jones, Microwave filters impedance-matching networks and coupling structures. Dedham, MA: Artech house, 1980.

[2] M. Makimoto, S. Yamashita, "Microwave resonators and filters for wireless communication: theory, design and application," New York: Springer, 2001.

[3] J. S. Hong, and M. J. Lancaster, Microwave filter for RF/Microwave application. New York: John Wiley & Sons, 2001.

[4] R. J. Cameron, C. M. Kudsia and R. R. Mansour, "Microwave filters for communication systems: fundamentals, design, and applications. Hobeken," New Jersey: John Wiley & Sons, 2007.

[5] I. C. Hunter, "Theory and design of microwave filters," New York: Artech House, 2001.

[6] J.-R. Lee, J.-H. Cho, and S.-W. Yun, "New compact bandpass filter using microstrip 4 resonators with open stub inverter," IEEE Microw. Guided Wave Lett., vol.10, no.12, pp.526-527, Dec.2000.

[7] L. Zhu and W. Menzel, "Compact microstrip bandpass filter with two transmission zeros using a stub-tapped half-wavelenght line resonator," IEEE Microw. Wireless Compon. Lett., vol.13, no.1, pp.18-18, Jan.2003.

[8] Q. Xue, K. M. Shum, and C. H. Chan, ""Novel 1-D microstrip pBG cells," IEEE Microw. Guided Wave Compon. Lett., vol.10, no.10, pp.403-405, Oct.2000.

[9] F. Zhang, J. Z. Gu, L. N. Shi, C. F. Li, and X. W. Sun, "Low pass filter with in-line beeline CMRC," Electron. Lett., vol.42, no.8, pp.472-474, Apr.2006.

[10] I; Wolff, "Microstrip bandpass filter using degenerate modes of a microstrip ring resonator," Electron. Lett., vol.8, no.12, pp.163-164, June,1972.

[11] J. –S. Hong, H. Shaman, and Y.-H. Chun, "dual-mode microstrip open loop resonators and filters," IEEE Trans. Microw. Theory Tech., vol.55, no. 8, pp. 1764-1770, Aug.2007.

[12] L. Zhu, S. Sun, and W. Menzel, "Ultra-wideband (UWB) bandpass filters using multiple mode resonator," IEEE Microw. Wireless compon. Lett., vol.15, no.11, pp.796-798, Nov.2005.

[13] R. Li and L. Zhu, "Compact UWB bandpass filter using stub-loaded multiple mode resonator," IEEE Microw. Wireless compon. Lett., vol. 17, no.1, pp.40-42, Jan.2007.

[14] X. Y. Zhang and Q. Xue, "Novel dual-mode dual band bandpass filters using coplanar-wavequide-fed ring resonators," IEEE Trans. Microw. Theory Tech., vol.55,no.10, pp.2183-2190,Oct.2007.

[15] C. –F. Chen, T.-Y. Huang, and R.-B. Wu, "Design of dual and triple passband filters using alternately cascaded multiband resonators," IEEE Trans. Micro. Theory Tech., vol.54, no.9, pp.3550-3558, Sep.2006.

[16] R. R. Monsour, B. Jolley, Shen Ye, F. S. Thomoson, and V. Dokas, On the power handling capability of high temperature superconductive filters. IEEE Trans. MTT-44, July 1996, pp.1322−1338.

[17] J.-S. Hong andM. J. Lancaster,Microstrip triangular patch resonator filters. IEEE MTT-S Dig. (1), 2000, pp.331−334.

[18] J. Watkins, "Circular resonant structures in microstrip," Electron. Lett. **5**, 1969, pp.524−525.

[19] I. Wolff and N. Knoppin, "Rectangular and circular microstrip disk capacitors and resonators," IEEE Trans. MTT-22, 1974, pp.857−864.

[20] H. Chaloupka, M. Jeck, B. Gurzinski, and S. Kolesov, "Superconducting planar disk resonators and filters with high power handling capability," Electron. Lett. **32**, 1996, pp.1735−1737.

[21] G. Matthaei, L.Young, and E. M. T. Jones, "Microwave Filters, Impedance-Matching Networks, and Coupling Structures," Artech House, Norwood, MA, 1980.

[22] E. G. Cristal and S. Frankel, "Design of hairpin-line and hybrid haripin-parallel-coupledline filters," IEEE MTT-S Dig. 1971, pp.12–13.

[23] HONG, J. S.; LI, S. "Theory and Experiment of Dual-mode Microstrip Triangular Patch Resonators and Filters," IEEE Transactions On Microwave Theory And Techniques, v. 52, n. 4, pp.1237-1243, April 2004.

[24] OVERFELT, P. L. "WHITE, D. J. TE and TM Modes of Some Triangular Cross-Section Waveguides Using Superposition of Plane Waves," IEEE Transactions On Microwave Theory And Techniques, v. 34, n. 1, pp.161-167, January 1986.

[25] WOLFF, I.; KNOPPIK, N. "Rectangular and Circular Microstrip Disk Capacitors and Resonators," IEEE Transactions On Microwave Theory And Techniques, v. 22, n. 10, pp. 857- 864, October 1974.

[26] CURTIS, J. A.; FIEDZIUSZKO, S. J. "Miniature Dual Mode Microstrip Filters," Acta Materialia, 51, pp. 5837-5866, 2003.

[27] Momentum, "RF Design Environment Documentation," Agilent Technologies, September 2005.

[28] I. Wolff and N. Knoppik, "Rectangular and circular microstrip disk capacitors and resonators," IEEE Transactions on Microwave Theory and Techniques, vol. 22, no. 10, pp. 857-864, Oct. 1974.

[29] J. Watkins, "Circular resonant structures in microstrip," Electronics Letters, vol. 5, no. 21, pp. 524-525, Oct. 1969.

[30] C.H.O. Chew, “Effects of Fringing Fields on the Capacitance of Circular Microstrip Disk,” IEEE Transactions on Microwave Theory and Techniques, vol. 28, no. 2, pp. 98-104, Feb. 1980.

[31] R. J. Cameron, “Advanced coupling matrix synthesis techniques for microwave filters,” IEEE Trans. Microw. Theory Tech., vol. 51, no. 1, pp. 1–10, Jan. 2003.

[32] Smain Amari et al., “Adaptative Synthesis and Design of Resonator Filters With Source/Load-Multiresonator Coupling”, IEEE Trans. Microwave Theory Tech., vol. 50, pp. 1969–1978, Aug 2002.

[33] S. Amari et al., “Adaptive synthesis and design of resonator filters with source/load multi resonator coupling,” IEEE Transactions on Microwave Theory and Techniques, vol. 50, no. 8, pp. 1969-1978, Aug. 2002.

[34] D. M.Pozar, “Microwave Engineering”, John Wiley & Sons, Inc .New York, 1998.

Chapter III
Results and Discussion

III.1. Introduction

This work aims to develop a tunable triple-mode bandpass patch filters using a circular resonator. To make the filters more compact, one of the effective ways is to modify the traditional resonator to generate additional modes, causing the resonator to have multiple resonant frequencies, thus one resonator in physical can be treated as multiple resonators in electrical.

Through the form, place and dimensions of the used slots, we can control the center frequency and the filter's bandwidth, as well as get good rejection of the second harmonic band.

The tunable patch filters are designed and simulated with the 3D EM software ADS (Advanced Design System) which is an electronic design automation software utilized to design RF/microwave modules, integrated MMICs for communications and aerospace/defense applications.

The substrate used to design the chosen geometries is Rogers RO3010 with a relative permittivity ε_r = 10.2 and thickness h= 0.635mm.

III.2. Analysis of the circular resonator

Initially we simulate a circular resonator of 8.1mm radius weakly coupled to the input and output line, these lines have a characteristic impedance of 50 Ω which results a thickness of 0.59 mm. The layout used in the simulation of the resonator can be seen in Figure III.1.

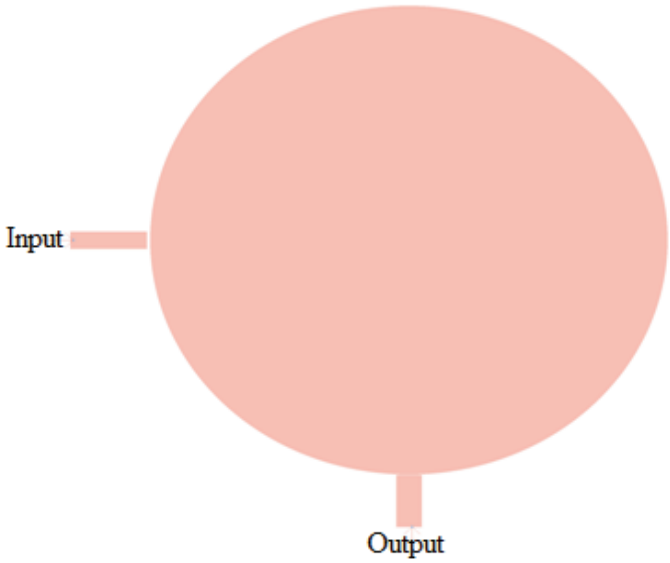

Figure III.1: Layout of the circular patch filter.

After the S-parameters simulation of this resonator we can distinguish the degenerate mode TMz_{110} (f_1= 3.38 GHz) and the second resonant mode TMz_{210} (f_2=5.714 GHz) as can be seen in figure III.2.

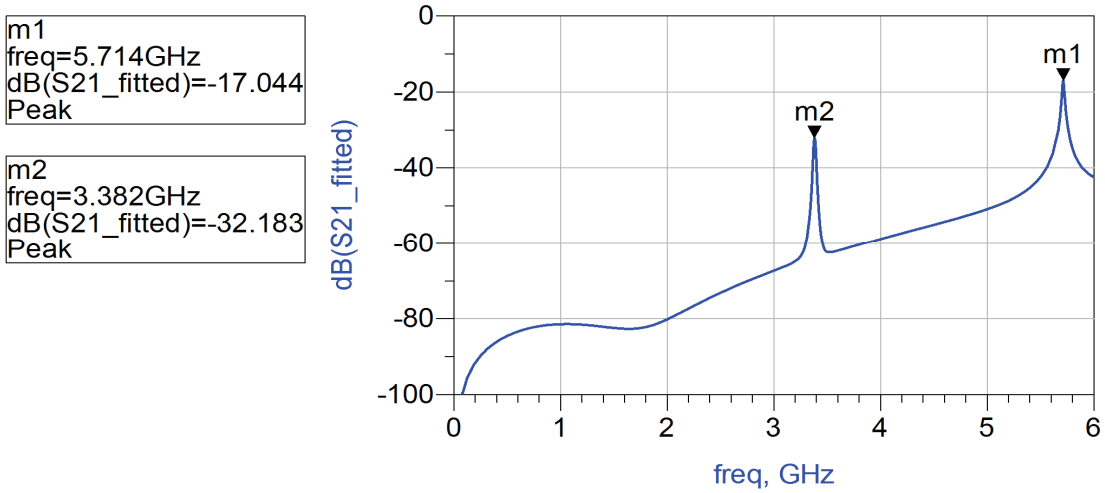

Figure III.2: Circular patch filter frequency response.

III.3. The circular patch filter (first structure)

When inserting slots inclined at 45 ° in the circular resonator it is possible to disrupt each of the degenerate modes and the second resonant mode, to change their frequencies as can be seen in Figure III.3.

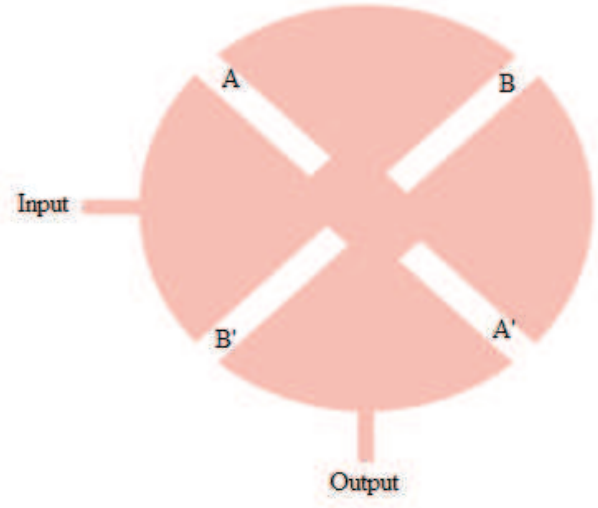

Figure III.3: Layout of the circular patch filter with four radial slots.

III.3.1 Influence of the dimensions of the slots on the frequency response

When analyzing the influence of each group of slots, A-A' and B-B' in the frequency response of the resonator, initial simulations showed that the most important influence on the response of the resonator was mainly caused by the length of the slots. Thus, the simulations started to be realized with slots of 1.1 mm wide, which resulted in a better return loss in the initial simulations of the circular patch.

A series of simulations was done using the layouts shown in Figures III.1 and III.3, varying the length of the slots and keeping its width constant.

III.3.1.1 Influence of the lengths A and A'

Figure III.4 shows the layout of the patch filter with only two slots AA’ in order to study the influence of the variation of these slots on the frequency response of the filter.

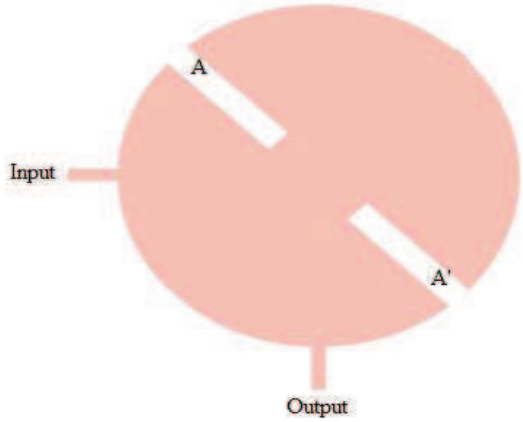

Figure III.4: layout of the patch filter with only two slots named A-A'.

Figure III.5 shows the S-parameters simulation results when the lengths A and A' vary while the width of the slots is kept constant.

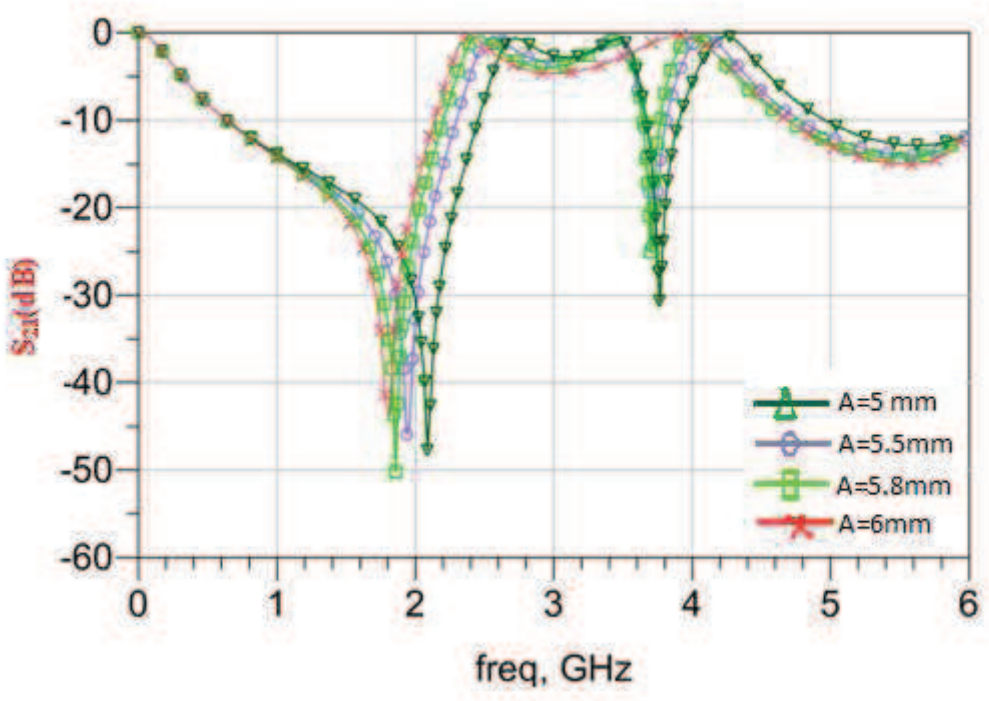

(a)

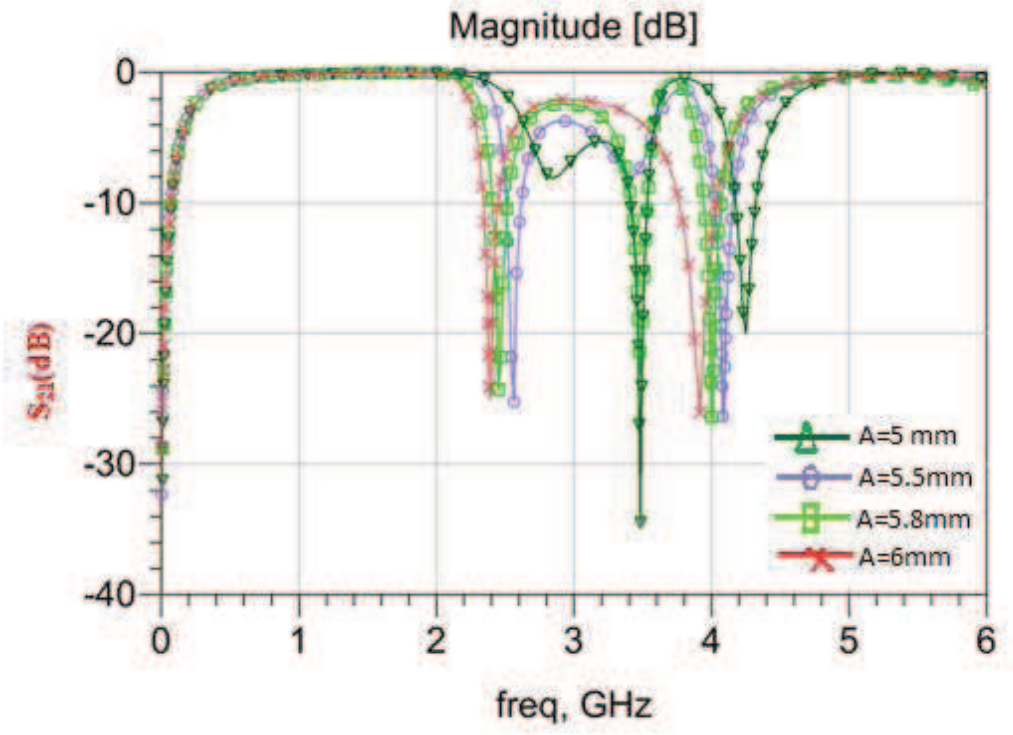

(b)

Figure III.5: The frequency of the three modes in relation with the length of the slots A-A'. (a): Insertion loss, (b): Return loss.

These figures show the behavior of the resonant frequencies depending on the length of the slots. In these figures, f_1 is the frequency of the dominant mode TMz_{110} - I, f_2 is the frequency of the dominant mode TMz_{110} - II and f_3 is the frequency of the second resonant mode, TMz_{210} (from the lower to the higher frequency).

Figure III.5 shows that f_2 does not change with the length of the slots A-A ' whereas f_1 and f_3 decrease with increasing the slots.

III.3.1.2 Influence of the lengths B and B'

Figure III.6 shows the layout of the patch filter with only two slots BB' in order to study the influence of the variation of these slots on the frequency response of the filter.

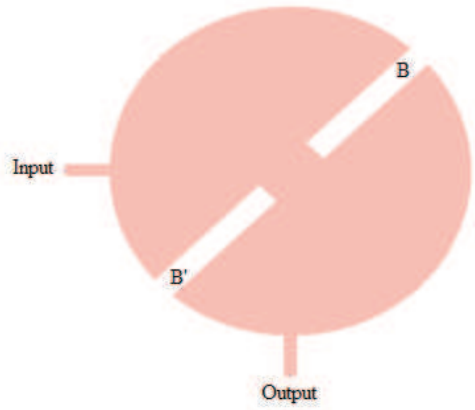

Figure III.6: Layout of the filter with two slots named B-B'.

Figure III.7 shows the S-parameters simulation results when the lengths B and B' vary while the width of the structure is kept constant.

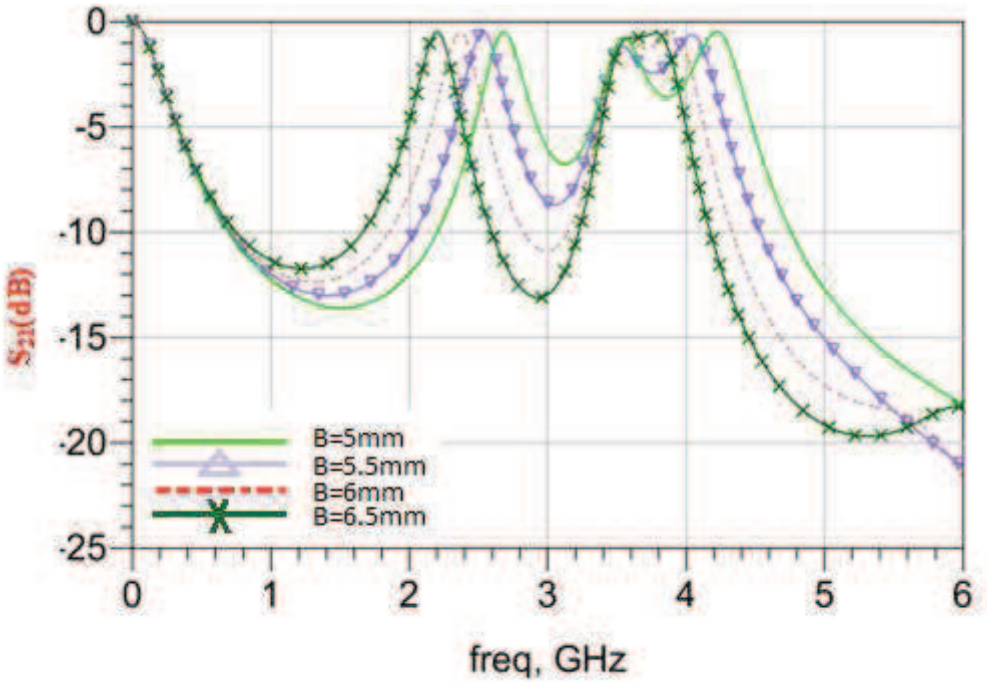

(a)

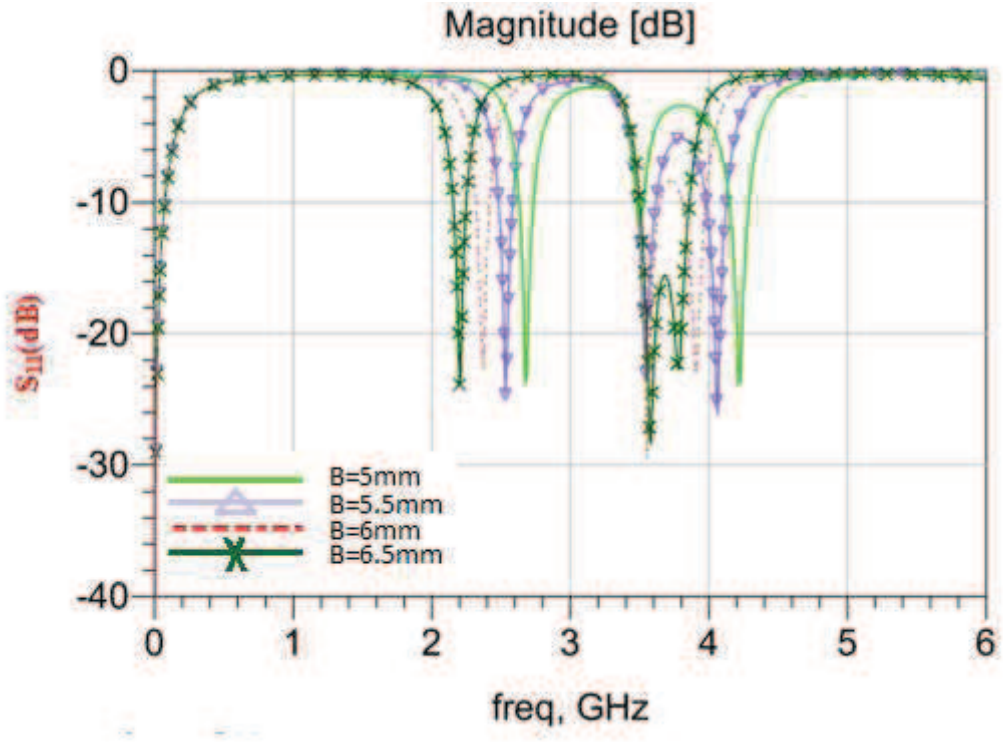

(b)

Figure III.7: The frequency of the three modes in relation with the length of the slots B-B'. (a): Insertion loss, (b): Return loss.

The variation of the length of the slots B-B' is shown in Figure III.6, say that f_1 and f_3 decreases while f_2 is minimally altered.

From the previous study concerns the influence of lengths of the slots AA' and BB' on the response of the filter, one can choose the right dimensions of the slots which have the butter performances and the most close to the wanted frequency.

III.3.2 Design and analysis of the 3 poles filter

Analyses and simulations of the modified circular patch resonator were applied to the bandpass patch filter design. The approximate dimensions of the slots were selected so that the three modes resonate around 2.4 GHz. Slots AA' have the same length, and so as for B and B'. However, the length of the pair A-A' differs slightly from the length of the pair B-B' determining the separation of the degenerate modes with respect to the input and output lines of the filter. Which are connected directly to the resonator through a line with a characteristic impedance of 50Ω.

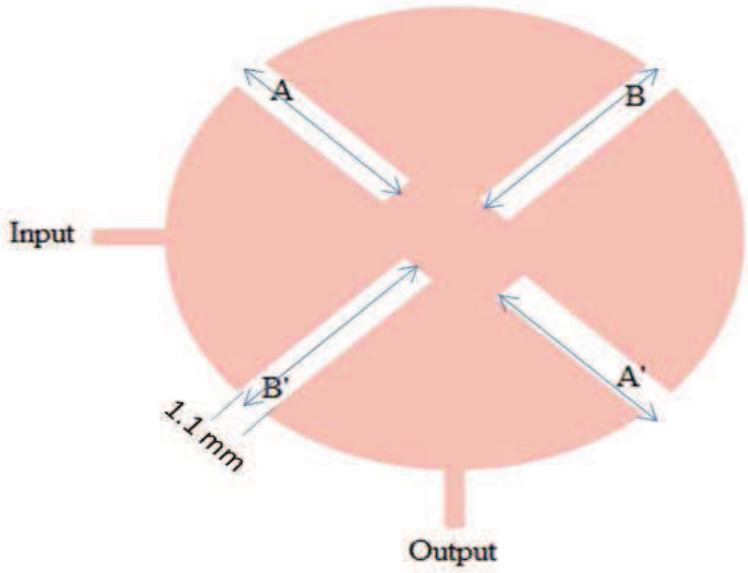

Figure III.8: Layout of the initial circular patch filter (dimensions in mm).

The final dimensions of the filter are presented in this table:

Parameters	dimensions [mm]
r (radius)	8.1
L1(AA')	5.8
L2(BB')	6.6
W	1.1

Table III.1: Dimensions of the filter.

The simulated frequency response of the triple-mode patch filter is shown in Figure III.9.

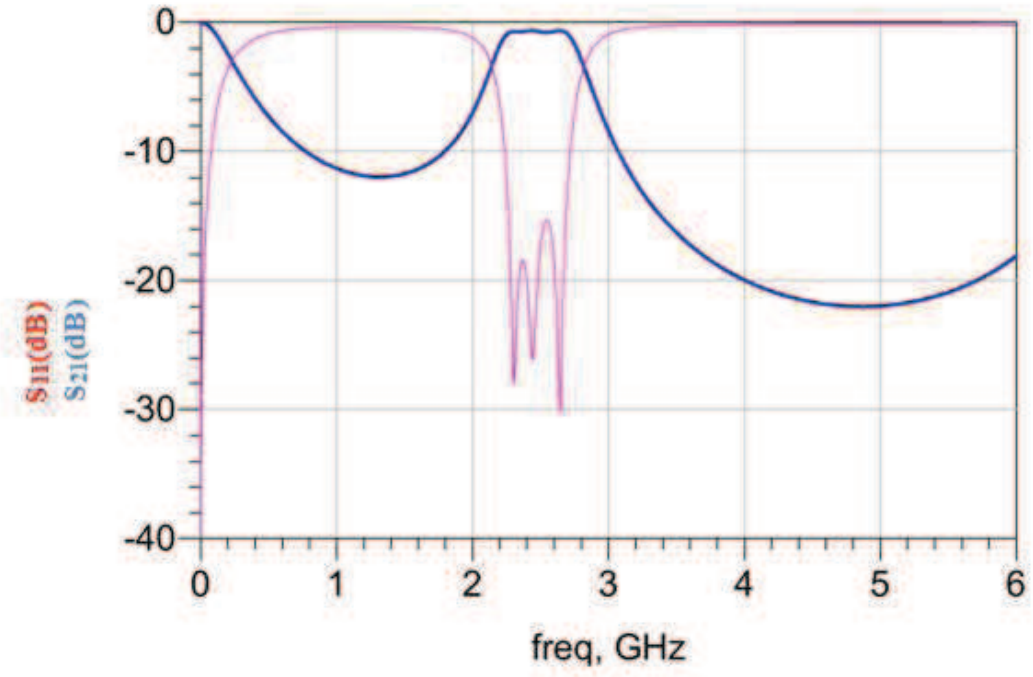

Figure III.9: Simulated frequency response of the unloaded triple-mode circular patch filter.

One clearly observes that the filter has a center frequency f_0 of 2.46 GHz, a bandwidth of 26% with f=2.15 GHz to f=2.8 GHz and three mode frequencies situated at f_1=2.3 GHz, f_2= 2.45 GHz and f_3=2.65 GHz. Moreover, the filter has an insertion loss of -0.6 dB and a return loss better than -15.7 dB. The filter has a total size of 18.2×18.2 mm^2

III.3.3 Tuning analysis

In order to verify how a patch filter behaves when capacitively loaded, the proposed patch filter is analyzed with capacitances across its slots as can be seen in figure III.10.

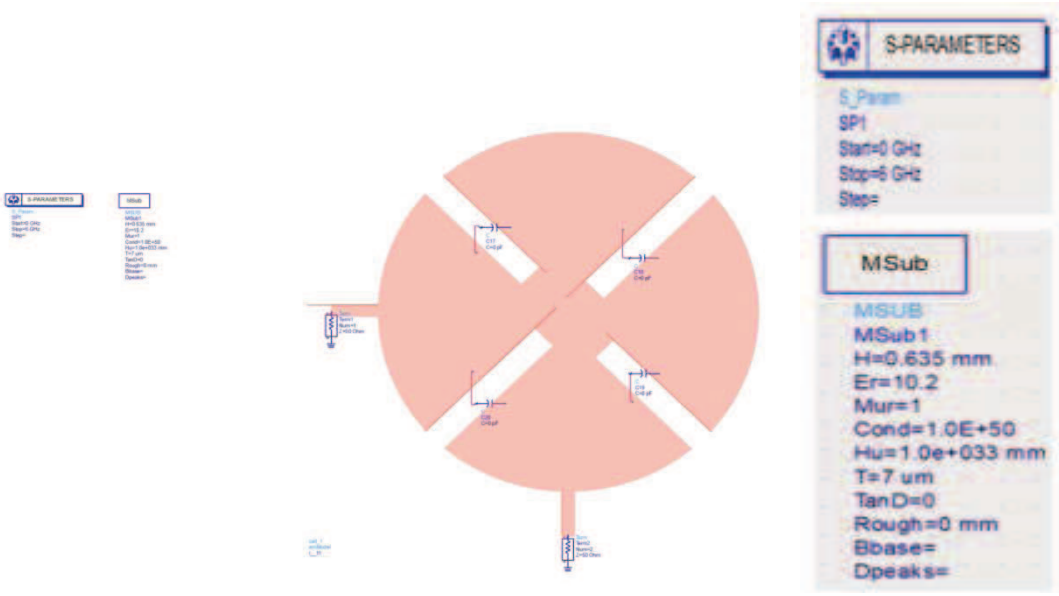

Figure III.10: Patch filter capacitively loaded.

The four capacitances were kept equal in order to simplify the study. At a specific capacitance (C_S), the modes superimpose destructively at the resonant frequency highly increasing the insertion loss.

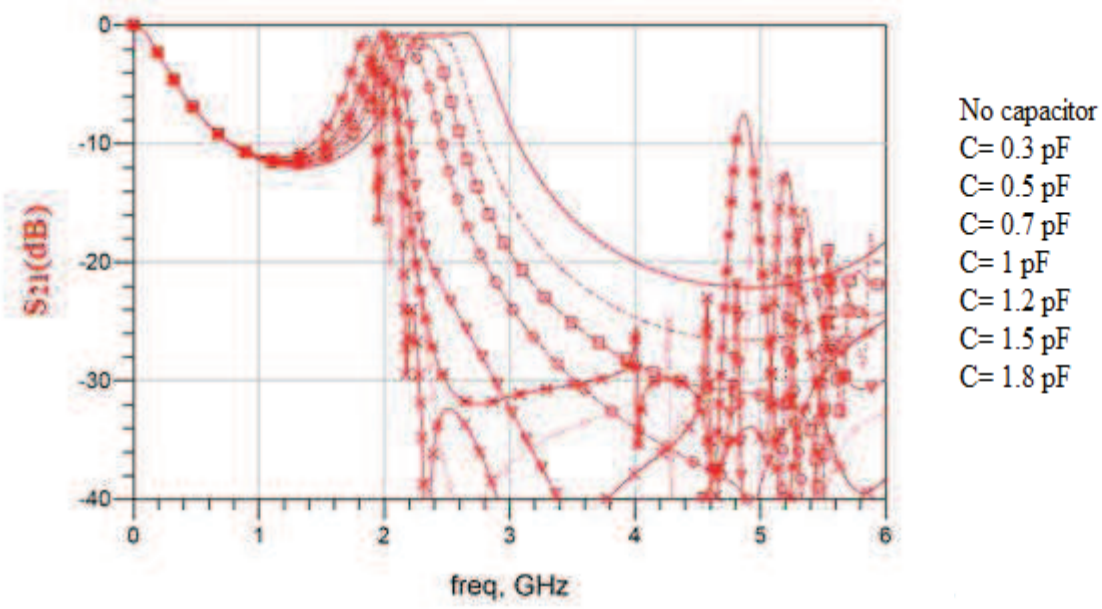

(a)

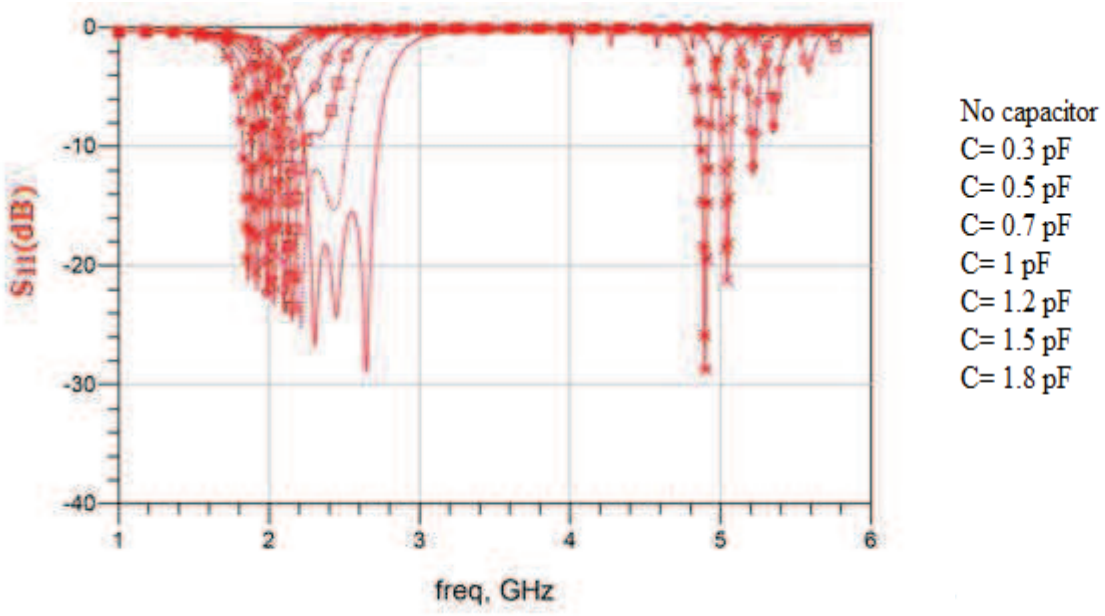

(b)

Figure III.11: Response of the circular patch filter capacitively loaded. (a): Insertion loss, (b): Return loss.

By further increasing the capacitances, the insertion loss decreases to its initial value up to a capacitance (C_{max}) in which the RL becomes worse than 12 dB due to the mismatch of the resonator impedance.

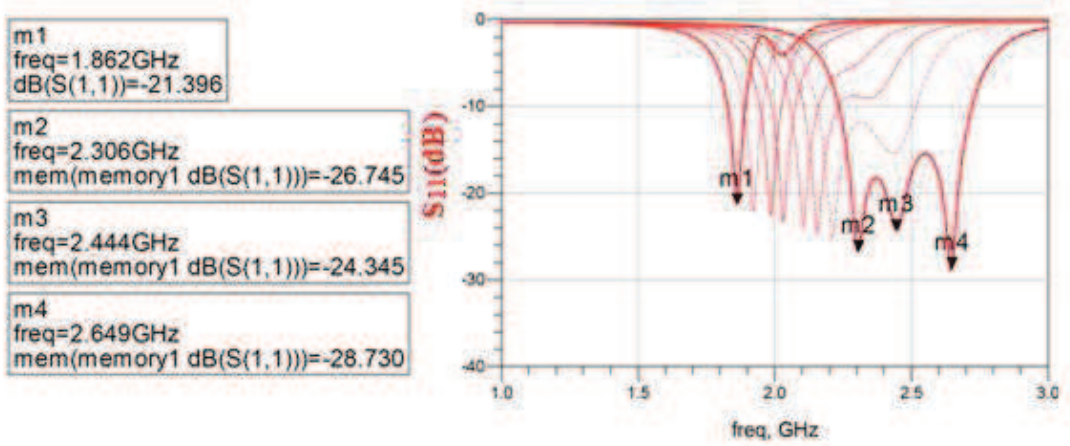

Figure III.12: Return loss of the filter with the modes frequencies.

The patch filter could be tuned by manually changing the capacitors. The capacitance varies from zero to 1.8 pF resulting in 28 % of center frequency tuning range, varying from 2.46 GHz to 1.86 GHz. At the same time, the filter's passband decreased from 26 % to 9 % for the same range of capacitances. These results are presented in Figures III.12 and III.13.

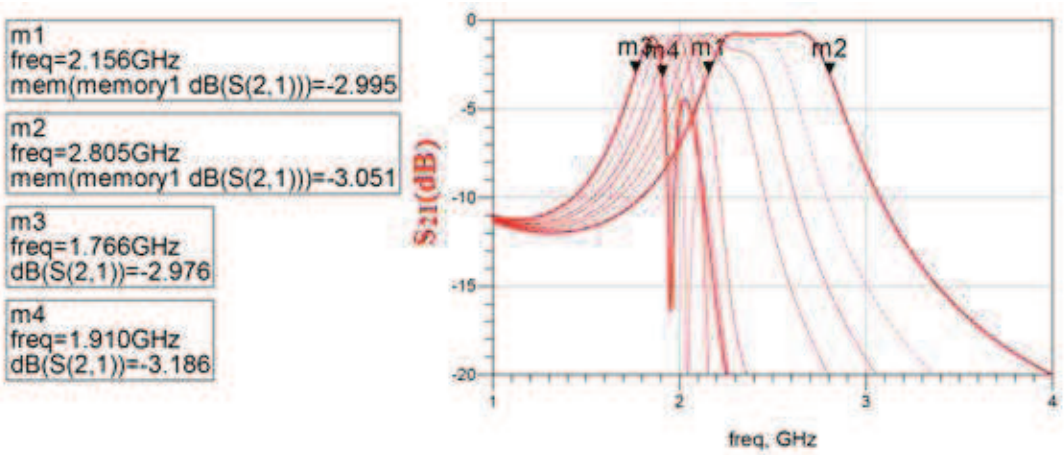

Figure III.13: Insertion loss of the filter with FBW-3dB.

When the capacitances are greater than 1.8 pF, the passband characteristic is deformed. The results are presented in the following table:

Values of capacitors (pF)	Center frequency (GHz)	FBW (%)
No capacitors	**2.46**	**28**
0.3	2.36	25.4
0.5	2.25	20.8
0.7	2.1	17
1	2	12
1.5	1.92	10
1.8	**1.86**	**9**

Table III.2: results of the patch filter loaded with four equal capacitors.

III.3.4 Varactor tuning

In order to obtain an electronically tuning, the filter was then analyzed considering the varactor diode model mentioned in the second chapter (the diode SMV1430 from Skyworks).

In order to clarify the study, the capacitance in each slot will be referenced as C_A, C_B, C_C and C_D, respectively, as illustrated in Figure III.16 and the frequency of the resonant modes $TMz_{1,1,0}$ odd, $TMz_{1,1,0}$ even, and $TMz_{2,1,0}$ will respectively be referred as f_1, f_2, and f_3.

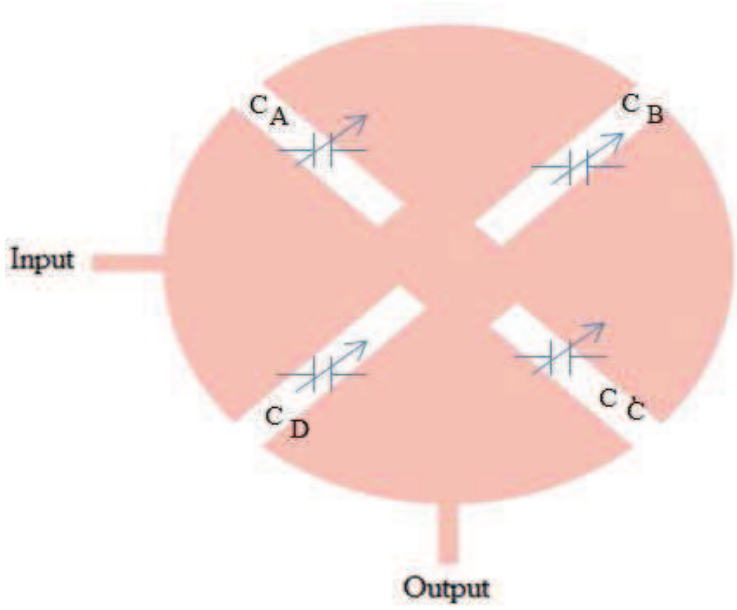

Figure III.14: layout of the circular patch filter loaded with four varactors.

III.3.4.1 The effect of C_A and C_C:

C_A and C_C have the same effect on the response of the filter, due to its symmetry. If these two capacitances are changed separately, the filter cannot be matched and the return loss is not acceptable. Therefore, the analysis was carried out with the influence of equal capacitances C_A and C_C, which vary together.

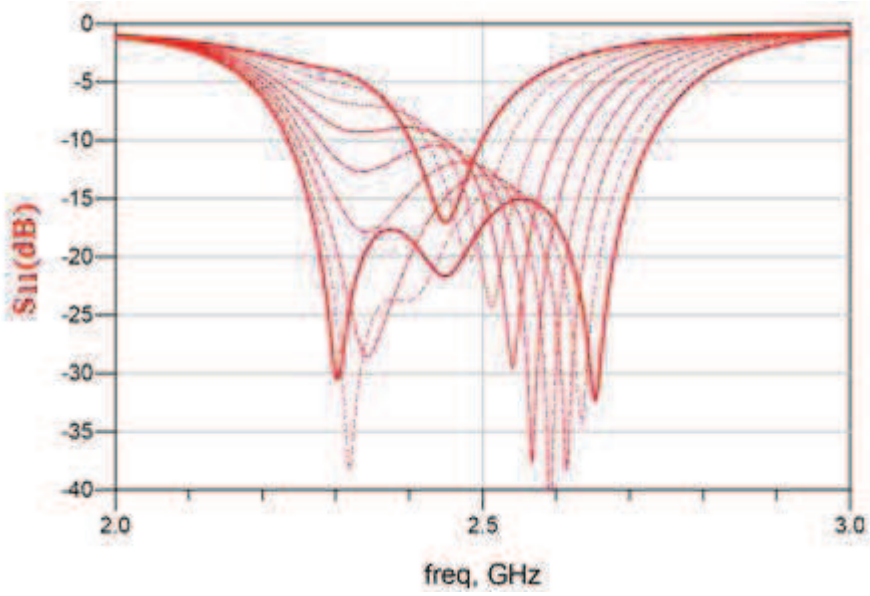

(a)

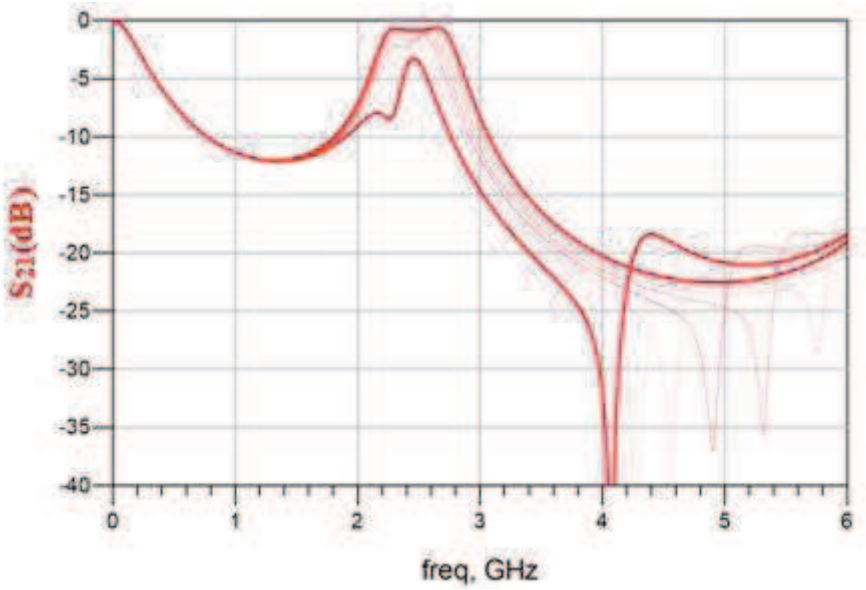

(b)

Figure III.15: simulated frequency response (varying C_A and C_C). (a): Insertion loss, (b): Return loss.

Figure III.15 shows the simulated frequency responses when varying both C_A and C_C. From the increase of these two capacitances, one can perceive two different effects in the mode frequencies: the decrease of f_2 approximating it to f_1, and the decrease of f_3.

Note that a very small capacitance already brings f_2 so close to f_1 that it is not possible to distinguish each other anymore.

In conclusion, the main effect of increasing C_A and C_C is to reduce both f_2 and f_3.

III.3.4.2 The effect of C_B:

Figure III.16 shows the influence of the variation of the capacitor C_B on the modes frequencies.

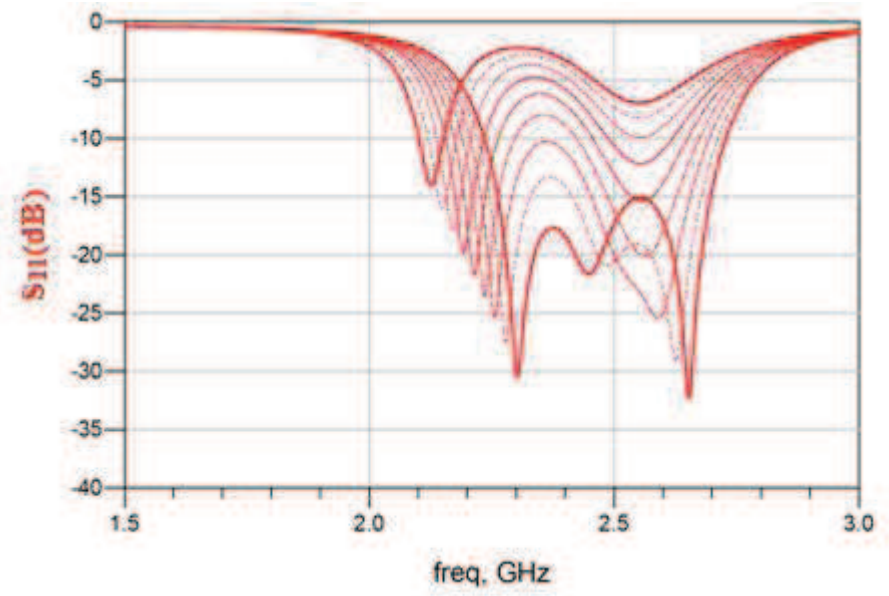

Figure III.16: Simulated frequency response (varying C_B).

A different behavior can be seen when varying C_B. The increase of this capacitance lowers both f_1 and f_3 at the same time, while slightly increasing f_2. Simulations showed that C_B has a stronger effect on f_3 than on f_1, reducing f_3 more than f_1. In conclusion, the main effect of increasing C_B is to reduce both f_1 and f_3, and slightly increase f_2.

III.3.4.3 The effect of C_D:

Figures III.17 and III18 shows the influence of the variation of the capacitor C_D versus the frequency response.

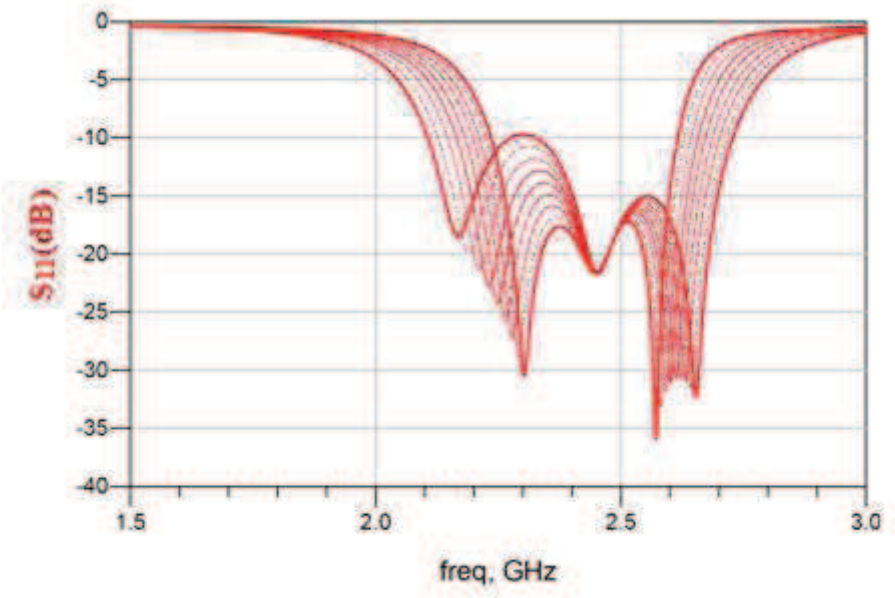

(a)

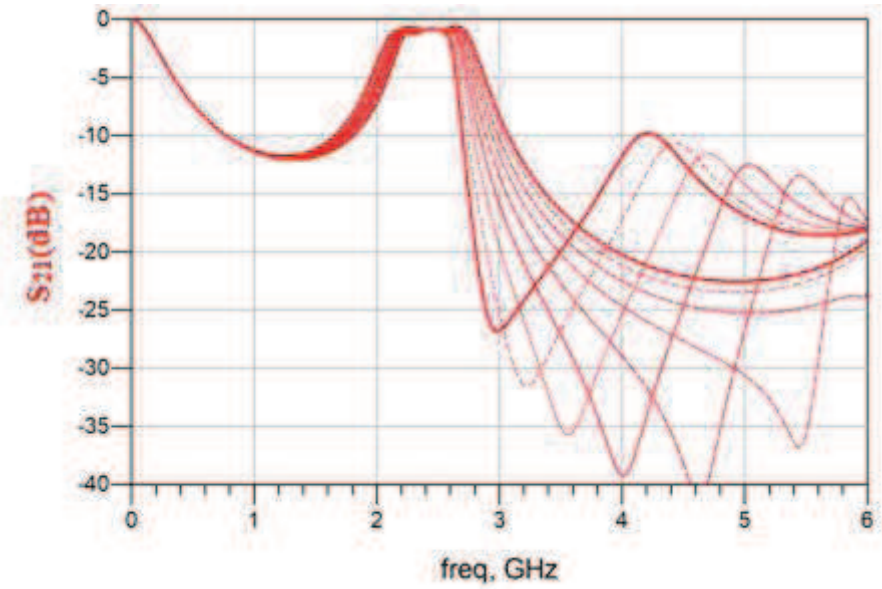

(b)

Figure III.17: Simulated frequency response (varying C_D). (a): Return loss, (b): Insertion loss.

C_D affects the filter response in another way. The analysis of the effect of C_D is much more complex because this capacitance affects several couplings at the same time. Initially, by increasing C_D, f_1 and f_3 decrease, and f_2 remains unchanged.

In conclusion, the effect of increasing C_D is to reduce both f_1 and $f3$, while keeping f_2 unchanged.

III.3.4.4 The effect of the four combined varactors

The study carried out in the above sub-sections has shown that when using the capacitances across the four slots, allowing this patch filter to be reconfigured by varactor diodes in terms of its center frequency, bandwidth, and rejection. The rejection is changed by bringing a transmission zero close to the upper side of the passband. Particularly for the susceptances, they all increased with the increase of each individual capacitance, and thus, the result of increasing all capacitances together is obviously a simultaneous decrease in the frequency of the three resonant modes.

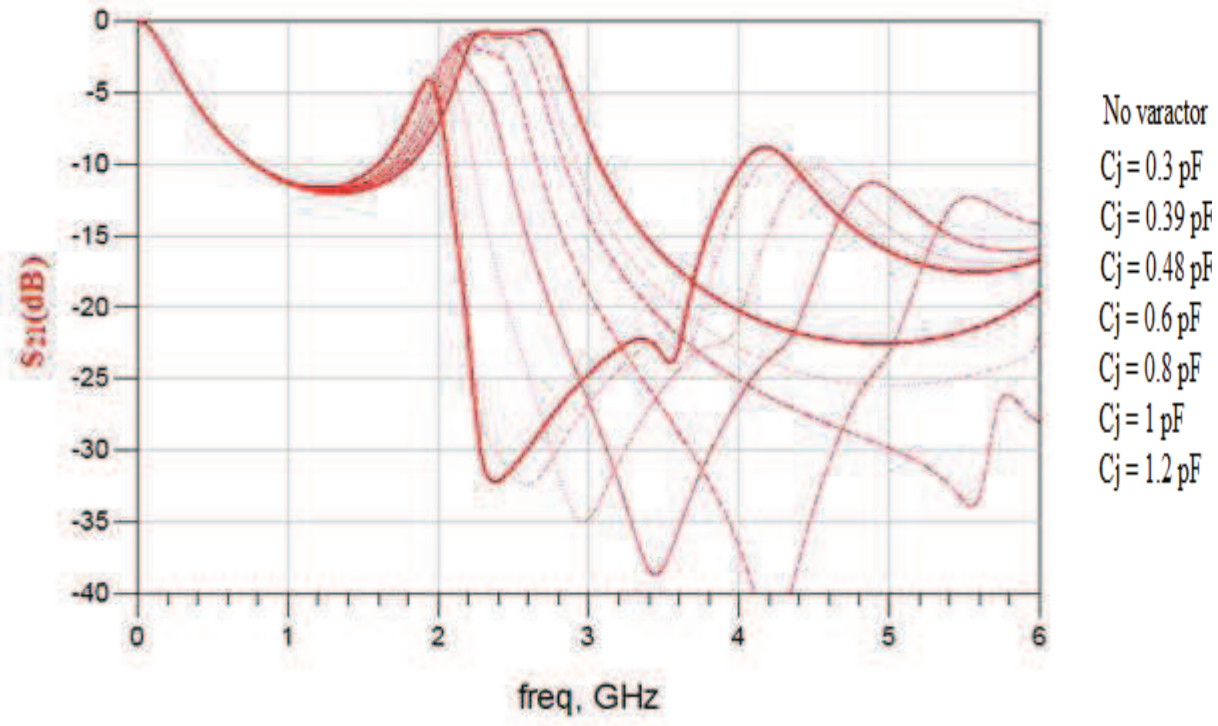

(a)

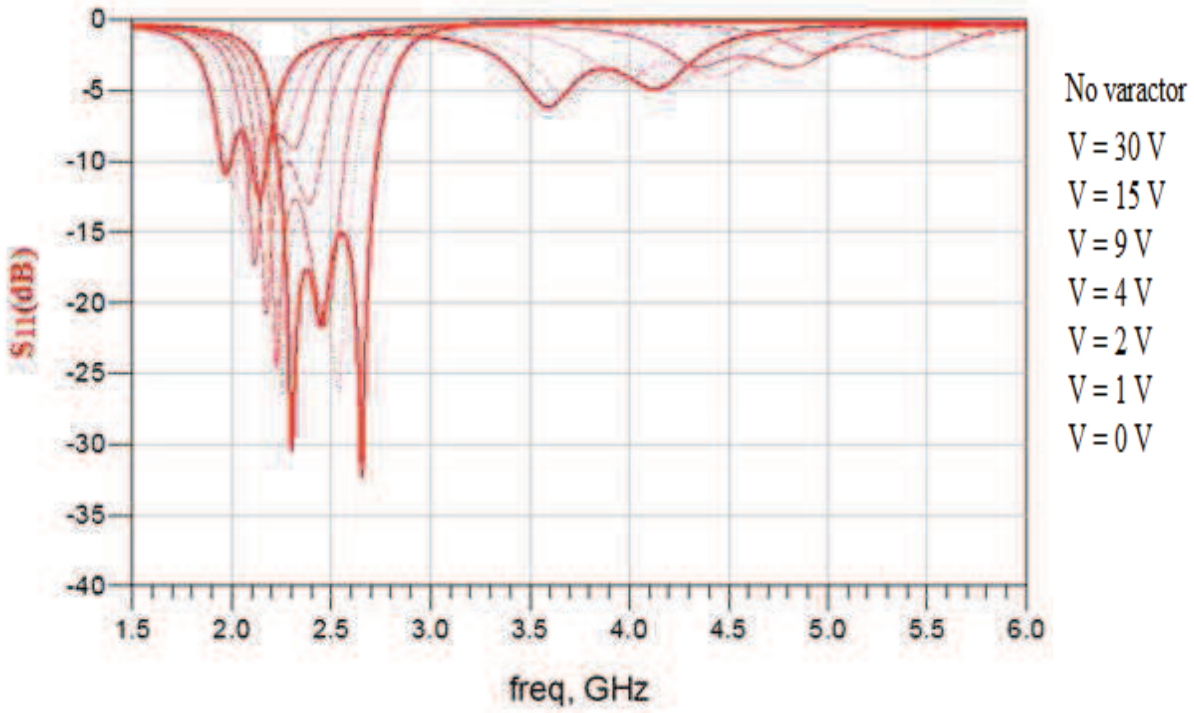

(b)

Figure III.18: simulated frequency response varying all the combined varactors.

(a): Insertion loss, (b): Return loss.

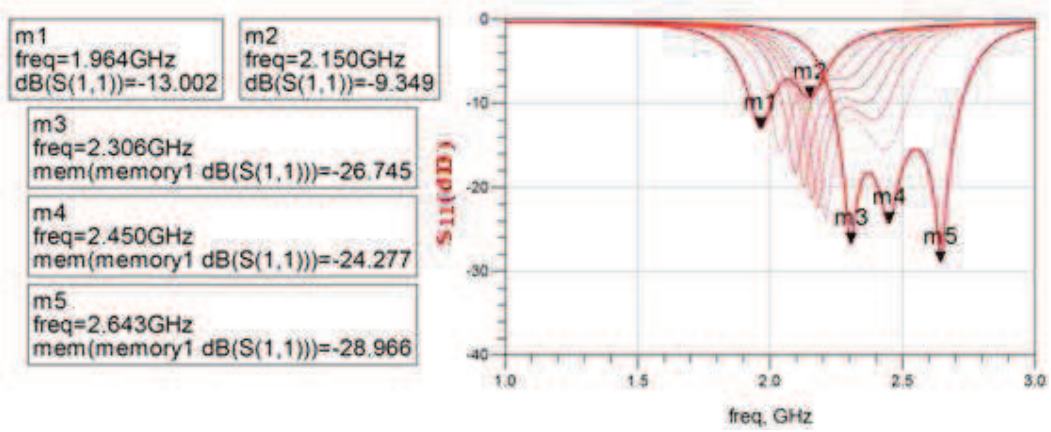

Figure III.19: frequency response with the different modes frequencies.

Simulations with equal capacitances at the four slots showed that both frequency and bandwidth decrease at the same time when increasing all the capacitances. Furthermore, the simulations with equal capacitances at the four slots in figure III.19, showed that a transmission zero is brought to the upper side of the passband. The center frequency of the tunable patch filter with varactor diodes could be tuned up to 2 GHz. The unloaded quality factor *Qu* of this filter was calculated from eq. (III.1):

$$Q_u = \frac{4.343}{FBW_{-3dB} IL} \sum_{i=1}^{N} g_i \qquad \text{(III. 1)}$$

Here, $N = 3$ thus, the 3rd order Butterworth elements of a low-pass prototype filter were considered: g1 = g3 = 1 and g2 = 2. At the initial frequency without tuning element (*fc* = 2.46 GHz and bandwidth = 28 %), the filter *Qu* equals 103. When the filter was tuned to the maximum frequency of the Tuning range (*fc* = 2 GHz and bandwidth = 12 %), *Qu* equals 41. The center frequency of the filer has a tuning range of 21% and a bandwidth tuning of 80%.

The tuning results of the first circular patch filter are resumed in the following table:

Values of capacitors Cj (pF)	Bias voltage (V)	Center frequency (GHz)	FBW (%)
No capacitors	-	2.46	28
0.3	30	2.32	23
0.39	15	2.28	21
0.48	9	2.25	18.6
0.58	5	2.22	14.8
0.7	3	2.19	13.6
0.8	2	2.16	12.7
1	1	2.11	12.4
1.2	0	2	12

Table III.3: results of the patch filter loaded with four equal varactors.

III.4. The circular patch filter (second structure)

This structure is presented for the first time; it is a circular resonator with two pairs of rectangular slots positioned orthogonally as to disrupt the modes to change their frequencies as can be seen in Figure III.23.

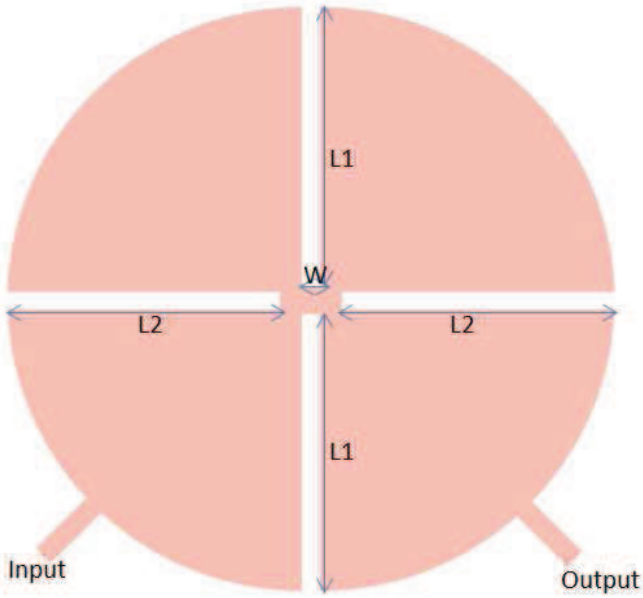

Figure III.20: Layout of the circular patch filter with four slots.

III.4.1 Influence of the slots on the frequency response

A series of simulations was done using the layouts shown in III.20, varying the length of the slots and keeping its width constant.

III.4.1.1 Influence of the length L1 (vertical slots)

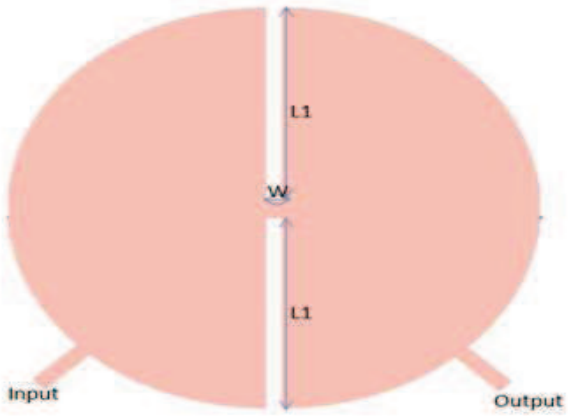

Figure III.21: Layout of the filter with two vertical slots.

When studying the influence of the length L_1, the simulation results showed that by increasing the length L_1 the bandwidth slightly increases as can be seen in figure III.22.

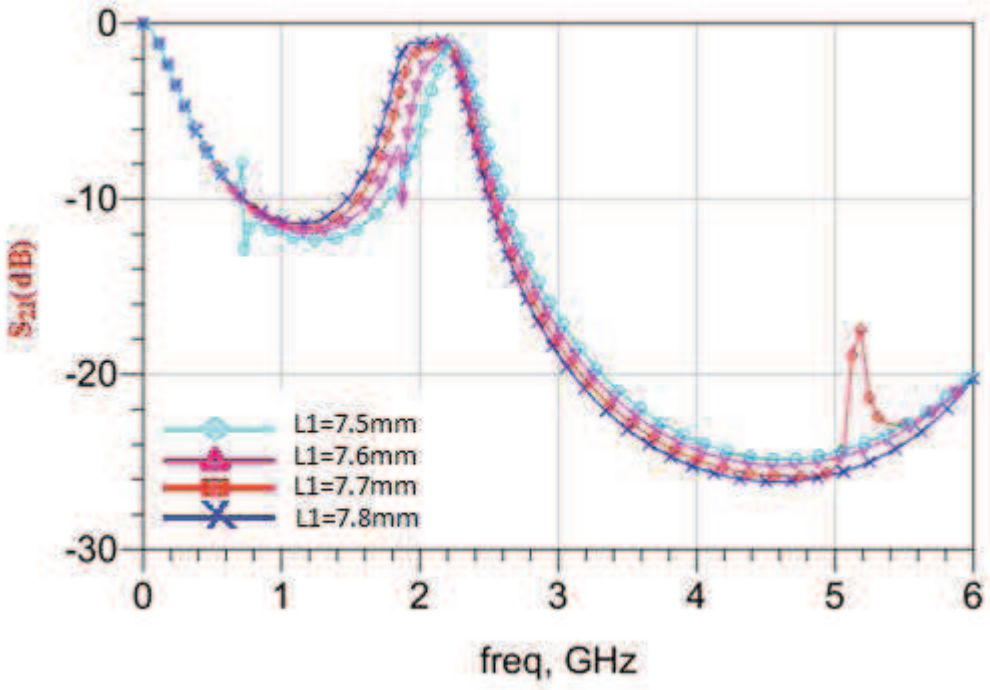

(a)

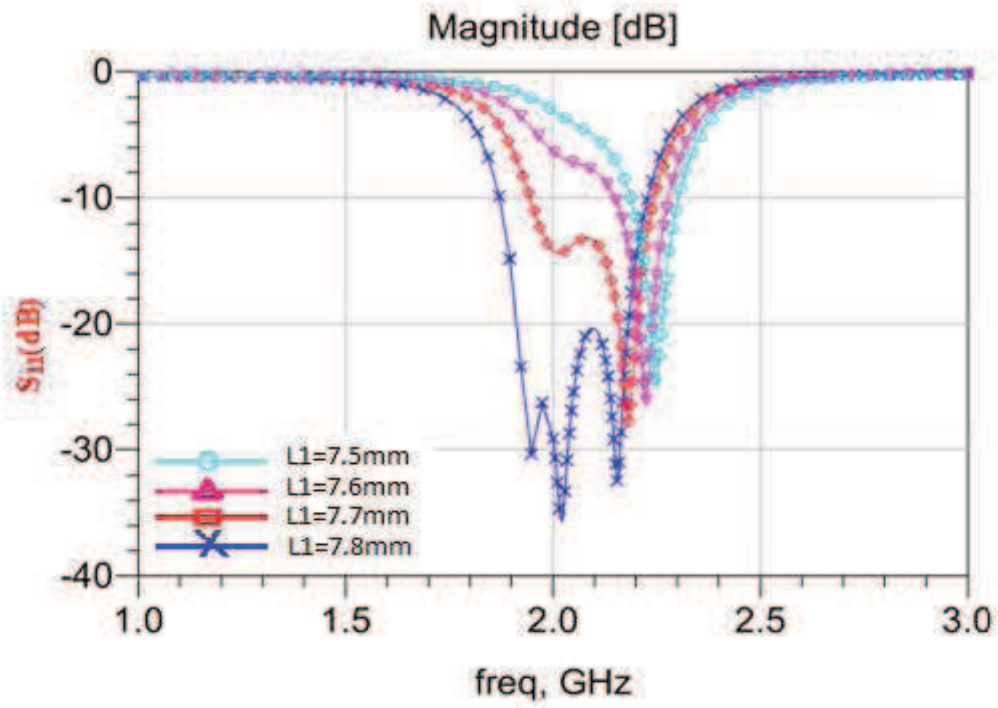

(b)

Figure III.22: The frequency of the three modes in relation with the length of the slots L1. (a): Insertion loss, (b): Return loss.

Also, the increase of the length of the vertical slots results in a decrease in the frequencies f_1 and f_3 while f_2 is minimally altered with a decrease in the return loss up to >20 dB.

III.4.1.2 Influence of the length L2 (horizontal slots)

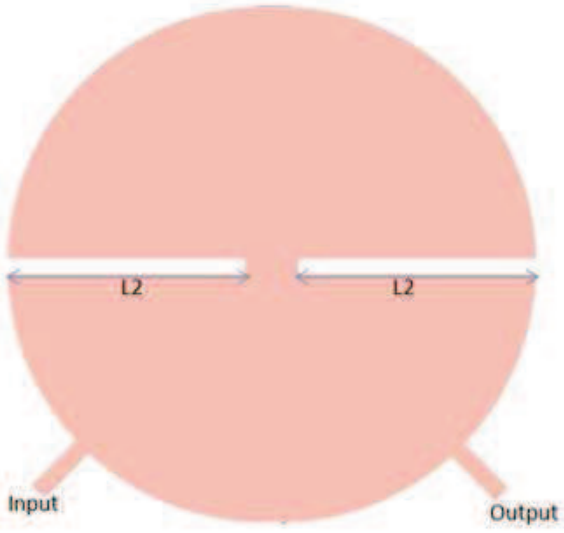

Figure III.23: Layout of the filter with two horizontal slots.

When studying the influence of the length L_2, the simulation shows that by increasing the length L_2 the bandwidth slightly decreases as can be seen in figure III.24.

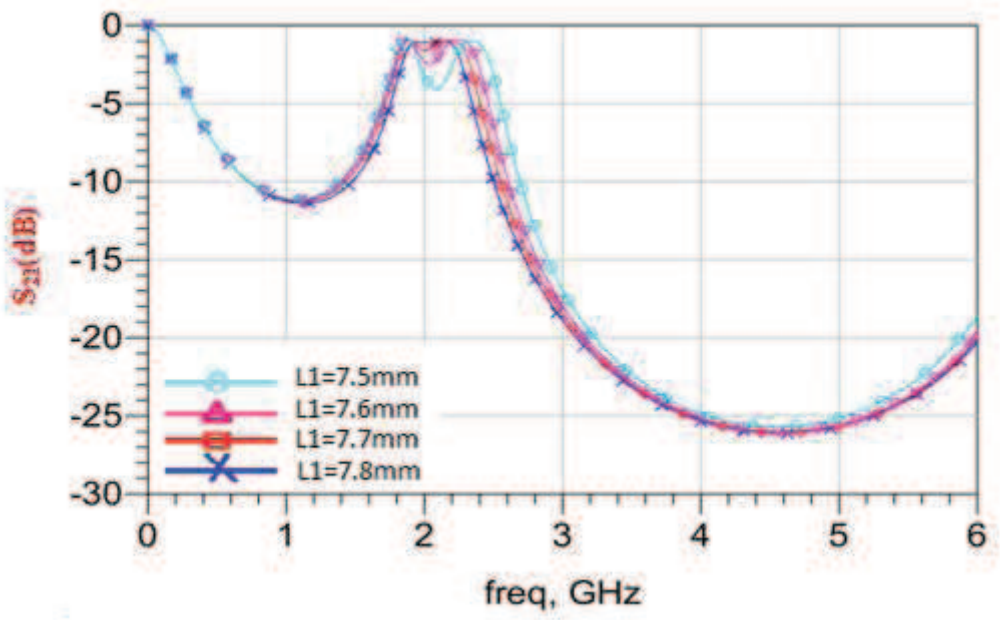

(a)

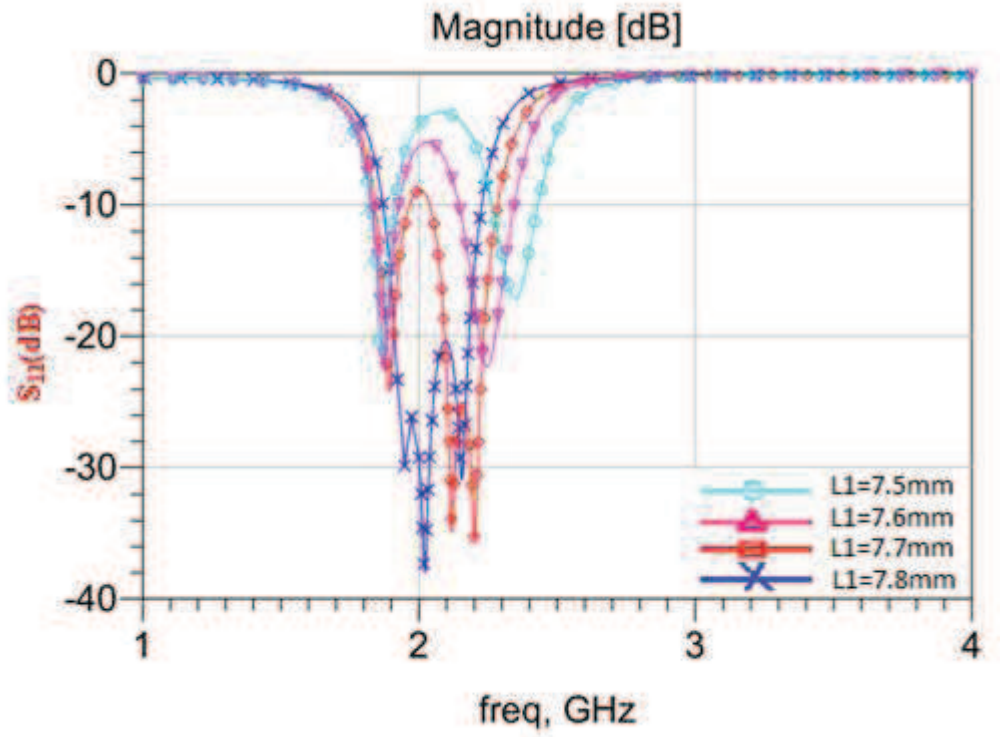

(b)

Figure III.24: Layout of the patch filter with horizontal slots.

Also, as the influence of L_1, the increase of the length of the vertical slots (L_2) results in a decrease in the frequencies f_3 and f_2 while f_1 slightly decrease.

III.4.2 Design and analysis of the 3 poles filter

Analyses and simulations of the new circular patch resonator were applied to the bandpass patch filter design. The approximate dimensions of the slots were selected so that the three modes resonate around 2 GHz. Vertical slots have the same length, and so as for horizontal slots. However, the length of the horizontal pair differs slightly from the length of the vertical pair determining the separation of the degenerate modes with respect to the input and output lines of the filter. Which are connected directly to the resonator through a line with a characteristic impedance of 50Ω.

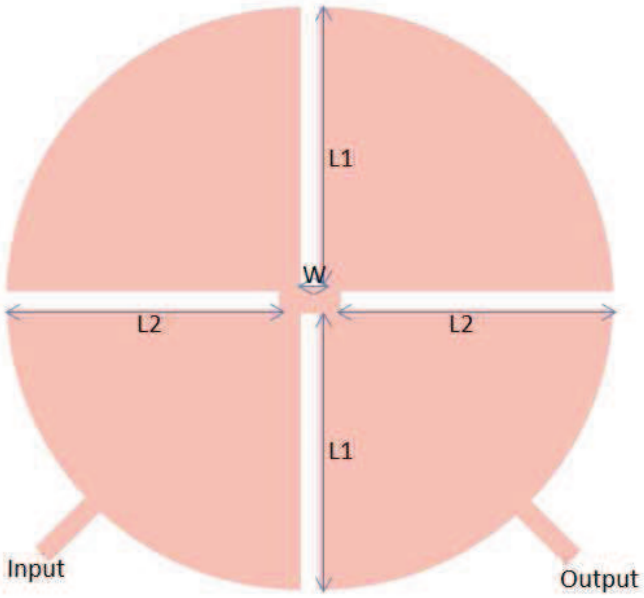

Figure III.25: Layout of the circular patch filter (dimensions in mm).

The final dimensions of the filter are presented in this table:

Parameters	dimensions [mm]
r (radius)	8.1
L1	7.8
L2	7.5
W	0.5

Table III.4: dimensions of the filter.

The band pass filter's response is shown in Figure III.26. The filter has a center frequency of f_c= 2.04 GHz, a bandwidth of 26% with f=1.81 GHz to f=2.3 GHz, the three mode frequencies localized at f_1=1.95 GHz, f_2= 2 GHz and f_3=2.16 GHz, an insertion loss of -1 dB and a return loss better than -20.38 dB. This filter has a total size of 18.2×18.2 mm^2.

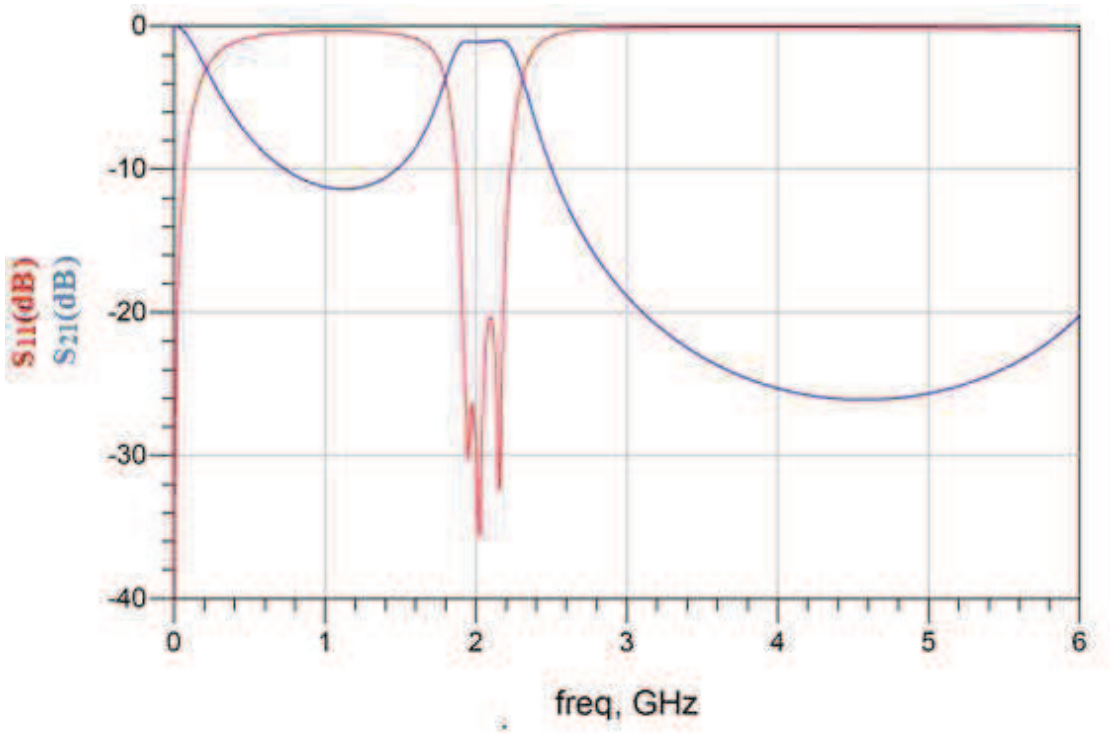

Figure III.26: Simulated frequency response of the unloaded triple-mode circular.

III.4.3 Tuning analysis

In order to verify how a patch filter behaves when capacitively loaded, the proposed patch filter was analyzed with capacitances across its slots.

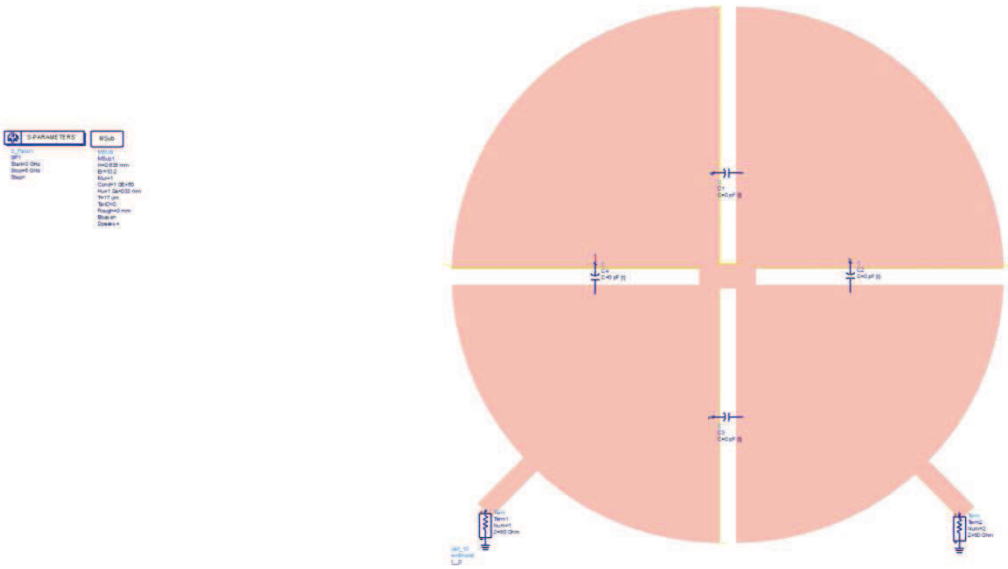

Figure III.27: Patch filter capacitively loaded.

The four capacitances were kept equal in order to simplify the study. At a specific capacitance (C_S), the modes superimpose destructively at the resonant frequency highly increasing the insertion loss.

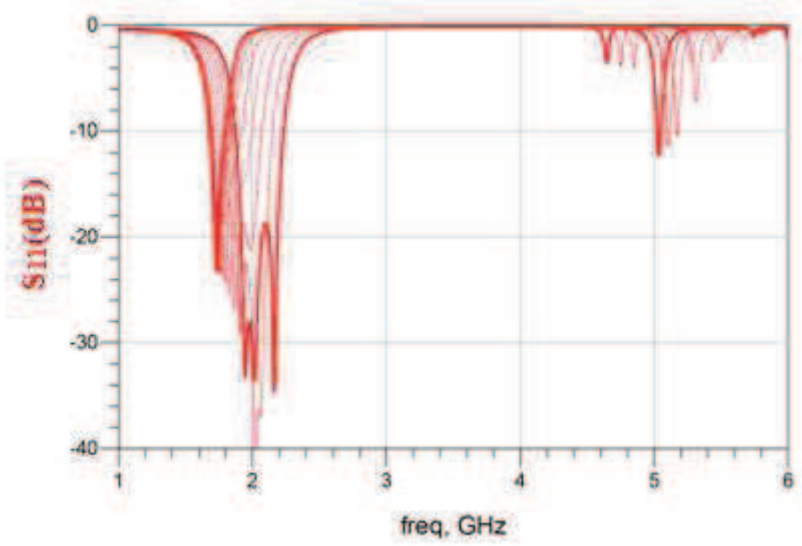

Figure III.28: Response of the circular patch filter capacitively loaded.

By further increasing the capacitances, the insertion loss decreases to its initial value up to a capacitance (C_{max}) in which the RL becomes worse than 12 dB due to the mismatch of the resonator impedance.

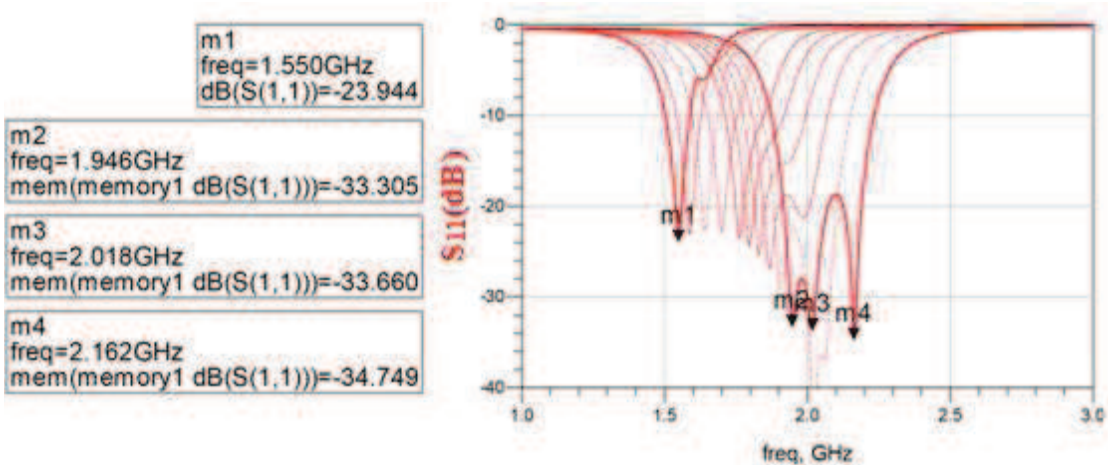

Figure III.29: Return loss of the filter with the modes frequencies.

The patch filter could be tuned by varying the capacitors. The capacitance variation from zero to 2.5 pF resulted in 27 % of center frequency tuning range, varying from 2.04 GHz to 1.55 GHz. At the same time, the filter's passband decreased from 26 % to 11 % for the same range of capacitances. These results are presented in Figures III.15 and III.16.

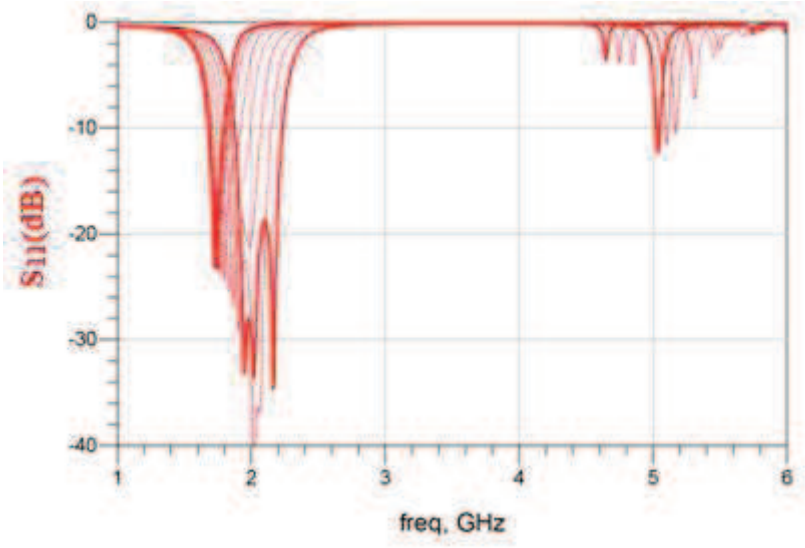

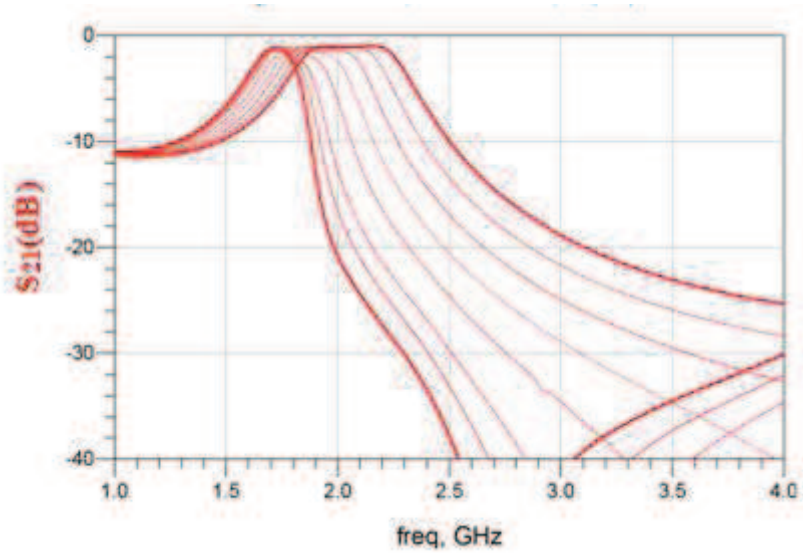

Figure III.30: Insertion loss of the filter with FBW-3dB.

When the capacitances are greater than 2.5 pF, the passband characteristic is deformed. The results are presented in table III.5:

Values of capacitors (pF)	Center frequency (GHz)	FBW (%)
No capacitors	**2.04**	**26**
0.3	1.95	22.4
0.5	1.9	20
0.7	1.81	18
1	1.76	14.6
1.5	1.68	12.6
1.8	1.64	11.7
2	1.6	11.2
2.5	**1.55**	**11**

Table III.5: Results of the patch filter loaded with four equal capacitors.

III.4.4 Varactor tuning

The filter was analyzed considering the same varactor diode used in the first structure. In order to clarify the study, the capacitance in each slot will be respectively referenced as C_A, C_B, C_C and C_D as illustrated in Figure III.31.

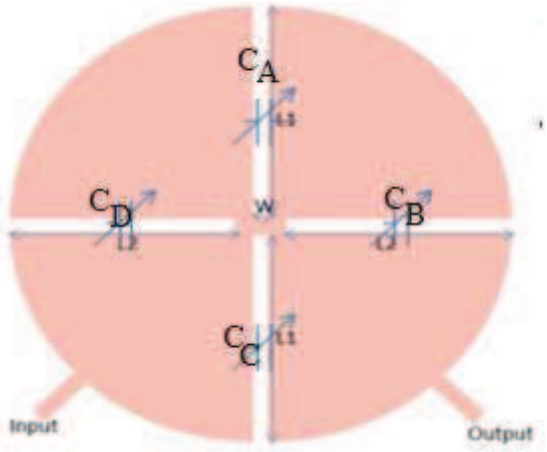

Figure III.31: Layout of the circular patch filter loaded with four varactors.

III.4.4.1 The effect of vertical slots*:*

C_A and C_C have the same effect on the response of the filter, due to its symmetry. Therefore, the analysis was carried out with the influence of equal capacitances C_A and C_C which vary at the same time.

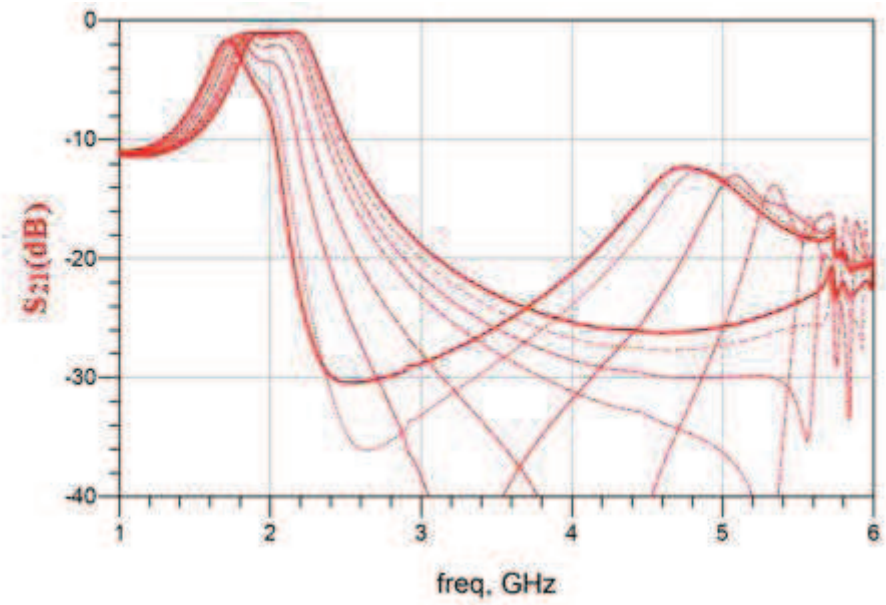

(a)

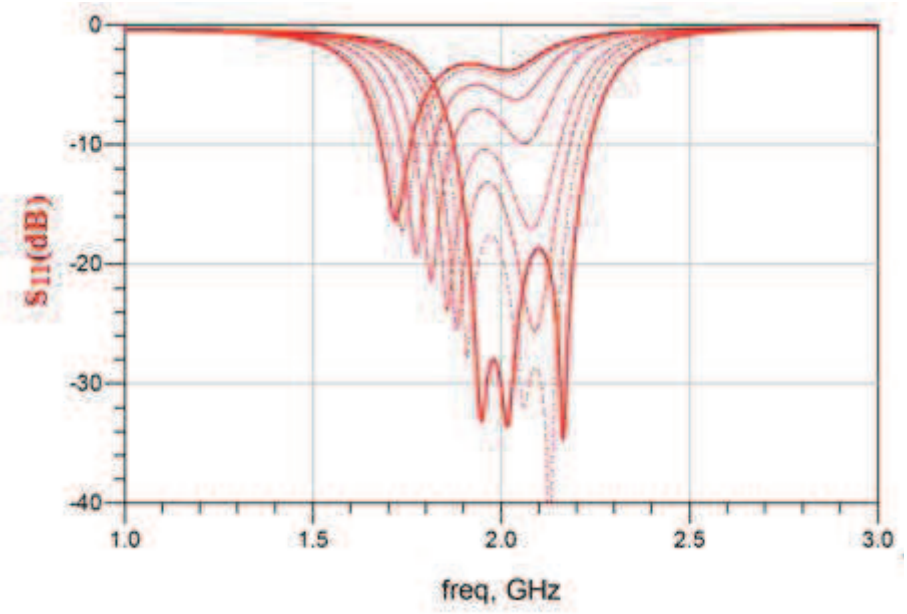

(b)

Figure III.33: Simulated frequency response by varying C_A and C_C vertical slots. (a): Insertion loss, (b): Return loss.

Figure III.33 shows the simulated frequency responses when varying both C_A and C_C. From the increase of these two capacitances, one can perceive two different effects in the mode frequencies: the increase of f_2 approximating it to f_3, and the decrease of f_1 and f_3.

In conclusion, the main effect in increasing C_A and C_C is to reduce both f_1 and f_3.

III.4.4.2 The effect of horizontal slots:

Figure III.34 shows the effect of the variation of C_B and C_D on the frequency response of the filter.

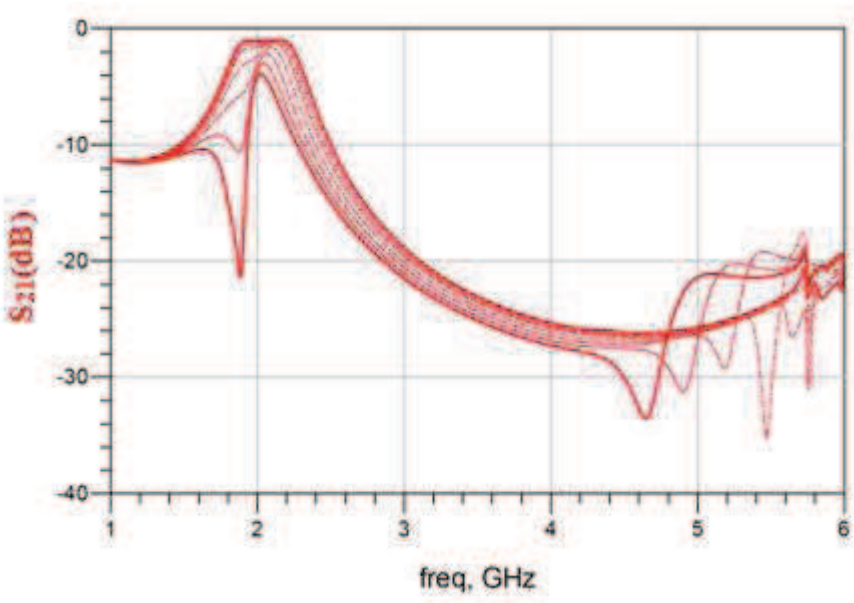

(a)

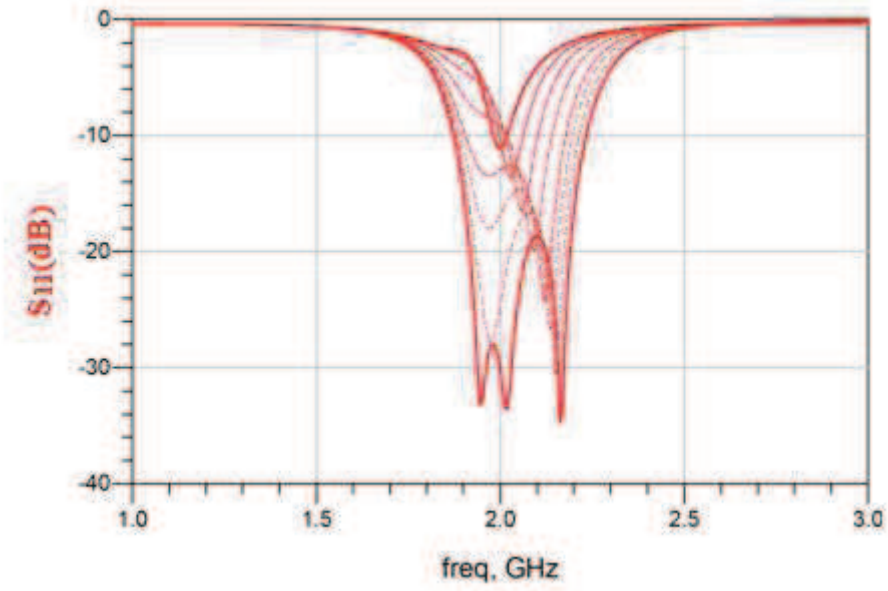

(b)

Figure III.34: Simulated frequency response by varying C_B and C_D. (a): Insertion loss, (b): Return loss.

A different behavior can be seen when changing C_B and C_D. The increase of this capacitance decreases both f_2 and f_3 at the same time, while slightly increasing f_1.

III.4.4.3 The effect of the four combined varactors

The study carried out in the above sub-sections has shown that when using the capacitances across the four slots, allowing this patch filter to be reconfigured by varactor diodes in terms of its center frequency, bandwidth, and rejection.

The rejection is changed by bringing a transmission zero close to the upper side of the passband. Particularly for the susceptances, they all increased with the increase of each individual capacitance, and thus increasing all capacitances together results a simultaneous decrease in the three resonant modes frequency.

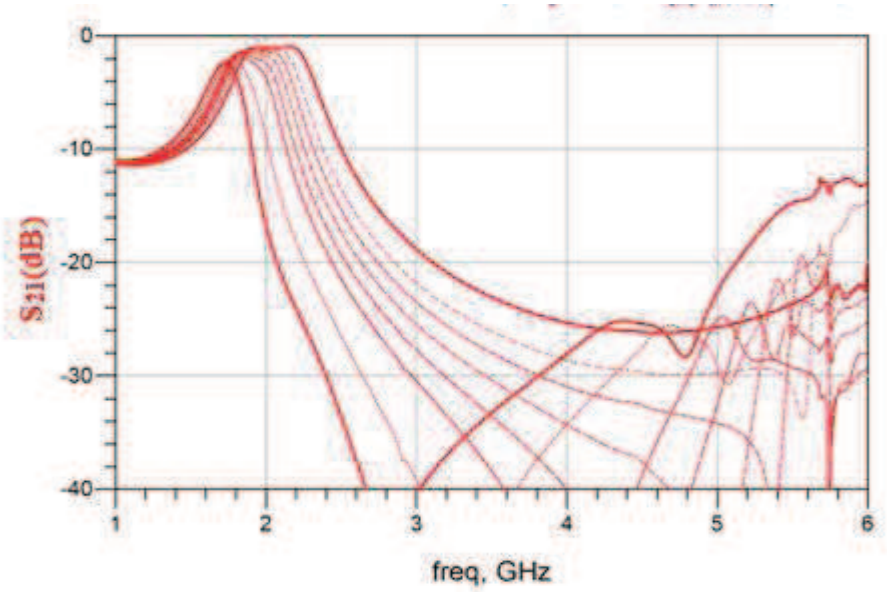

(a)

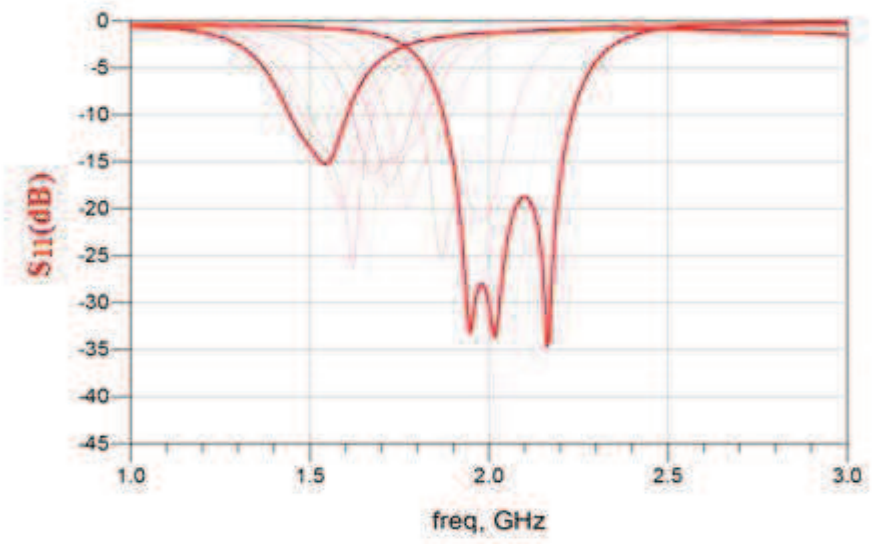

(b)

Figure III.35: Simulated frequency response when varying all the combined varactors. (a): Insertion loss, (b): Return loss.

The patch filter could be tuned by varying the capacitors. The capacitance variation is from zero to 1.2 pF results in 28 % of center frequency tuning range, which varies from 2.02 GHz to 1.54 GHz. At the same time, the filter's passband decreased from 26 % to 13 % for the same range of capacitances. These results are presented in Figures III.34 and III.35.

Simulations with equal capacitances at the four slots show that both frequency and bandwidth decrease at the same time when increasing all the capacitances.

The center frequency of the tunable patch filter with varactor diodes could be tuned up to 2 GHz. The unloaded quality factor *Qu* of this filter was calculated.

At the initial frequency without tuning element (*fc* = 2.02 GHz and bandwidth = 26 %), the filter *Qu* equals 74. When the filter was tuned to the maximum frequency of the Tuning range (*fc* = 1.54 GHz and bandwidth = 13 %), *Qu* equals 44.5. The center frequency of the filer has a tuning range of 27% and a bandwidth tuning of 67%.

Values of capacitors Cj (pF)	**Voltage**	**Center frequency (GHz)**	**FBW (%)**
No capacitors	-	**2.02**	**26**
0.3	30	1.94	22
0.39	15	1.92	21
0.48	9	1.9	19
0.58	5	1.83	17.7
0.7	3	1.8	17
0.8	2	1.75	15.6
1	1	1.62	14.2
1.2	**0**	**1.54**	**13**

Table III.6: Results of the patch filter loaded with four equal varactors.

III.5. Comparison between the two structures

The tunable circular patch filters designed in this chapter used a single bias voltage. Because of that, its tuning characteristic was a simultaneously *fc* and bandwidth tuning, without independent control.

Why the second structure is better than the first one?

First of all from figure III.36, we can see that the return loss in the new structure is better than the first one (RL_1=-15 and RL_2=-20).

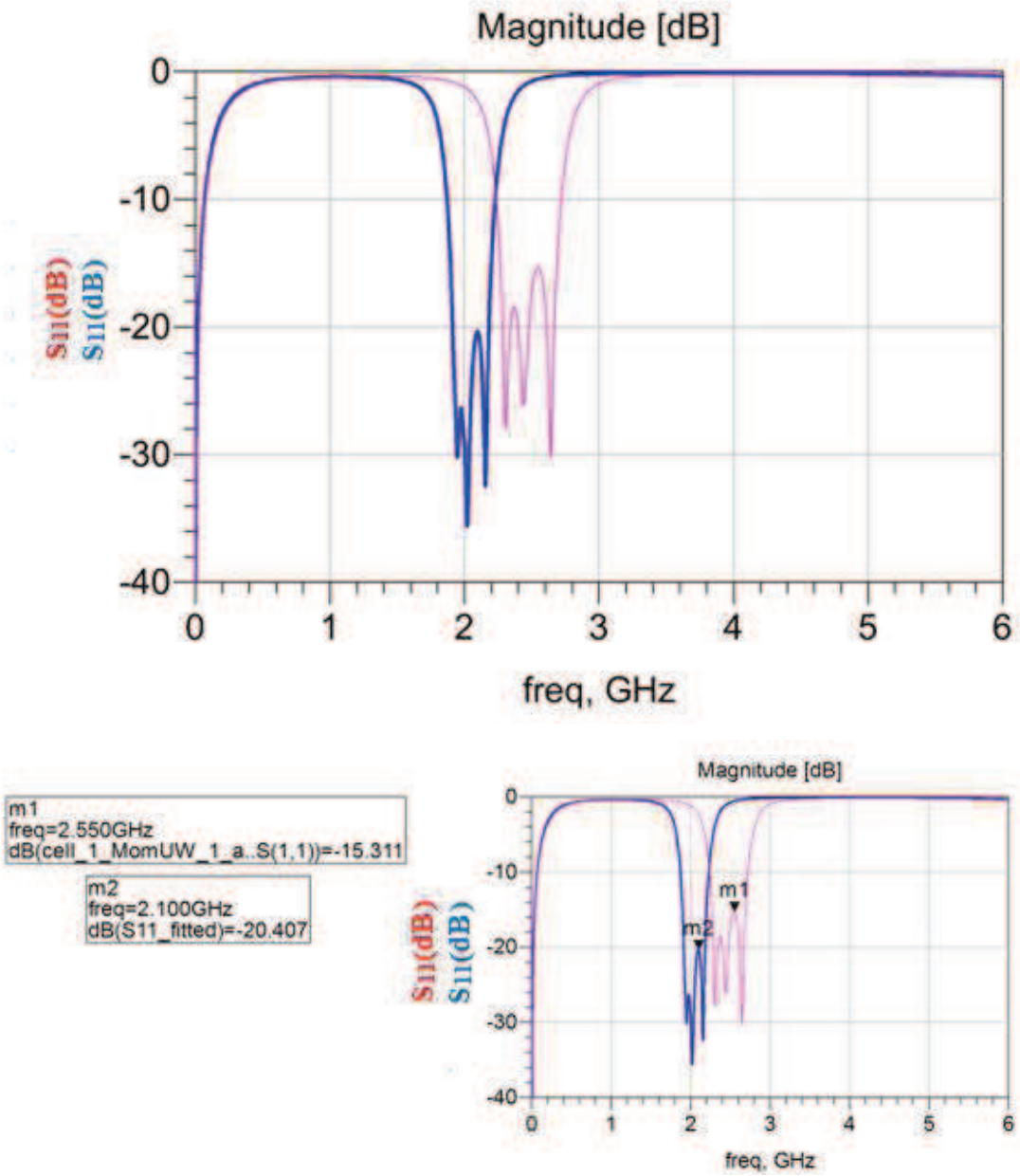

Figure III.36: Simulated S_{11} of the two circular patch filters.

Secondly and from figure III.37 the bandwidth of the filter is narrower (BW_1= 28% and BW_2= 25.7%), for the insertion loss its better in the first structure (IL_1= -0.6 and IL_2= -0.9). We notice also a sharper cut off frequency in the right side of S_{21}.

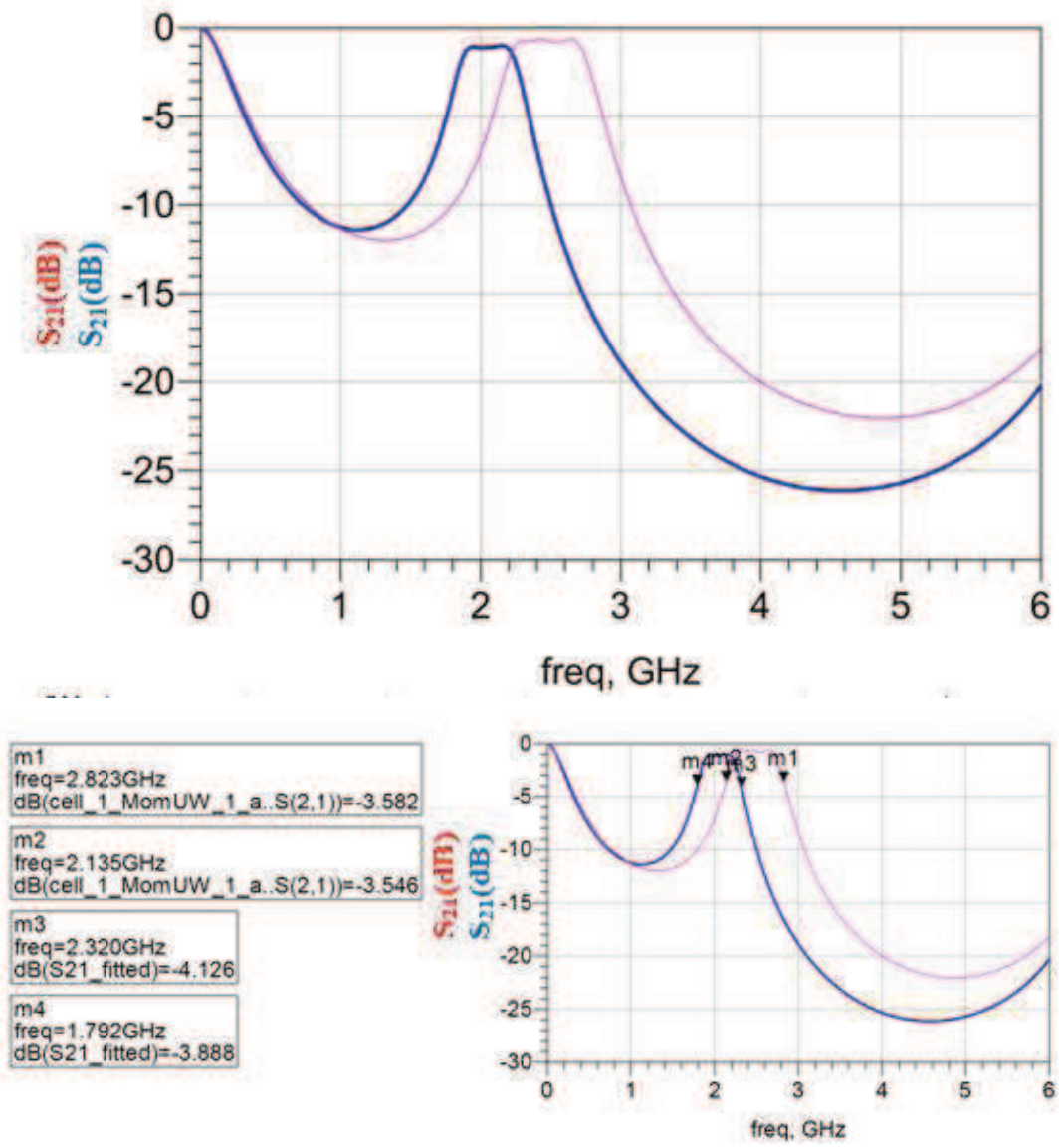

Figure III.37: Simulated S_{21} of the two circular patch filters.

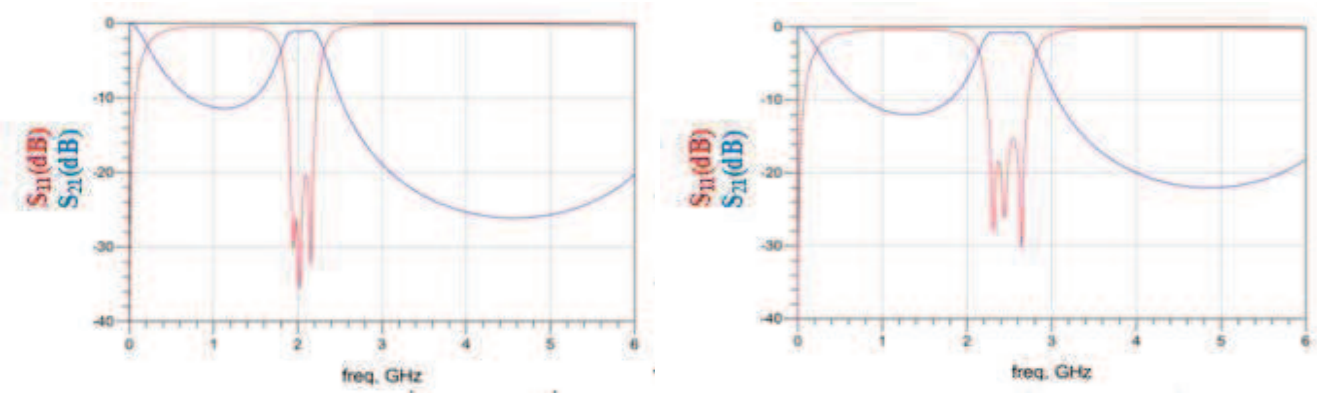

(a) **(b)**

Figure III.38: Simulated frequency response of the two circular patch filters.

(a): the second filter's response, (b): the first filter's response.

III.5.1 Tuning range

When the filter was tuned to the minimum frequency of the tuning range fc_1 = 2.36 GHz and bandwidth = 25%, fc_2 = 1.96 GHz and bandwidth = 24 %. When the filter was tuned to the maximum frequency of the tuning range fc_1 = 2 GHz and bandwidth = 12 %, fc2 = 1.54 GHz and bandwidth = 13%.

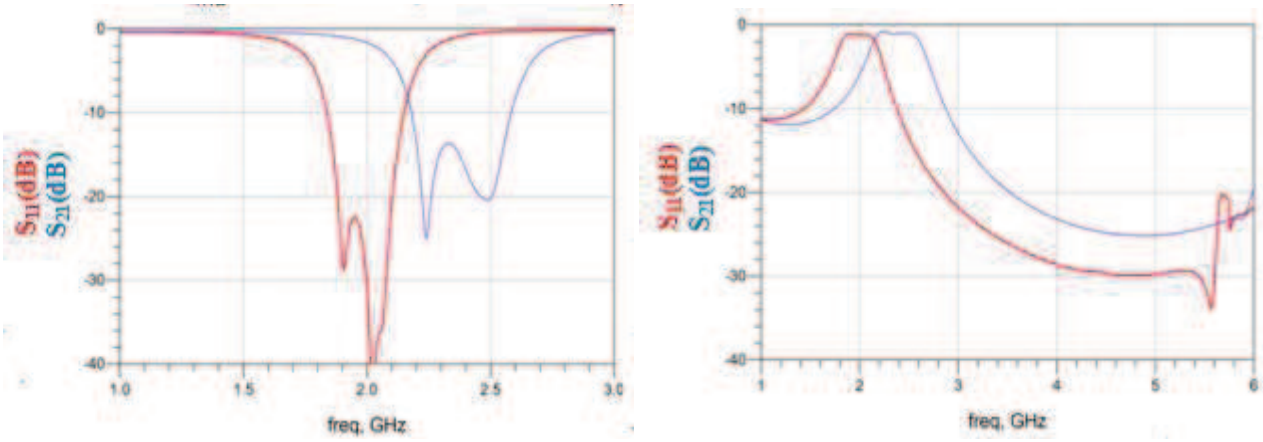

(a) **(b)**

Figure III.39: Minimum frequency of the tuning range of the two circular patch filters.

(a): Return loss, (b): Insertion loss.

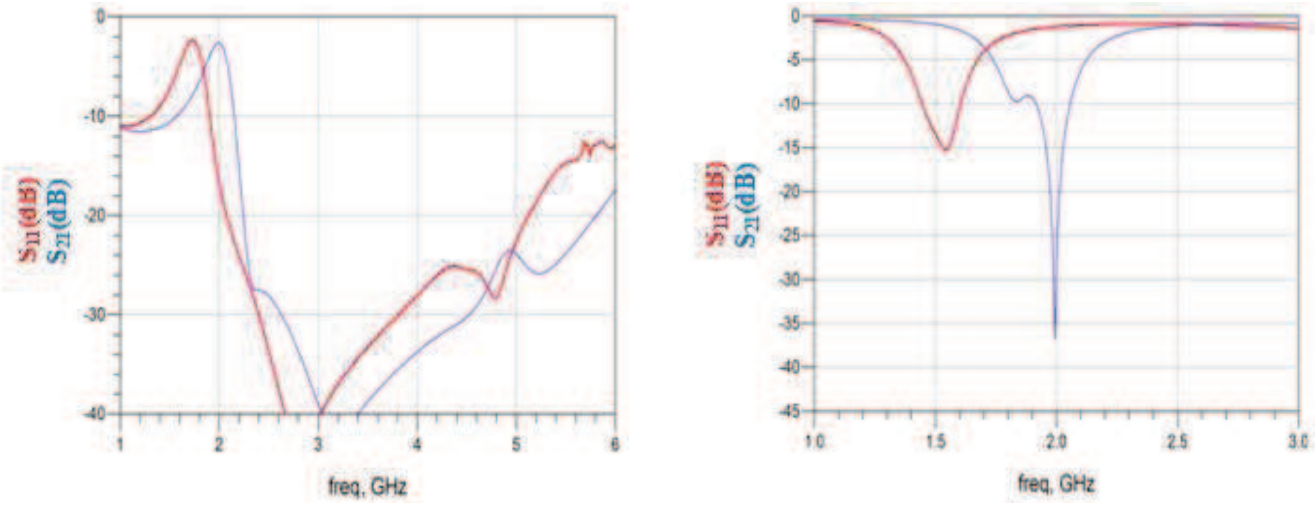

(a) **(b)**

Figure III.40: Maximum frequency of the tuning range of the two circular patch filters. (a): Return loss, (b): Insertion loss.

Considering the bandwidth tuning range, the first filter achieved a high range of 80% and considering the center frequency, the filter achieved a very good tuning range of 21%. The second filter achieved a bandwidth tuning range of 67% and a center frequency tuning range of 28%.

This table compares the designed tunable patch filters of this work and the tunable filters presented in the literature:

Ref	Topology	tuning element	DC bias	F_{min} (GHz)	IL_{max} (dB)	Tunability
1	square ring	varactor diode	5.5 V	2.45	1.6	
2	open loop	VO_2 switch		9.0		5.4%
3	stub	PIN diode		1.9	4.1	50%
4	ring and stub	PIN diode		2.4	1.35	20%
5	combline	varactor diode	20 V	0.75	5.0	18%
6	meander loop	varactor diode	20 V	1.68	7.6	41%
7	folded	GaAs varactor diode	20 V	1.39	2.5	26%
8	combline	BST varactor	100 V	11.7	10	20%
9	folded	varactor diode	20 V	1.06	3.5	5.5%
10	CPW ring	BST varactor	35 V	1.8	2.5	10%
11	triangular patch	PIN diode	10 V	10	3.3	60%
12	square patch	PIN diode	10 V	8.9	3.7	10%
13	triangular patch	GaAs varactor diode	22 V	3	3	15%
This work	**circular patch1**	**GaAs varactor diode**	**30 V**	**2**	**3.5**	**21%**
This work	**circular patch2**	**GaAs varactor diode**	**30 V**	**1.54**	**3**	**28%**

Table III.7: Comparison between the designed tunable filters of this work and those presented in the literature.

III.6. Conclusion

In this work, we have studied and designed two tunable patch filters using varactor diodes electronically controlled by a DC bias voltage. The designed filters are based on a circular patch resonator.

The first filter is a triple modes bandpass filter using a circular patch filter with four slots inclined at 45°. This filter was designed at 2.4 GHz using a single voltage for biasing all the varactors and its center frequency was tuned simultaneously with the bandwidth, reaching so 21% of center frequency tuning and 80% of bandwidth tuning.

The second filter is also a triple mode bandpass filter using the same circular patch with changing the position and the dimensions of the slots. This circular patch was modified with two pairs of slots perpendicular to each other. However, this filter was designed at 2 GHz. The center frequency was also tuned simultaneously with the bandwidth, reaching respectively higher tuning ranges of 28% and 67%.

The final part of this chapter was a comparison between the two designed tunable bandpass patch filters. It is important to note that the proposed tunable bandpass patch filter represents a good improvement not only on the structure but also on the filter characteristics. Indeed, this filter is centered at f = 2.02 GHz with a bandwidth of 26% which is equivalent to 260 MHz, it has an insertion loss of -0.9 and return loss over 20 dB. Moreover, the frequency tuning range is 28% from 2.04 GHz to 1.54 GHz while the bandwidth tuning range reached 67%.

References

[1] Y.-M. Chen et al., "A reconfigurable bandpass-bandstop filter based on varactor-loaded closed-ring resonators [Technical Committee]," IEEE Microwave Magazine, vol. 10, no. 1, pp. 138-140, Feb. 2009.

[2] D. Bouyge et al., "Applications of vanadium dioxide (VO2)-loaded electrically small resonators in the design of tunable filters," Proceedings of the 40th European Microwave Conference, vol. 22, no. 3, pp. 822-825, Sep. 2010.

[3] A. Miller and J.-sheng Hong, "Wideband Bandpass Filter with Reconfigurable Bandwidth," IEEE Microwave and Wireless Components Letters, vol. 20, no. 1, pp. 28-30, Jan. 2010.

[4] C.H. Kim and K. Chang, "Ring Resonator Bandpass Filter with Switchable Bandwidth Using Stepped-Impedance Stubs," IEEE Transactions on Microwave Theory and Techniques, vol. 58, no. 12, pp. 3936-3944, Dec. 2010.

[5] M. Sanchez-Renedo, "High-Selectivity Tunable Planar Combline Filter With Source/Load-Multiresonator Coupling," IEEE Microwave and Wireless Components Letters, vol. 17, no. 7, pp. 513-515, Jul. 2007.

[6] M.R. Al Mutairi et al., "A Novel Reconfigurable Dual-Mode Microstrip Meander Loop Filter," 2008 38th European Microwave Conference, no. October, pp. 51-54, Oct. 2008.

[7] M.A. El-Tanani and G.M. Rebeiz, "A Two-Pole Two-Zero Tunable Filter With Improved Linearity," IEEE Transactions on Microwave Theory and Techniques, vol. 57, no. 4, pp. 830-839, Apr. 2009.

[8] J. Sigman et al., "Voltage-Controlled Ku-Band and X-Band Tunable Combline Filters Using Barium-Strontium-Titanate," IEEE Microwave and Wireless Components Letters, vol. 18, no. 9, pp. 593-595, Sep. 2008.

[9] C.-K. Liao et al., "A Reconfigurable Filter Based on Doublet Configuration," 2007 IEEE/MTT-S International Microwave Symposium, pp. 1607-1610, Jun. 2007.

[10] Y.-H. Chun et al., "BST-Varactor Tunable Dual-Mode Filter Using Variable Zc Transmission Line," IEEE Microwave and Wireless Components Letters, vol. 18, no. 3, pp. 167-169, Mar. 2008.

[11] C. Lugo and J. Papa polymerou, "Single switch reconfigurable bandpass filter with variable bandwidth using a dual-mode triangular patch resonator," IEEE MTT-S International Microwave Symposium Digest, 2005., vol. 00, no. C, pp. 779-782, 2005.

[12] C. Lugo and J. Papa polymerou, “Dual-mode reconfigurable filter with asymmetrical transmission zeros and center frequency control,” IEEE Microwave and Wireless Components Letters, vol. 16, no. 9, pp. 499-501, Sep. 2006.

[13] A.L.C. Serrano, " Synthèse et Conception de Filtres Patch Accordables de Microondes," Université de São Paulo, mai 2011.

Conclusion

In this work, we have proposed two structures of tunable patch filters based on a circular patch resonator.

The first designed filter is a triple modes bandpass filter that uses a circular patch filter with four slots inclined at 45°. The second filter has the same structure as the first but the position and the dimensions of slots have been changed in order that the two pairs of slots are perpendicular to each other.

The circuit was simulated in a copper box with air above and below it. The thickness of copper cladding was set as 17 μm. The circuit was simulated by the full wave EM simulation ADS. The modeling circuit of the GaAs varactor was simulated using the Advanced Design System (ADS).

The frequency responses of patch resonators and filters were simulated using the tool 3D planar Momentum / ADS, which allows the analysis circuit planar with arbitrary topologies. Thus, one can see that the 3D planar EM simulator, Momentum / ADS, used in the design of resonators and filters, proved to be an efficient tool having good compromise between processing time and accuracy.

The important part of this work is a comparison between the two proposed tunable bandpass patch filters. Indeed, the second proposed tunable bandpass patch filter represents a good improvement not only on the structure but also on the filter characteristics. Simulation shows that it is possible to continuously tune the center frequency of the patch filter from 1.54 GHz to 2.02 GHz in a bias range from 0V to 30 V. Within this range, the bandwidth of this filter varies from 26% to 13 %, which leads to a bandwidth tuning range of 67%. All results show insertion loss lower than 3 dB.

Concluding this dissertation, the main objectives were achieved, a new structure have been presented in the filter microwave bandpass resonators using planar patch with the development of miniaturized filters having low loss and good power.